Synthetic Lethality and Metabolism in Ewing Sarcoma : Knowledge Through Silence

Anneliene Jonker

UNIVERSITE PARIS XI

FACULTE DE MEDECINE PARIS-SUD

ECOLE DOCTORALE DE CANCEROLOGIE

Année 2014 N°

THESE

Pour obtenir le grade de

DOCTEUR DE L'UNIVERSITE PARIS XI

Discipline : Cancérologie

Présentée et soutenue publiquement

Par

Anneliene Hechtelt Jonker

Le 8 septembre 2014

Synthetic Lethality and Metabolism in Ewing sarcoma: Knowledge through Silence

Directeur de thèse : Dr. Olivier Delattre

JURY

Dr. Christine Perret	Présidente
Dr. Karoly Szuhai	Rapporteur
Dr. Alessandra Boletta	Rapporteur
Dr. Franck Perez	Examinateur
Dr. Olivier Delattre	Directeur de thèse

UNIVERSITE PARIS XI

FACULTE DE MEDECINE PARIS-SUD

ECOLE DOCTORALE DE CANCEROLOGIE

Année 2014 N°

THESE

Pour obtenir le grade de

DOCTEUR DE L'UNIVERSITE PARIS XI

Discipline : Cancérologie

Présentée et soutenue publiquement

Par

Anneliene Hechtelt Jonker

Le 8 septembre 2014

Synthetic Lethality and Metabolism in Ewing sarcoma: Knowledge through Silence

Directeur de thèse : Dr. Olivier Delattre

JURY

Dr. Christine Perret	Présidente
Dr. Karoly Szuhai	Rapporteur
Dr. Alessandra Boletta	Rapporteur
Dr. Franck Perez	Examinateur
Dr. Olivier Delattre	Directeur de thèse

Acknowledgements

Completing a Ph.D. and writing this thesis was an amazing adventure that would not have been possible without the help of many extraordinary people that have somehow taken part in this journey. I once presented my Ph.D. results by saying that “Great things are done by a series of small things brought together,” and my Ph.D. journey has certainly been a series of many people brought together.

First of all, a splendid thanks to the members of my jury; Christine Perret, Franck Perez, Alessandra Boletti and Karoly Szuhai. Thank you for taking the time and effort to read this manuscript and the guidance on the way. Karoly, I cannot do more than to acknowledge you enormously, not only for being one of my reviewers, but also for being a fantastic mentor over the years. If there is one person that has encouraged me to do research over the last 6 years (Tigger still looks at me every day) and to keep feeling stupid every day, it has been you!

Olivier, thank you for having accepted me in your lab and for your guidance in doing this Ph.D. I know I did not make life any easier for you, with all my extra-curricular activities, but thank you for continuing to believe in my project and me all the way. Without you this crazy, wonderful, mind wrecking journey would not have started and certainly not have come to an end today.

Didier, we might sometimes have suffered together or apart throughout my thesis, but we made it to the end together and that is worth it. Thank you for your help along the way and for making it together so far. Good luck with your next steps in life!

My Ph.D. certainly would not have been possible without the help of many wonderful colleagues. Sandrine and Carole, thank you for mothering over me and explaining me French bureaucracy. Thomas, Mr. Serious, thank you for explaining me that even you do experiments four times before counting them as the first time and thank you for helping me with Mr. Coconut. It has encouraged me to keep having faith so many times! Virginie, thank you for being my neighbor on the other side of the window, for your happiness, but most certainly for indirectly introducing me to other French people. Virginie, thank you for your company in the lab at nights, I still miss you these days and off course thank you for our little cinemas together. Without you, I certainly would not have learned to speak French this quickly. Sarah, despite the fact that I won our bet, I am happy to have lost in the long run. Everything is a matter of time and perseverance! Zhi-Yan, thank you for being my neighbor for so many years, supporting my chaotic behavior and my fear for mice; it was a pleasure! Karine, thank you for your assistance





in so many little things, for new protocols and for your positive energy, I have appreciated it enormously. Georges-Alain and Sarah, it was a pleasure doing a Ph.D. with you! Mr. Serious nr 2, Franck, thank you for answering all the everlasting questions I keep on asking. And last but not least, Marie-Ming, without your positive energy it certainly would have been less fun! Finally, a big thank you to all Neuro, Rhabdo and Bioinfo colleagues, and everyone else from u830 with whom I had so many wonderful exchanges, in both scientific and non-scientific ways! FX for the little P3: thanks for giving me the sign on the door “I was here.”

An overwhelming thank you goes to both the ADIC and YRLS, without whom I certainly would not have completed my Ph.D. Thank you to all its active members for having kept me sane and happy in Paris. Thank you, Alexandre, Susanne, Sofia, Morgan, Claas, Tommy, Xavier, Maxime, Charlotte and many, many more! And as you are almost part of the A-team: thank you Genevieve, Jacqueline, Mélanie and Alysia! To the complete “wireless”- and A-team, it is thanks to you that I managed to create so many contacts, make new friends, and see the ins and outs of science!

Finally, a big, big thank you to all my dear friends and family that have supported me while doing a Ph.D.; it is an enormous pleasure to have friends and family from all continents of the world in my life and to be allowed to take part in yours, but it is an even bigger pleasure to see some of you here today, tomorrow and yesterday and knowing that you will be there in the future adventures to come!

At last, but certainly not least, to my great loves: my university taught me “the future is for those who believe in the beauty of my dreams,” but it is with you that I learned and understand the real meaning of this. Thank you so much for continuing to let me dream and for the future ahead of us.

Table of content

Index Figures

List of abbreviations

αKG	α-ketoglutarate
AA	Amino Acids
ACTA1	Actin 1
ACTB	β-actin
ADP	Adenosine diphosphate
AHR	aryl hydrocarbon receptor
AKT	Protein Kinase B
AML	Acute myelogenous leukemia
AML1	Runt-related transcription factor 1
AMP	Adenosine monophosphate
AMPK	AMP-activated protein kinase
AP-1	activator protein 1
ATP	Adenosine triphosphate
BCR-ABL	Philadelphia chromosome, translocation of BCR and ABL
BRAF	V600E B-rat fibrosarcoma
BRCA1/2	breast cancer 1/2, early onset
CAS9	CRISPR asssociated protein 9
CAV	Caveolin
CBP	CREB-binding protein
CCND1	cyclin D1
CDKN2A	Cyclin dependent kinase inhibitor 2A (P16)
CEMS	Capillary electrophoresis–mass spectrometry
CML	chronic myelogenous leukemia
c-MYC	transcriptional activator Myc
CREB	cAMP response element-binding protein
DNA	Deoxyribonucleic acid
DSB	double stranded breaks
EGFR	epidermal growth factor receptor
EIF2A	Eukaryotic translation initiation factor 3 subunit A
EML-ALK	echinoderm microtubule-associated protein-like 4-anaplastic lymphoma kinase
ER	Endoplasmic reticulum
ERG	v-ets erythroblastosis virus E26 oncogene like
ERK	extracellular-signal-regulated kinases
EWSR1	EWS RNA-Binding Protein 1
EZH2	Histone-lysine N-methyltransferase
FAS	Fatty acid synthesis
FASN	tumor-associated fatty acid synthase
FBS	Fetal bovine serum
FC	Fold Change
Fli-1	Friend leukemia virus integration
FUS	Fused in Sarcoma/Translocated in Sarcoma
GATA2	GATA binding protein 2

GAPDH	Glyceraldehyde 3-phosphate dehydrogenase
GC-MS	gas chromatography–mass spectrometry
GCL	glutamate cysteine ligase
GGT	γ-glutamyl transpeptidase
GI30	concentration for 30% of maximal inhibition of cell proliferation
GIST	Gastro-intestinal stromal tumor
GLI1	Glioma-Associated Oncogene Homolog 1
GLUT1	Glucose transporter 1, SLC2A1
GLUT2	Glucose transporter 2, SLC2A2
GLUT3	Glucose transporter 3, SLC2A3
GLUT4	Glucose transporter 4, SLC2A4
GLUT6	Glucose transporter 6, SLC2A6
GSH	reduced glutathione
GSK-3β	Glycogen synthase kinase 3β
GSSG	oxidized glutathione
GSR	glutathione reductase
HIF	Hypoxia induced factor
HIF1A	Hypoxia-inducible factor 1-alpha
HK	Hexokinase
HR	homologous recombination
HTERT	Telomerase reverse transcriptase
IDO1	indoleamine 2,3-dioxygenase 1
IDO2	indoleamine 2,3-dioxygenase 2
IDH1/2	Isocitrate dehydrogenase 1/2
IGF	insulin growth factor
IGF-1R	insulin growth factor receptor 1
IGFBP3	Insulin-like growth factor-binding protein 3
JAK	Janus kinase
KIF11	Kinesin family member 11
KIT	c-Kit, CD117
KMO	kynurenine 3- monooxygenase
Krebs cycle	citric acid cycle
LC-MS	liquid chromatography–mass spectrometry
LEF1	Lymphoid enhancer-binding factor 1
LKB1	liver kinase B1
LOH	Loss of heterozygosity
LOX	Lysyl oxidase
Luc	Luciferase
MAFB	V-maf musculoaponeurotic fibrosarcoma oncogene homolog B
MAPK	mitogen-activated protein kinase
Mb	mega bases
MDH	malate dehydrogenase
MEI	Malic enzyme 1
MIC2	CD99 antigen
MS	Mass spectrometry

MST1R	macrophage-stimulating 1 receptor tyrosine kinase
mTOR	mammalian target of rapamycin
MYC	Myc Proto-Oncogene Protein
NAD+	nicotinamide adenine dinucleotide
NADPH	nicotinamide adenine dinucleotide phosphate
NF-κB	nuclear factor κB
NFATc2	nuclear factor of activated T-cells, cytoplasmic 2
NHE-1	Na+/ H+ exchanger-1
NLS	nuclear localization signal
NMR	nuclear magnetic resonance spectroscopy
NR0B1	dosage-sensitive sex reversal, adrenal hypoplasia critical region, on chromosome X, gene 1
NSCLC	non-small-cell lung carcinoma
OR6C70	olfactory receptor, family 6, subfamily C, member 70
P16	cyclin-dependent kinase inhibitor 2A
P21	cyclin-dependent kinase inhibitor 1
P300	E1A binding protein p300
P38 MAPK	P38 mitogen-activated protein kinases
PARPI	Poly (ADP-ribose) Polymerase I
PAX5	Paired box protein
PC-1/2	Polycystin-1/2
PDGFR	platelet derived growth factor receptor
PFK	Phosphofructokinase
PFKFB3	6-Phosphofructo-2-Kinase/Fructose-2,6-Biphosphatase 3
PI3K	phosphatidylinositol triphosphate kinase
PIT1	POU domain, class 1, transcription factor 1
PK	Pyruvate kinase
PKD1	polycystic kidney disease 1 (autosomal dominant)
PKM2	pyruvate kinase M2
PLK1	polo-like kinase 1
POLR2B	DNA-directed RNA polymerase II subunit
PNT	pointed
PPP	pentose phosphate pathway
PRKCB	protein kinase PKC-ß
RAD52	RAD52 human homolog
RAS	RAS, Ki-RAS, Ki-rat sarcoma gene
RBD	RNA-binding domain
RBL2	Retinoblastoma-Related Protein 2
RBX1	RING-box protein 1
RGG	arginine-glycine-glycine rich
RMS	Rhabdomyosarcoma
RNA	ribonucleic acid
RNP	RNA recognition motif
ROS	reactive oxygen species
RPS6	ribosomal protein S6

RTK	receptor tyrosine kinase
shRNA	short hairpin RNA
shCT	control shRNA, shRNA with scramble insert
shEF1	shRNA against EWS-FLI1
shPKD1	shRNA against PKD1
siRNA	small interfering RNA
siCT	scramble siRNA
siEF1	siRNA against EWS-FLI1
SP1	Transcription factor Sp1
SSB	single-strand breaks
STAT	Signal Transducers and Activators of Transcription
STK33	serine-threonine kinase 33
TCA	Krebs cycle, citric acid cycle
TDO2	tryptophan 2,3-Dioxygenase
TFIID	Transcription factor II D
TGFBR2	transforming growth factor β receptor II
TRPP	Transient Receptor Potential Polycystic
TP53	Tumor protein p53
TRYX3	trypsin X3
TSC	tuberous sclerosis
TXNL4A	thioredoxin-like 4A
VEGF	vascular endothelial growth factor
VHL	von Hippel-Lindau tumor suppressor
VIM	Vimentin
WNT	wingless-type MMTV integration site family
2-DG	2-deoxyglucose
$1C^{start}$	Starting point of 1C infected cells
$1C^{end}$	Final time point (10 doublings) of 1C infected cells
1C dox^{end}	Final time point (10 doublings) of 1C dox infected cells

Foreword

Ewing sarcoma, first described in 1921 by James Ewing, is the second most commonly occurring pediatric bone tumor with median peak incidence at age 15[1]. Ewing sarcoma primarily occurs in bone, especially in the pelvis, the diaphyseal regions of the long bones and bones of the chest wall, but a small part of primary tumors arises in extra skeletal soft tissue. Ewing sarcoma is aggressively treated with a combination of surgery and chemotherapy and while the overall survival rate of Ewing patients is around 70-75%, the survival rate for metastatic cases remains low (35%)[2–6].

Ewing sarcoma is associated with chromosomal translocations leading to the formation of a fusion protein between the EWS RNA binding protein and an ETS transcription factor. In about 85% of the cases, the translocation involves the *EWSR1* and *FLI1* genes, leading to the expression of the chimeric protein EWS-FLI1[7]. Other translocation leading to the expression of fusion proteins such as EWS-ERG, EWS-ETV1, EWS-EIAF and EWS-FEV are observed in the remaining cases[8–10]. *EWS-FLI1* is a transforming oncogene as shown by tumorigenic properties of EWS-FLI1-expressing NIH3T3 cells and by knockdown experiments in Ewing sarcoma cell lines[11–13]. The chimeric protein acts as an aberrant transcription factor and regulates cell growth and differentiation, which is regarded as a strong indicator that it induces transformation. Additionally, this oncogene is expected to aberrantly regulate hundreds of genes, which may finally contribute to tumor growth and/or metastasis.

For a long time, it has been known that metabolism in tumors is different from normal tissues, with the Warburg effect, the concept that tumors prefer anaerobic glycolysis even in the abundance of oxygen, as its most known phenomenon[14,15]. Recently this concept has regained more and more attention, being described as one of the new cancer hallmarks[16]. There are several reasons to investigate this aspect in the context of Ewing sarcoma; first, it has long been known that Ewing sarcomas are small round tumor cells that have a very high content of glycogen. EWS-FLI1 has been shown to down-regulate IGF-1 and to impair the IGF-1/IGF-1R signaling pathway[17]. Finally, previous unpublished data from expression profiling of Ewing tumors indicated that EWS-FLI1 directly regulates some members of the glycolysis pathway. Therefore, studying the *EWS-FLI1* gene fusion becomes an essential step in understanding the metabolism of Ewing sarcoma.

Fortuitously, such the experimental environment to perform such a study are available, as Tirode et al. previously developed in the lab of Olivier Delattre a tetracycline-inducible cell line model that conditionally regulates the expression of the *EWS-FLI1* fusion gene[18]. This model allows performing EWS-FLI1 inhibition/reactivation experiments from which transcriptomic expression time series profiles were generated. Additionally, in the lab, there is a vast amount of transcriptomic data available for both Ewing sarcoma cell lines and Ewing sarcoma tumors, allowing for a better investigation of the biology related to this tumor. Taking advantage of the above described tetracycline inducible cell line, the metabolic impact of EWS-FLI1 was investigated, using mass spectrometry-analysis with cells of Ewing sarcoma in shEWS-FLI1 on and off conditions.

A parallel avenue of investigation that will be described in this thesis is the search for new therapeutic targets in EWS-FLI1 fusion protein-carrying Ewing sarcomas. In recent years, the search for a better therapeutic target for Ewing sarcoma as for many other cancers has focused on the development of personalized therapy, driven by the premise that it will increase therapeutic efficacy and reduce toxicity. However, the development of drugs for these targets that selectively kills tumor cells, without causing damage to the normal cells of the body remains challenging. In these challenging cases, the concept of synthetic lethality has been advanced as a potential approach. Synthetic lethality refers to the phenomenon of cell death caused by two mutations acting together, where each mutations alone does not contribute to a decrease in cell viability. Synthetic lethality in cancer research has shown some striking examples, such as Poly (ADP-ribose) Polymerase I (PARP1) inhibition in breast cancers where both alleles of Breast cancer 1 or Breast cancer 2 (*BRCA1/2)* were inactivated. Using a high-throughput shRNA approach, we investigated whether it is possible to identify synthetic lethal genes in the context of Ewing sarcoma.

Before setting down the results of the study that are presented in this dissertation, an introduction will be presented to establish a structural template for the discussion of set results. The introduction can be broadly categorized in three parts. Firstly, a general overview on Ewing sarcoma will be presented. The second part will discuss metabolism in the setting of cancer research. Finally, the concept of synthetic lethality and high-throughput genetic screenings will be presented and discussed.

Introduction

1. General aspects of Ewing sarcoma

A. Clinical aspects

A.1 Historical context

The American pathologist James Ewing, named "Cancer Man" by Times magazine in 1931, first described a new bone tumor, "diffuse endothelioma of bone," in 1921, two years after he published the first edition of his cancer textbook, in which he classified many different cancer types[19,20]. He reported a 14-year-old girl with a tumor of the radius, the pathology of which was distinctly different from, at that time already well know, osteosarcoma. He described the tumor with the somewhat ambiguous term "round cell sarcoma," as the cells appeared to resemble blood vessels of the bone and he consequently called it endothelioma of bone. In the same report he described six other cases, which he had come to observed in a period of four months. In the years following this publication several other case reports were published concerning the topic using different names, none of which agreed on the origin of the tumor, kick starting a still unresolved debate[21]. Eventually, the French pathologist Oberling eponymously christened the tumor as Ewing sarcoma, thus the tumor becoming James Ewing's eponym[22].

A.2 Histogenesis

Ewing sarcomas are a group of mostly undifferentiated, highly aggressive, small round cells tumors, that mostly affect the long bones and the soft tissues[23]. They are defined by a chromosomal translocation between chromosomes 11 and 22, leading to a fusion protein between the EWS RNA binding protein and an ETS transcription factor[24,25]. This translocation characterizes about 85% of the cases, leading to the fusion gene *EWS-FLI1*. It is this genetic marker comprised of a group of tumors with variable status and physical location that defines Ewing sarcoma[26–28].

A.3 Epidemiology

Ewing sarcoma, a malignancy of childhood and adolescence, is the second most commonly occurring bone tumor[29]. This tumor can be considered "rare" with a yearly incidence of about 1.3 per million[30]. The average age of diagnosis is around 15 years of although 20-30% of cases are diagnosed in the first decades of life, 20% of cases are

discovered in the third decade and cases continue to be diagnosed at a later age, although with a lesser frequency[1]. There is a slight male predominance, with males being slightly more affected then females, with a ratio of 1.3:1[31]. Despite very low incidence rates, some familial cases have been described, however the disease is not linked to any hereditary syndrome[32–34]. Ewing sarcoma primarily occurs in the Caucasian population, with very few described cases of African or Asian origin[30,35–38].

A.4 Clinical characteristics

Ewing sarcoma most commonly occurs in bones, more specifically in the long or the flat bones of the axial skeleton. They tend to arise from the diaphyseal rather than the metaphysial portion of the bone[23]. Even though Ewing sarcoma can be found in any part of the body, the most affected are the large bones such as the pelvic bone, the femur, the tibia, the humerus and the scapula (Figure 1). Most common symptoms are loco-regional pain, followed by a palpable mass[39]. Generally, the duration of symptoms prior to diagnosis can be between weeks to months, with a median of 3-9 months[40–42]. Fever or weight loss is observed in about one third of patients, often correlated with metastatic disease[40–43]. About one fourth of patients has a detectable metastasis at diagnosis, which is often (35%) related to the lung, as well as isolated bone/bone marrow involvement, combined lung- and bone metastases and rarer sites[6,23].

Ewing sarcomas are presented at a macroscopic level as solid, greyish, often necrotic and hemorrhagic. More common histological features include undifferentiated uniform small round cells, with hyperchromatic nuclei, inconspicuous nuclei and scant cytoplasm[44]. Mitotic activity is low. Cells are usually (90%) positive for CD99 antigen (MIC2) and vimentin (VIM), however this antigen is non entirely specific for Ewing sarcoma[45].

A.5 Treatment

The standard of care is neo-adjuvant chemotherapy, followed by surgery and radiation. The standard protocol of treatment in Europe requires 6 cycles of chemotherapy consisting of a combination of 5 different chemotherapeutic agents: vincristine, doxorubicin, ifosfamide, etoposide and cyclophosphamide (Euro-E.W.I.N.G 1999). Disease can respond drastically to treatment, with initial response being a marker of better outcome[46]. However, despite a good initial response and the intensive

treatment, Ewing sarcoma holds a propensity for deadly recurrence for both local and metastatic disease[46,47]. Several prognostic factors have been identified, the disease stage i.e. the presence or absence of metastasis at diagnosis, being the most important one. Other factors include the response to chemotherapy, tumor site and volume, the age of the patient and the extent and site of metastasis[48–50]. The average 5-year overall survival rate of patients with Ewing sarcoma is approximately 70-75%[2–4]. Nevertheless, the long-term survival for patients with metastatic, refractory or relapsed disease is significantly reduced being around 35%, indicating the need for novel therapeutic targets[5,6].

B. Molecular genetics of Ewing sarcoma

B.1 Characterization of the fusion gene EWS-FLI1

The unifying genetic event of Ewing sarcoma, the chromosomal translocation, t (11; 22)(q24; q12), was first described more than 30 years ago[25]. The resulting fusion is a combination between the N-terminal region of EWS RNA-Binding Protein 1 *(EWSR1*), an RNA binding protein and the C-terminus of an ETS transcription factor, Friend leukemia virus integration (*FLI1*)[7]. This fusion has its expression under the control of the *EWSR1* promoter, which is ubiquitously expressed. The reciprocal *FLI1-EWS* fusion is rarely expressed and the der (11) is even lost in certain cases. There are at least 12 different types of the fusion *EWS-FLI1*, containing different combinations of exons from *EWSR1* and *FLI1*[51]. However the most common ones are type 1, a fusion between *EWSR1* exon 7 to *FLI1* exon 6 and type 2, a fusion between *EWSR1* exon 7 to *FLI1* exon 5[52]. Type 1 accounts for about 60% of *EWS-FLI1* fusions, whereas type 2 does for 25%[53]. Clinically, no significant prognostic value of the fusion type on the risk of progression or relapse was found as reported by the recent prospective Euro-E.W.I.N.G[53–56].

B.2 Other fusion types

In the 15 % of remaining cases of Ewing sarcoma that do not harbor an *EWS-FLI1* translocation, the *EWSR1* gene is most often fused with other genes of the *ETS* family. In a majority (10%) of the cases v-ets erythroblastosis virus E26 oncogene like (*ERG)* is implicated in a translocation t(21;22)(q22;q12), however other genes of the *ETS* family implicated with *EWSR1* are *ETV1*, *ETV4*, *E1AF* and *FEV*, or more exceptionally *ZSG*[8–10,57–59] (Figure 2). In the remaining rare cases another member of the *TET* family, Fused in

Sarcoma/Translocated in Sarcoma (*FUS)* is implicated, forming the fusion *FUS-ERG* or *FUS-FEV*[60,61]. Recently, a group of round cell tumors have been identified that harbor morphologic commonalities and certain degree of biologic overlap with Ewing sarcoma, that have been defined as Ewing-like tumors. In this group *EWSR1* can be merged with a non-*ETS* family member, of which *EWS-NFATc2* is an example, as the even more exceptional *EWS-SP3*, *EWS-POUF5F1* and *EWS-SMARCA5*[62–65]. Additionally, a small number of cases negative for *EWSR1* have been characterized carrying *BCOR-CCNB3* or *CIC-DUX4* fusions[66–68]. *EWSR1* gene fusions are thought to be the initiating oncogenic event and are critical for proliferation and tumorigenesis[69].

B.3 Secondary alterations

Ewing sarcoma is characterized by a relatively simple karyotype with a few numerical and structural aberrations. Secondary chromosomal alterations are a common phenomenon in Ewing sarcoma, with more then 75 to 80% of cases being affected[70,71]. Most common alterations are trisomy 8 and 12 and a deletion of 16q as a result of an unbalanced translocation t(1;16)[72,73]. In additional cases, other aneuploidies have been identified; structural chromosome 1 aberrations resulting in gains of chromosome 1q or relative losses of 1p, as well as a loss of chromosome 16q[72]. Although several studies have been published on this topic, there is a disagreement concerning the correlation of chromosomal alterations with clinical parameters[74–78]. Common mutations in human malignancies are infrequent in Ewing sarcoma; mutations in Tumor protein p53 (*TP53)* and cyclin dependent kinase inhibitor 2A (*CDKN2A*), encoding for the proteins p14 and p16*,* have been identified in 10 up to 20% of cases and generally carry an unfavorable outcome[79–81].

C. The ETS family

C.1 The *ETS* transcription factors

The *ETS* family of transcription factors, initially derived from the name of the erythroblastosis virus, E26, which carries the *v-ets* oncogene, is one of the largest, conserved gene families of transcription factors and is unique to metazoans[82,83]. So far 28 genes have been identified in humans whereas 27 mouse homologues have been listed[84,85]. ETS family of transcriptions factors are characterized by sequence homology within their ETS DNA binding domain, a domain of 85 amino acids that is localized most often in the C-terminus region (therefore conserved in Ewing sarcoma). The ETS

domain, highly conserved in evolution, forms a winged helix-turn-helix structural motif that binds to the consensus sequence GGAA/T[84].

A further sub-classification of ETS family members is possible on the basis of high amino acid conservation of the ETS domain and the presence of other conserved domains[86,87]. A subset of the ETS transcription factors additionally has a pointed (PNT) domain in the N-terminus. This domain is also organized in a helix-turn-helix motif and allows for homo-oligomerization, hetero-dimerization and transcriptional repression[88–92]. Additionally, certain ETS family members contain two possible transcriptional activation domains, at both their N- and C-terminus regions[93].

Family members can act either as transcriptional regulators or repressors, of which activity is regulated by phosphorylation and protein-protein interactions[94,95]. These interactions between the different members of the ETS family as well as with other transcription factors allows for transcriptional regulation depending on the cellular context.

C.2 The ETS biological functions

ETS transcription factors are involved in regulating a variety of biological pathways. They regulate gene expression by functional interaction with other transcription factors and co-factors on composite DNA-binding sites. Well-known ETS interactions are the interaction between the ETS and the Jun family proteins, the mitogen-activated protein kinase (MAPK) signaling proteins, extracellular-signal-regulated kinases (ERK), POU domain, class 1, transcription factor 1 (PIT-1) and P38 mitogen-activated protein kinases (P38) SAPK[96–99]. For the precise transcriptional regulation, ETS is thereby is dependent on interaction with other factors[100]. ETS thus interacts with several other transcription factors such as SAP-1a, activator protein 1 (AP-1), Runt-related transcription factor 1 (AML1), Lymphoid enhancer-binding factor 1 (LEF1), Transcription factor Sp1 (SP1), transcriptional activator Myb (c-MYB), Paired box protein (Pax-5), nuclear factor κB (NF-κB), Stat-5 and V-maf musculoaponeurotic fibrosarcoma oncogene homolog B (MAFB)[96,101].

C.3 The TET family

TLS/FUS, EWS, TAF15 are part of a family called the TET family of proteins and they perform various roles in gene expression. The TET family members are predominantly

localized in the nucleus and they are expressed in all human tissues[102–104]. These proteins are highly related and characterized by an amino terminus rich in Gln, Gly, Ser and Tyr, as well as by a conserved RNA-binding domain (RBD), a arginine-glycine-glycine rich (RGG) regions that may affect RNA binding and a Cys2–Cys2 zinc finger that may bind nucleic acids, although some variation exists between the TET proteins[105]. EWS contains several copies of a hexapeptide repeat of Ser-Tyr-Gly-Gln-Gln-Ser, where the second amino acid is always a Tyr and the fourth always a Gln[61]. It is suggested that the multiple Tyr residues are needed for transcription activation, however with the region being vastly anarchic, it seems likely that organization is not a key element[61,106].

The secondary structure of TET proteins is defined by the RBD, which folds into a sheet of parallel β-strands perpendicular to two α-helices[107]. In the RBD, RNA recognition motif (RNP)-1 and RNP-2 bind to the RNA directly via hydrogen bonds and ring stacking[105]. Additionally, single strand DNA can also bind to the RBD. The RBD domain is the most conserved domain of the TET family of proteins. Additionally, the TET proteins may bind to nucleic acid via their zinc finger[108]. Furthermore, TET proteins contain three RGG, that may be responsible for an increased affinity of RNA to TET's RBD or zinc finger[107].

Full-length EWS associates with members of the transcriptional machinery, including RNA polymerase II, Transcription factor II D (TFIID) and CREB-binding protein/ E1A binding protein p300 (CBP)/(p300), indicative of a role in transcription activation[109,110].

The expression profile of ETS family members is variable. In normal cells, EWS is expressed ubiquitously; it localizes generally in the nucleus and exceptionally in the cytoplasm and various subcellular compartments[104,111]. Localization of EWS in different subcellular compartments reflects its dynamic distribution during cell cycle.

C.4 The TET biological functions

The TET proteins have a large variety of biological functions, being involved in several aspects of cell growth control, in addition they also have been shown to have roles in transcription and splicing, DNA repair and RNA transport in neurons. TET proteins directly associate with members of the transcriptional machinery, such as RNA Polymerase II, TFIID and CBP/p300, but they also regulate transcription through contacting activators and repressors[105,109,110,112]. The reverse is also true, in that TET also

represses transcription by RNAP II[113]. TET proteins do not work alone, but work together with a variety of other proteins, to play a regulatory role in different cellular processes.

TET proteins have been thought to be important in pre-mRNA splicing, by interacting with SR proteins[114–116]. TET proteins also play a role in the DNA repair pathway. It was shown that TET proteins homologously pair DNA, an exclusive activity to TET and PSF, a splicing factor[117].

C.5 EWS-FLI1

The *EWSR1* gene codes for the EWS protein, a member of the TET family of proteins, whereas the *FLI1* gene, a member of the ETS family of proteins, codes for the FLI1 protein (Figure 3). The fusion protein EWS-FLI1 contains the amino-terminus of EWS and the carboxy-terminus of FLI1. This resulting fusion protein works as an oncogene through its function as aberrant transcription factor, but can also work as a transcriptional repressor[13,118–121].

The amino-terminus part of EWS in the fusion protein contains several serine-tyrosine-glycine-glutamate repeats, resembling a transcriptional activation domain[59]. The transcriptional activator function of EWS-FLI1 is thus due to binding of this domain with a heterologous DNA-binding domain[13,119,122]. The carboxy-terminus domain of FLI1 in the EWS-FLI1 fusion protein contains the *ETS* DNA binding domain and recognizes a GGAA/T core motif, equal to other *ETS* family members or a specific $(GGAA)_{n>7}$ microsatellite repeat that is specific to this oncogene[84,87,100,123–125]. The fusion protein between EWS and FLI1 is constitutively expressed, due to the *EWSR1* promoter[7,13,126–128].

Several activatory and repressive mechanisms by EWS-FLI1, such as protein-protein interactions and post-translational modifications have been described in literature[129]. Examples of post-translational modifications of EWS-FLI1 have been shown by the phosphorylation of Ewing sarcoma cell lines, which modulates DNA binding and transcriptional activity. Additionally, it was shown that EWS-FLI1 undergoes O-GlcNAcylation, which may alter the protein's intracellular half-life, thus altering of the transcriptional function of EWS-FLI1[129,130].

Where normal EWS directly associates with the general transcriptional machinery, EWS-FLI1 does not appear to be stably associated with the RNA polymerase II complex[109]. However, EWS-FLI1 does interact with the RNA polymerase II subunit

RPB7[110]. EWS-FLI1 also interacts with RNA helicase A[131]. Another component of the transcriptional apparatus of EWS-FLI1 is CBP[121,132].

C.6 EWS-FLI1 targets

EWS-FLI1 acts as an aberrant transcription factor that targets a number of downstream genes, contributing to the process of oncogenesis in Ewing sarcoma. EWS-FLI1 binds to GGAA microsatellites to activate down-stream targets. Several techniques have been used to identify and visualize the variety of downstream targets of EWS-FLI1, most notably RNAi, followed by microarray or ChIP-analysis, allowing for identification of up-regulated and down-regulated targets. A variety of target genes of EWS-FLI1 are necessary for different processes of tumorigenesis, being cell proliferation, evasion of apoptosis, drug-resistance, cell cycle control, evasion of growth inhibition, immortalization, angiogenesis, adhesion and maintenance of pluripotency, such as cyclin D1 (CCND1), Insulin-like growth factor-binding protein 3 (IGFBP3), Glutathione S-transferase Mu 4 (GSTM4*),* cyclin-dependent kinase inhibitor 1 (p21), transforming growth factor β receptor II (TGFBRII), Telomerase reverse transcriptase (hTERT), vascular endothelial growth factor (VEGF), Caveolin (CAV), dosage-sensitive sex reversal, adrenal hypoplasia critical region, on chromosome X, gene 1 (NR0B1), NKX2.2, Glioma-Associated Oncogene Homolog 1 (GLI1), Histone-lysine N-methyltransferase (EZH2) and protein kinase PKC-ß (PRKCB) respectively[120-122,125-127, 129-142]. Among the EWS-FLI1 regulated genes, some represent direct targets of EWS-FLI1, others function as indirect targets[143]. In addition to up-regulated genes, EWS-FLI1 thus also down-regulates a variety of genes; EWS-FLI1 may repress as many, if not more, genes than it up-regulates. In comparison to the up-regulated genes, the mechanism of repression by EWS-FLI1 is still indefinable[144,145]. The down-regulated genes are also involved in a variety of cellular processes and oncogenesis, signifying that this part of EWS-FLI1 targets is equally important for tumorigenesis[12,120,121]. Examples of proteins which expression is down-regulated by EWS-FLI1 are Lysyl oxidase (LOX) and TGFBR2, that function as tumor suppressors in Ewing sarcoma[120,146].

Summary and directions for introductory section on Ewing sarcoma

- *Ewing sarcoma, the second most commonly occurring pediatric bone tumor, is most often caused by a translocation of EWS-FLI1.*
- *EWS-FLI1 represses and activates a network of target genes.*
- *Ewing sarcoma is treated with conventional chemotherapy, radiation and localized surgery, but despite aggressive treatment, survival rates in recurrent and metastasized cases remain especially low.*

Characterizing the downstream events of EWS-FLI1 has added to the growing knowledge about Ewing sarcoma. However, with the characterization of downstream signaling cascades below EWS-FLI1, the question arises of the role of metabolics in the tumor. Metabolic changes are more and more seen as an essential driving process in tumor biology and an integrated part of cell biology. It might therefore be of great interest to visualize the metabolic network of EWS-FLI1, in order to integrate metabolic pathways with available genetic data and therefore allow for a better general understanding of the disease.

Additionally, a high need for the identification of new therapeutic targets in the treatment of Ewing sarcoma remains, as survival rates in Ewing sarcoma in metastatic and relapse cases are low. Making use of the concept of synthetic lethality, the idea that two combined mutations lead to cell death while both alone do not alter cell viability, might be an interesting concept and a way forward to find those new therapeutic targets.

2. Cancer metabolism

A. Historical aspects

It is generally believed that the field of cancer cell metabolism was started by Otto Warburg's observations. This process involves the intracellular chemical reactions that convert nutrients and endogenous molecules into the energy and matter that sustain the cancer cell. Otto Warburg, a German truly interdisciplinary scientist with a PhD in chemistry and a degree in medicine, had supposedly set himself the goal to cure cancer[147]. In the golden age of biochemistry (roughly the 1920s till 1960s), Otto Warburg sought out several ways to improve quantification of biological research, such as the use of thin tissue slices for physiological research, improved manometric techniques and the single-beam spectrophotomer, which allowed him to make several major contributions to the research on metabolism and cancer research[148–151]. He carried out one of the pioneering studies of cancer cell metabolism, with slices of living tissue where he observed a pattern specific to cancer cells: while in normal tissues lactate production occurs almost exclusively during oxygen deprivation, it was not ablated in the slices of cancer cells in the presence of oxygen[15]. This phenomenon, named the Pasteur effect after the work from Louis Pasteur by Warburg and later called the Warburg effect, attracted the attention of other scientists and was followed by several other publications validating and continuing upon his experiments[152–155].

Although Warburg won the Nobel Prize for a different study on respiration, he is best remembered for his research on metabolic research in cancer and most specifically the Warburg effect. About 90 years later, the concept of cancer cell metabolism is still a remarkably exciting issue in many ways. Over the last decade, researchers have started to unravel the precise biological nature behind metabolic changes and shown that these altered metabolic processes can be a necessary factor in tumor development, rather than just being a consequence of cancer.

A. Metabolic pathways in the cell

B.1 Metabolism: catabolism, anabolism, waste disposal

Metabolism is commonly defined as the entire of biochemical processes in living organisms that either produce or consume energy[156]. The entire of the cell's metabolism in eukaryotes is rather complex with about 10000 metabolic reactions currently known

in the Kyoto Encyclopedia of Genes and genomes, catalyzed by more then 16000 enzymes[156,157]. Generally, the metabolism can be divided into three different parts: anabolism, catabolism and waste disposal, essential for energy homeostasis and macromolecular synthesis in humans. Several major nutrients, such as glucose, amino acids and fatty acids are used via anabolism to create all macromolecules, needed for cell growth (lipids, proteins, nucleic acids and polyamines) and energy storage (glycogen, lipids, proteins), requiring the input of energy. When needed, these macromolecules are broken down in a series of degradative chemical into smaller units, mostly releasing energy, a process called catabolism. As complex chemical units are broken down in smaller units via catabolism, waste products such as ammonia, carbon dioxide and reactive oxygen species, are produced.

B.2 Metabolism as integrated part of cell biology and disease

In our current on-going exploration of cell biology and disease, the revelation of more and more metabolic pathways and metabolites has urged us to no longer see metabolism just as independent series of pathways, but as an integrated world. Metabolism influences and is influenced by almost every process in the cell[156]. Numerous regulatory mechanisms connect cell signaling to the orchestration of metabolic pathways, most noticeably in cell growth, where metabolism helps to implement cell growth programs.

B.3 Roles of “metabolic” genes in cell signaling

Cell growth and proliferation are promoted and controlled by extracellular ligands (Figure 4). Most of these ligands bind to the cell surface receptors and initiate signal transduction cascades. Activation of these, but also numerous other pathways, alter the phosphorylation states of numerous targets, eventually leading to the coordination of cellular activity which leads to cell growth and division. However, tight control of metabolism is absolutely essential for the transition from a resting state to a dividing state of the cell. In order to maintain a bioenergetics state permissive for cell growth, growth factor signaling is effectively increasing the surface expression of transporters of essential nutrients such as glucose[156,158]. This provides energy and metabolic precursors to produce molecules. The phosphatidylinositol triphosphate kinase/ Protein Kinase B/ mammalian target of rapamycin (PI3K/ AKT/ mTOR) pathway is an example of such a pathway that stimulates surface receptors to allow for a rapid increase in nutrient

uptake and the appropriate distribution of these nutrients in the corresponding anabolic and catabolic pathways[159]. The balance between the corresponding anabolism and catabolism pathways are dynamically regulated by diverse cell signaling pathways that are also involved in sensing the energy status of the cell. The previously indicated PI3K/ AKT/ mTOR pathway promotes anabolism and suppresses catabolism, whereas AMP-Activated protein kinase (AMPK) does the reverse, providing a negative feedback loop for those pathways. AMPK acts as energy sensor for nutrient availability, at times when the bioenergetics state of a cell is compromised. Adenosine monophosphate (AMP) and Adenosine diphosphate (ADP) promotes activation of AMPK by enhancing the phosphorylation of one of its kinase domains, promoting phosphorylation of a number of downstream targets, thus inactivating energy consuming and growth promoting pathways as lipid synthesis[160].

B.4 Essential metabolic pathways

Cell signaling pathways thus dynamically influence and control several metabolic pathways in order to influence the cell's growth processes and energy balance. Alternatively, the metabolism also affects cell signaling in a variety of ways providing substrates for posttranslational modifications that modulate protein trafficking, localization and enzymatic activity[156]. A systematic understanding of a variety of pathways by which metabolism influences cellular signaling can be performed by broadly dividing the set pathways into the following three pathways:

- Energy metabolism pathways (such as glycolysis, the Krebs cycle (TCA cycle or citric acid cycle) and the oxidative phosphorylation)
- Cellular redox status pathways (such as the methionine- glutathione pathway, the taurine pathway and the cysteine pathway)
- Biosynthesis pathways (such as the biosynthesis of nucleotides via the pentose phosphate pathway, lipid and fatty acid synthesis, the urea cycle and gluconeogenesis).

The different pathways will be described in more detail in the following paragraphs.

B.5 Energy metabolism

Energy metabolism is the common process by which cells obtain and consume the energy needed to stay alive, to grow and to reproduce. Adenosine triphosphate (ATP) is a universal energy carrier. Glucose is the preferred source of energy in all organisms. For the breakdown of glucose and the synthesis of ATP, there are two major metabolic processes, either anaerobic or aerobic, being anaerobic glycolysis and oxidative phosphorylation.

Glycolysis, which occurs exclusively in the cytosol, a molecule of glucose is converted into 2 molecules of pyruvate, a process that requires 2 molecules of ATP to get started. The released energy after this step are 4 molecules of ATP, thus a net release of 2 molecules of ATP and electrons, which are trapped in the reduction of 2 molecules of NAD+ to NADH. In the absence of oxygen, pyruvate is subsequently reduced to lactate which is excreted to the bloodstream. However, in the presence of oxygen, a more complex energy-yielding process, called oxidative phosphorylation, takes place. After glycolysis, a carbon is removed from pyruvate as CO_2, resulting in 2 remaining original carbons, attached to Coenzyme-A and the production of a molecule of NADH. The complex that is formed is called Acetyl Co-A.

These molecules then enter into the Krebs cycle inside mitochondria and yield 1 ATP and traps high-energy electrons in 3 NADH and 1 FADH. In several previous steps, electrons have been trapped in either NADH or FADH, which are consequently used to produce ATP through chemiosmosis. Oxidative phosphorylation has a much higher energy yield than glycolysis, resulting in a total of 30 net ATP molecules, but it thus requires oxygen as an electron acceptor. ATP is one of the main substrates for phosphorylation in kinase cascades, thus influencing cell signaling. Alternative metabolic pathways involved in energy synthesis are gluconeogenesis, glycogen metabolism, fatty acid metabolism and amino acid metabolism.

B.6 Redox status

An important pathway involved in maintaining the redox status of a cell is the glutathione pathway. Reduced glutathione (GSH) has traditionally been considered as an antioxidant that protects cells against oxidative stress. So, when a loss of GSH and formation of glutathione disulfide occurs, this is considered a classical parameter of

oxidative stress that is increased in diseases. In most cells, GSH is synthesized through a two-step reaction; first, γ-glutamylcysteine is formed from cysteine and glutamate, catalyzed by the enzyme glutamate cysteine ligase (GCL)[161]. Following this reaction, glycine is added by glutathione synthase and becomes GSH. The availability of cysteine and the activity of the enzyme GCL are the two rate limiting aspects of the formation of GSH.

Glutathione exists in two forms, the thiol-reduced form, GSH and the disulfide-oxidized form (GSSG)[162]. In cells, GSH is the predominant and accounts for > 98% of total GSH[163–165]. Cells have three major storage spaces of GSH, being the cytosol, which accounts for most GSH, the mitochondria and for a very small part the endoplasmic reticulum (ER)[105–107]. The ratio between GSH and GSSG is extremely important to maintain redox homeostasis and the ratio between both metabolites is tightly controlled. The cell uses three different ways to tighten the ratios: firstly, GSSG can be reduced back to GSH by glutathione reductase (GSR) or exported out of the cell, secondly, cells control the import and export of cysteine, one of the rate limiting steps of the glutathione pathway and thirdly, cells can up-regulate an enzyme called γ-glutamyl transpeptidase (GGT), an enzyme that transfers the glutamate from GSH to an acceptor amino acid[161,169–171]. Next to its role in the redox homeostasis, GSH is also of vital importance in detoxification of xenobiotics and has roles in cell proliferation, apoptosis, immune function and fibrogenesis[172].

B.7 Biosynthesis

De novo fatty acid synthesis is the formation of fatty acids from acetyl-CoA and malonyl-CoA precursors through a series of enzymatic reactions. This process usually takes place in the liver. The enzymes of fatty acid synthesis are packed together in a complex called fatty acid synthases (FAS). FAS takes place in the cytosol from Acetyl-CoA. Acetyl-CoA, derived from pyruvate in the mitochondria, has to be transported to the cytosol via a citrate shuttle. In this shuttle, acetyl-Coa is condensed with oxaloacetate by citrate synthase, to form citrate. Citrate is then transported to the cytosol and broken down into the two individual components. Oxaloacetate in the cytosol is reduced to malate by malate dehydrogenase (MDH) and malate is transported back into the mitochondria to participate in the Krebs cycle. Acetyl-CoA is turned into malonyl-CoA, at which point malonyl-CoA is destined to feed into the fatty acid chain tail. In reverse, in fatty-acid β-oxidation fatty acid molecules are broken down in the mitochondria

to generate acetyl-coA, which enters the citric acid cycle, when fatty acids are needed as energy source[173]. Acetyl-CoA is thus an essential metabolite for the dynamic balance between carbohydrate metabolism, fatty acid synthesis and fatty acid β-oxidation, feeding into the citric acid cycle, participating to the cell's energy supply, or when more biosynthesis is necessary, participating to fatty acid synthesis.

All in all, looking at three groups of metabolites, in the energy metabolism pathways, the redox pathways and the biosynthesis pathways, it becomes clear that metabolites are omnipresent in every aspect of cell biology. Cellular functions cannot be seen as separate from cellular metabolism; for the correct functioning of the cells the balance between different cellular, genetic and metabolic pathways is of utmost importance. Disturbances of the metabolites and the metabolic pathways can thus be foreseen to be necessary for the development and growth of tumors.

C. Hallmarks of cancer: metabolic reprogramming

C.1 Cancer: altered cellular metabolism

Cancer is marked by altered cellular metabolism, recently defined as an emerging hallmark, contributing to the malignant transformation, initiation, growth and maintenance of tumors[16]. The increased cell proliferation, a well-defined trademark of cancer development, due to a deregulation of the control of cell proliferation falls together with a vast amount of changes in metabolism, to keep up with the neoplastic progression[16]. The aggressive tumor growth is hypothesized to need a metabolic and genetic reorganization to meet the new demands in energy supply, cellular redox status to protect the cells from oxidized stress from the microenvironment and the increase of biosynthetic demands caused by the fast tissue growth (Figure 5)[174–176].

C.2 Alterations in metabolism: Cause and effect?

One of the major questions concerning the metabolic programming is what drives this metabolic switch in cancer cells, seeing that some of the metabolic changes seem somewhat counterintuitive at first sight. By now, numerous cancer mutations have shown to be of influence for the reprogramming of tumor metabolism, more specifically mutations in oncogenes (such as Myc Proto-Oncogene Protein (*MYC*) and RAS) and mutant tumor suppressors that regulate glucose metabolism[174,177]. Additionally, several oncogenic mutations have been discovered in metabolic enzymes, such as isocitrate

dehydrogenase 1 and 2 (*IDH1* and *IDH2*) in gliomas and acute myelogenous leukemia (*AML*)[178–180]. Cancer mutations are thus found in specific enzymatic and metabolic pathways, direct linking to the cellular metabolism, but also other oncogenic mutations affect a high amount of signaling pathways and processes for tumorigenesis, directly linked to the cellular metabolism.

In looking at both the intrinsic and extrinsic molecular mechanisms of cellular cancer metabolism, we see that support is needed to provide a basis for the increasingly dividing and altering cancer cells, being a fast and efficient ATP generation to maintain the tumor's energy level, an increased biosynthesis of the four major classes of macromolecules, carbohydrates, proteins, lipids and nucleic acids and a intensified continuation of the redox status. Some of the changes are seen as well in fast proliferating cells, however if their supply of intracellular nutrients becomes spares, these cells adapt by slowing down their proliferation or switching back to alternative metabolic pathways. There are several ways that the tumor benefits from the switch in alternative metabolic pathways; first, by making switches in metabolism the tumor cells ensure themselves by having a constant supply of nutrients required for macromolecule synthesis. Secondly, by making switches to their energy metabolism, they use an excessive amount of nutrients from their environment, so they starve their neighbors and gain place for the growth of the tumor. Thirdly, the excessive nutrient feeding from normal tissue to tumor cells can promote the generation of ROS. By acting on growth inhibiting phosphatase enzymes, this can promote the proliferation of the cancer cell and additionally enhance the mutation rate by inducing DNA damage[181].

D. Changes in energy status

D.1 Energy status and the Warburg effect

The best-characterized metabolic shift observed in tumor cells is the Warburg effect, a shift from ATP generation through oxidative phosphorylation and the Krebs cycle to glycolysis, even when enough oxygen is present (Figure 6). Tumor cells thus convert most of the glucose to lactate rather then further metabolizing the pyruvate in the mitochondria in the Krebs cycle. The advantage of ATP production through glycolysis is that it is far more rapid, although the net energy outcome is far less efficient. The tumor cells therefore need to implement an extremely high rate of glucose transport

into the cell, to meet the increased energy needs.

The question arises what are the exact reasons behind this metabolic shift, that despite its speed of ATP production is nevertheless a lot less efficient. Currently, four consequences have been hypothesized to be of importance in this shift. First, cells that rely on oxidative phosphorylation to generate their energy supply require a relative constant quantity of oxygen to be present. However, in cancer cells, the oxygen tensions are fluctuating due to the inconstant hemodynamics of distant blood vessels, so in using glycolysis cells are not dependent on oxygen and are thus able to stand these fluctuations[182].

Second, when cancer cells rely on glycolysis rather then oxidative phosphorylation, cells produce rather a lot of lactate, the end product of anaerobic glycolysis. These acid conditions favor tumor invasion and suppress a number of anticancer immune effectors[183–185].

As a third reason, tumors have the additional option to metabolize glucose through the pentose phosphate pathway (PPP), which generates a supply of nicotinamide adenine dinucleotide phosphate (NADPH) that allows the cells antioxidant defenses against both the microenvironment and chemotherapeutic agents, but NADPH can also contribute to fatty acid synthesis.[186,187]

Fourthly, cancer cells use the intermediates of the glycolytic pathway for anabolic reactions, more specifically for biosynthesis of fatty acids, cholesterol and isoprenoids. The tumor cells can derivate pyruvate towards a truncated Krebs cycle, where the acetyl-CoA is exported from the mitochondria via the citrate shuttle to become available for fatty acid synthesis[186–188].

D.2 Changes in energy & signaling pathways

Several cell-signaling pathways are known to be involved in the regulation of the metabolic shift from the Krebs cycle to anaerobic glycolysis, being PI3K, HIF, p53, MYC, AMPK and liver kinase B1 (LKB1). The PI3K pathway is one of the most frequent altered pathways in cancer. Proteins involved in this pathway are subject to a number of common oncogenic mutations, for example in *PTEN*, but also mutations in the *PI3K* complex, or by aberrant signaling from receptor tyrosine kinases (RTKs)[189]. The PI3K

pathway thus plays a dual role in the cancer metabolism, by providing growth, survival and proliferation signals to the cancer cell, but also influencing the cells metabolism, thus being crucial for the oncogenic effects of this signaling pathway[190]. AKT, downstream of PI3K, activates the hypoxia induced factor (HIF) and MYC transcription factors, stimulates the expression and membrane translocation of glucose transporters 1 and 4 (GLUT1 and GLUT4 respectively) and phosphorylates glycolytic enzymes (hexokinase and 6-Phosphofructo-2-Kinase/Fructose-2,6-Biphosphatase 3 (PFKFB3))[181,188,191–193]. AKT also activates fatty acid synthesis through the phosphorylation of ATP citrate lyase, joined by the derivation of pyruvate by HIF from the Krebs cycle[181,194]. Some of these actions can be reinforced by p53[181]. AMPK is known to oppose the effect of AKT, functioning as a metabolic checkpoint. Tumor cells need to overcome this checkpoint, in order to continue their massive proliferation; by suppressing AMPK signaling fuel signals are uncoupled from growth signals, allowing the tumor cells to divide under abnormal nutrient conditions[194–197].

E. Changes in biosynthesis and redox status

E.1 Cancer and increased biosynthesis

Metabolic changes in the cancer cell go beyond the Warburg effect and adaptations in the energy dynamics. Cancer cells have an abnormal increase in biomass, essential for their increased cell proliferation; hence have an important need for macromolecular biosynthesis. No matter how big the supply of ATP, without sufficient precursors of fatty acids, lipids, nucleotides and amino acids (AA), cells cannot proliferate. Pyruvate kinase M2 (PKM2), an isozyme that is present in limited types of normal proliferating cells, but present in high levels in cancer cells, slows down glycolysis. Even though this seems counterintuitive, this allows for carbohydrate metabolites to enter other subsidiary pathways, such as the hexosamine pathway, the UDP-glucose synthesis, glycerol synthesis and PPP. These pathways generate the required macromolecule precursors necessary for cell proliferation[198–200].

E.2 Cancer and altered redox status

PKM2 also reduces the level of NADPH, a metabolite resulting from the promotion of oxidative PPP[194]. NADPH is an essential cofactor for many enzymatic reactions in the macromolecular biosynthesis, but is also a crucial antioxidant. At moderate levels,

reactive oxygen species (ROS) induce stress-responsive genes such as hypoxia induced factor 1 alfa (HIF1A), which in turn increases pro-survival genes such as GLUT1 and VEGF[201,202]. However, when ROS levels become too high, they can among many effects create major damage to the macromolecule biosynthesis[203–206]. Here, NADPH and GSH play a major role, by controlling the increased level of ROS and repair ROS induced damage[207].

Many tumors are addicted to glutamine, the most common AA[208,209]. Glutamine is used in a large variety of reactions and thus of high importance. After glutamine has entered the cell, it is turned into glutamate by the glutaminase enzymes, which could then be turned directly into GSH, but it can also be converted to α-ketoglutarate (αKG), from which it enters the Krebs cycle. From here, a part of the glutamine-derived carbon can exit the Krebs cycle as malate and serve as a substrate for Malic enzyme 1 (MEI), which produces additional NADPH[210]. Glutamine is also a critical metabolite for lipid synthesis, in that it supplies carbon to maintain citrate production at the start of the Krebs cycle, from which it supports the production of acetyl-CoA and NADPH for fatty acid synthesis[210]. The excess carbon is efficient as it allows for faster incorporation into biomass, facilitating the increase in cell proliferation[200]. Cancer cells generally engage widely in net lipid synthesis to create phospholipids for membrane assembly and lipid-derived signaling intermediates[181].

F. The study of cancer metabolism

F.1 Metabolomics: Large scale metabolic studies

Metabolic pathways are numerous, with a high variety of metabolites present. To get a better grasp of cancer cell metabolism, one can make use of metabolomics analysis, which has the potential to prove insight into metabolic pathways in specific cells, cell types or tissues. Metabolomics is the study of the identification, quantification and characterization of the different metabolites simultaneously within a biologic system[211]. It takes into account genetic regulation, altered enzymatic activity and changes in metabolic reactions and metabolites. It therefore reflects changes in phenotype and function of the cells[212,213]. Metabolism varies extensively between populations, individuals and different tissues of the human body, but also in disease processes and medical treatment.

F.2 Metabolomics: different ways of metabolic profiling

Metabolic profiling is a systematic analytical tool used to identify different metabolites from cellular processes. There are several types of analytical tools available, such as nuclear magnetic resonance spectroscopy (NMR), mass spectrometry (MS), Capillary electrophoresis–mass spectrometry (CEMS), tracer-based studies and metabolic foot-printing[213]. While all methods have their advantages and disadvantages, the tool most commonly used to determine the composition of diverse sample types as well as changes to that composition following perturbation is MS. After the ion peaks of the different metabolites are organized by mass, retention time and peak area, which allows for the identification of the different metabolites, the spectra is compared to a standard reference library to allow for identification of the specific metabolite[214]. Usually, metabolic studies use non-targeted approaches where the analytical conditions are optimized to detect as many metabolites as possible, however, targeted metabolic analysis are also possible, which are optimized for the detection of a specific metabolite or set of metabolites[214]. When looking at metabolomics studies performed, more and more studies have picked up an interest in metabolics as a translational tool for the identification and treatment of cancer in a clinical setting[212,215,216]. Different body fluids and tissues of individuals can be "metabotyped," a phenotyping involving the comprehensive analysis of the metabolic state of biological fluids or tissues that are sampled in the clinic[217].

G. Metabolic targeting as cancer therapy

G.1 Metabolics as a way of targeted therapy?

Cancer therapy has long targeted the increased cell proliferation of tumor cells for treatment. However, with the current growing interest in cancer metabolics, the question arises whether there could be a way for new drugs to target the cancer's metabolic pathways and thus specifically target the cancer cells. Hereby one aims to turn the cancers' adaptive metabolic mechanisms against the tumor, as being superman's kryptonite. Metabolic targeting for cancer is currently investigated, in an effort to identify molecules that specifically inhibit key metabolic steps in different tumors. There are three ways the cancer's metabolism is currently targeted; by means of indirect inhibition of tumor metabolism, by means of targeting nucleotide synthesis and by targeting glycolysis and PPP. When inhibiting enzymes in metabolic pathways,

it is preferential to inhibit those that are primarily expressed in the tumor of interest. Several therapeutic targets are currently being used to indirectly inhibit the tumor, but targeting upstream regulators of metabolic pathways.[218] Generally, theses genes include *PI3K, AKT, mTOR, AMPK, HIF* and insulin growth factor receptor 1 (*IGF1R*) (see B, metabolic pathways of the cell). Targeting these pathways can be clinically beneficial, by means of metabolic inhibition. IGF1R, one of the signaling receptors upstream of AKT and PI3K, has shown potential in the treatment of many different cancers, pediatric cancers included, but nevertheless resistance is a common phenomenon[219].

G.2 Examples of metabolic drugs in cancer

Targeting the nucleotide biosynthesis is not a new phenomenon, with the first anticancer drugs aimed at inhibiting DNA synthesis, which have been used as chemotherapeutic agents in the clinic[218]. Nevertheless, as this target has proven to be rather unspecific, attention has nowadays shifted towards inhibiting pathways that supply intermediates to be used in nucleotide biosynthesis, namely the PPP, glutaminolysis, the TCA cycle and fatty acid synthesis[218]. For example, C75, a small compound specifically inhibits the increased tumor associated fatty acid synthase (FASN), thereby inhibiting FAS, which has proven to be of interest for specific tumors[220]. C75 inhibition has been tested in both human prostate and breast cancer xenografts and has led to a significant antitumor effect in these xenografts[221,222].

Glycolysis can be blocked by the inhibition of several enzymes, being hexokinase (HK), phosphofructokinase (PFK) and pyruvate kinase (PK), all of which are rate-limiting steps in glycolysis[223]. The goal is to block the enzymatic activity of these enzymes and thereby compromise the increased glycolysis in cancer. One of the available HK inhibitors, 2-deoxyglucose (2-DG), competitively inhibits HK, so that the access of glucose to the enzyme is blocked[223]. This drug and others are currently in pre-clinical studies. Due to the accumulation of 2-DG in the cell, there is a depletion of ATP production[224]. PFK, one of the other enzymes, is very sensitive to pH changes and therefore, Na+/ H+ exchanger-1 (NHE-1) inhibitors, a Na+/H+ exchanger that increases the pH in cancer cells, thereby decreasing PFK activity and thus glycolysis[225–229]. PKM2, an enzyme that is primarily expressed in cancer cells but rarely in normal proliferating cells, can be inhibited to limit the generation of ATP in cancer cells by limiting the glycolytic flux[230,231]. One of the PKM2 inhibitors, Shikonin, a active small-molecule chemical, inhibits PKM2 activation, thereby restoring mitochondrial respiration and diminishing the levels of lactate as a

glycolysis marker[232]. A variety of the above described and other drugs is currently in clinical trials, either alone as monotherapy or as addition to conventional therapy.

Summary and directions of metabolomics and cancer

- *Metabolomics, the study of all biochemical pathways in a living organism, has gained more and more attention over the last years, with several methods of analysis being available, such as NMR and MS.*
- *Metabolomic research in cancer has prevailed that most metabolic alterations fall into three groups, being changes in the energy metabolism, changes in the cellular redox status and changes in the biosynthesis.*
- *Metabolomic research in cancer has seen an increase in popularity over the last decade, a revival around 90 years after the Warburg' effect was first described.*

It is more then likely that the metabolism of Ewing sarcoma is altered in comparison to the normal cell (of origin). EWS-FLI1 regulates the IGF1R pathway, an important molecular player in the glucose metabolism, located upstream of PI3K and AKT and has been shown to be efficiently inhibited by IGF1R inhibitors in some pediatric tumors. However, a better understanding of the metabolism of Ewing sarcoma and its regulation by EWS-FLI1 will lead to an overall better understanding of the tumor mechanism and discovery of novel targets for intervention.

3. Synthetic lethality

A. The concept of synthetic lethality

Synthetic lethality occurs when two otherwise non-lethal mutations together result in an unviable cell (Figure 7A). Bridges, followed by Dobzhansky and by Sturtevant, has first described this phenomenon in studies using Drosophila melanogaster, from which the latter author named the phenomenon[233–235]. Since then, numerous researchers have build on this idea and searched for synthetic lethal genes in additional model organisms. In Saccharomyces cerevisiae the concept of synthetic lethality reached its apogee, where numerous synthetic lethal screens have been carried out in yeast in the last decade through the use of a simple plasmid dependency assay[236]. Genomic methodologies for the search of synthetic lethal interactors begin to take shape by using a variety of techniques, such as RNAi screens, allowing for combination of knockdown to be analyzed not only in model organisms, but also in human cell lines.

B. The introduction of synthetic lethality in cancer

B.1 Cancer and the development of targeted therapy

The trademark of conventional chemotherapy for cancer is the ability to kill rapidly dividing cells, thus being non-specific for its target cells. This changed with the discovery of molecular therapeutic targets for specific genomic abnormalities in cancer offering the promise of higher specificity and less side effects. Certain targeted drugs delivered on that promise, showing impressive and durable responses. Most noticeably is the example of Imatinib, a small molecule that inhibits the tyrosine kinase driver BCR-ABL in chronic myelogenous leukemia (CML) and c-KIT (KIT) and platelet derived growth factor receptor α (PDGFR-α) in gastro-intestinal stromal tumor (GIST)[237–244]. This concept was extended to some other intractable cancers, for example treating non-small-cell lung carcinoma (NSCLC) expressing mutated epidermal growth factor receptor (*EGFR*) with EGFR inhibitors, melanomas with the activating V600 B-rat fibrosarcoma (*BRAF*) mutation with a kinase inhibitor and NSCLC patients with the EML4–ALK fusion protein with an ALK inhibitor[245,246].

Additionally some impressive results have been obtained by the monoclonal antibody trastuzumab in breast cancers with HER2/ ERBB2 receptor tyrosine kinase.

targets[247]

However, often the responses to single agent drugs are relatively short lived and primary or secondary drug resistance is a commonly seen phenomenon and considered the major obstacle in targeted cancer therapy[248,249]. Even though drugs targeting an oncogene with a gain of function mutation have provided possibilities of targeted treatment, no pharmacological inhibition is possible whenever the mutation concerns a tumor suppressor gene. To overcome resistance and to specifically target cancer cells but not normal cells, the exploitation of the concept of synthetic lethality has shown to be of great potential[250–253]. This concept, originally taken from model organisms such as drosophila and yeast, is often but not necessarily based on the interaction of two genes, that both contribute to essential cell processes, however the range of synthetic lethal predictions revealed by synthetic lethality studies varies from predicted to unexpected connections[254–256].

B.2 Different paths towards synthetic lethality

Several scenarios can be the underlying cause of synthetic lethality in cancer. In the simplest scenario, parallel pathways contribute to an essential cellular process. So while alternative pathway will allow the tumor cell to adapt to the mutation, if both pathways are mutated this will lead to a double targeting of the essential pathway and thus a synthetic lethal effect. However, synthetic lethality does not necessarily occur in clearly linked pathways, but can also occur in two divergent pathways that are both required for a reaction to a cellular insult, or a pathway that is only connected to another pathway as a result of a gain-of-function oncogenic mutation[256]. For finding these kinds of more complex synthetic lethal interactors, high-throughput screening may prove to be particularly useful.

As previously stated, synthetic lethal targeting of cancer cells could be beneficial to the treatment of specific types of cancer; only the cancer cells that harbor a previous non-lethal mutation will be killed by the targeting of the second gene, while the normal cells that do not contain the mutation will not be significantly affected. Using the concept of synthetic lethality therefore increases selectivity towards the specific tumor. Synthetic lethality poses a therapeutic opportunity above other strategies in several situations; first, for targets that have proven difficult to be modulated therapeutically by other situations. For example, while often drugs attempt to disrupt gain of function

mutations, tumors are equally often driven by loss of function mutations in tumor suppressor genes[257–259]. As the re-entry of these complexes has proven difficult to restore by gene therapy, here synthetic lethality could be a possible treatment[260–262]. Secondly, not all oncogenes are targetable by pharmacological intervention, thus synthetic lethality being an option for these untreatable cancers. Thirdly, synthetic lethal therapeutic agents can be provided either alone by monotherapy, or in combination with more conventional treatments[263–265]. Finally, as the progression of the tumor is constant and exist of multiple steps, the so-called driver mutations change in the different steps of progression. Here, synthetic lethality could target a range of mutations occurring from tumorigenesis to metastatic spreading, being an option for metastatic disease, where currently not many options are possible yet[256].

C. Methods designed to find synthetic lethal interactions

C.1 Different tools to find synthetic lethality

The concept of synthetic lethality has become a more and more often used tool in the search for new targets in cancer. The search for synthetic lethality is no longer limited to model organisms. The advances in technology have made it possible to screen for synthetic lethal genes in a large scale. Most notably, the use of RNAi, by using small interfering RNA (siRNA) or by vector-encoded short hairpin RNA (shRNA) libraries, has proven a useful tool in the search for this phenomenon. Alternatively, or in combination with this approach, libraries of small molecules, enabling for genome-wide high throughput screenings of different cancer cells. Finally, two brand-new players on the horizon could hold promise to find synthetic lethal therapeutic agents, being ORF screening and the newly developed efficient knockout technique RNA-guided human genome engineering via CRISPR asssociated protein 9 (cas9)[266,267].

C.2 Array- based screenings

Synthetic lethal screens can be either array-based or performed in a pooled manner. Generally, siRNA and compound library screenings are performed in an array-based or multi-well manner, whereas shRNA screenings can be performed in a pooled fashion. When using an siRNA approach, individual siRNAs are transfected into cancer cells in a multi-well plate format. As siRNAs only transiently knock down the gene of interest, usually 3-5 days, the readout follows usually quickly after transfection. At least

two conditions are needed to determine the synthetic lethal effect, being the condition containing the primary mutation and the condition without (either naturally or experimentally inhibited). Different readouts can be performed, such as measuring cell number, cell viability or the rate of apoptosis. The synthetic lethal genes are the genes whose inhibition impairs proliferation or viability in the mutated cancer cells, whereas it does not impair the viability in the cells that do not harbor the mutation of interest. Several interesting works have used this type of screening, such as a paper by Steckel et al that discovered the synthetic lethal interaction between *KRAS* and GATA binding protein 2 (GATA2)[268]. Not every cell type efficiently takes up the siRNA following transfection, or shows effect by siRNA transfection, nor is the knockdown of expression very long-lived, being the drawbacks of this technique. Also, siRNA screens, being plate-based techniques, limit the amount of targets that can be tested.

Compound based screenings are performed in a similar manner as siRNA based screens, being that the cells with or without the mutation are plated and left to adhere for a day, after which the compounds are added. Hereafter the cells are left to incubate and readout for viability, apoptosis or cell number is performed to find drugs that have a differential effect on both conditions. Additionally, synthetic lethal chemical enhancer screens are performed, in order to find pathways whose inhibition synergizes with the pathway targeted by a cancer drug.[269] With these dropout screens, one tries to identify drugs which combination is particularly potent, so cells are plated and exposed to the presence or absence of the drug of interest, followed by the addition of a library of drugs. Cells that are exposed to a combination of drugs that has an added effect, will die, or will show a very diminished cell proliferation, whereas cells that are grown in the absence of the secondary drug will not be severely affected in their proliferation. For this it is important that the cells are exposed to a relatively low dose of drugs, for example the GI30 (dose of drug that causes 30% growth inhibition), in order to allow these combinations to be identified.

C.3 Pooled screenings

When using a synthetic lethal shRNA approach, shRNAs are inserted into a lentiviral vector, after which cells are infected with the shRNA. shRNA has the ability to deliver long-term gene silencing, depending on the type of vector and allows for infection of a wide-range of cells.[269] shRNA screens can be performed in arrayed or pooled format, of which the pooled format is nowadays the most cost-efficient and

often used. Hereby, thousands of shRNAs are introduced in cell lines, with or without the primary mutation, followed by puromycin selection and growth of the cell population. After a number of doublings, the cells are harvested, after which the DNA is harvested and the barcodes extracted and the relative abundance of the specific shRNAs can be determined by deep sequencing and compared between both conditions.

Synthetic lethal genes targeted in cells that do not harbor the primary mutation will resist to the expression of the specific shRNA, thus will continue to divide, while the cells that do harbor the primary mutation will enter growth arrest or dies upon knockdown of the gene. Most pooled shRNA approaches use a bar-coded shRNA, to facilitate identification and quantification of the different shRNAs. As RNAi techniques have well-established off target effects, it is generally recommended that only genes that have multiple independent shRNAs or siRNAs are identified as candidates in the screen.[270] Pooled shRNA approaches have as a major advantage that thousands of genes can be analyzed simultaneously, in several cell lines, to enable a better understanding of genes and pathways whose silencing is essential for cell proliferation and survival. Several interesting synthetic lethal genes have come out of pooled shRNA screenings, such as a recent paper describing the interaction between loss of *BRCA1* and *CCNE1* amplification[271].

C.4 Advantages and disadvantages of different screenings

We classify different screening techniques in those with a bottom-up or top-down approach. In the current section we discus the advantages and disadvantages of both approaches.

- Top-down approaches. This approach of screening is an RNAi based approach.
  - Advantages: allows for direct target identification and can find genes involved in different signaling pathways, thus providing a better understanding of the biology behind the involved pathway[256].
  - Disadvantages: technique is that RNAi does not automatically lead to a therapeutic solution; there might not be a compound available to block the identified synthetic lethal gene, or it might not be possible to develop one. Another disadvantage of screening by RNAi based techniques is the discovery of false negatives after a screening, caused by non-specificity of the sh/ siRNA[256].

- Bottom-up approaches. This approach of screening is performed using small compound libraries screenings.
  - Advantages: identified candidates have a "ready-to-use" compound available, thus the trajectory from candidate to the implementation of the actual drug could in theory be faster. Drugs that are available and previously tested for their safety in other diseases could be beneficial in other conditions.
  - Disadvantages: a compound does not necessarily mean that a target or pathway is identified. Therefore, it could be that the identified compound does not directly lead to a better understanding of the biology (of disease) or genetic interactions of the target pathway[256].

Universal limitations: Of course both ways of screening in vitro in cell line models have their limits, as in that drugs are also influenced by the tumor environment, which is not taken into account when screening in a cell line model. However, performing genetic screenings in vivo is technically extremely challenging to say the least, extremely time consuming and also comes with more than its fair share of limitations due to the choice of model.

D. Examples of synthetic lethality in cancer research

D.1 Different synthetic lethal targets

About 75 years after the introduction of synthetic lethality, the concept has first been suggested in its possible application in cancer targeting[250]. Nevertheless, it has only been recently that synthetic lethality in cancer made it to the clinic. A variety of pathways have been shown to be implicated in synthetic lethality, such as DNA repair mechanisms, *KRAS* (*RAS*) mutations, loss of function mutations of the tumor suppressor genes *p53*, *Rb* and von Hippel-Lindau tumor suppressor *(VHL)*, as well as disruption of interactive protein kinase networks[272–277]. Nonetheless, more and more pathways are found to be synthetic lethal in specific cancer contexts. Below, two examples of synthetic lethality pathways in cancer research, being the *BRCA1/2* and the *KRAS* pathway, are described.

D.2 Synthetic lethality in combination with BRCA1/2

Even though several examples are available, one of the most prominent examples is PARP inhibition in tumors with a dysfunctional *BRCA1/2* mutation (Figure 7B)[278–280], which has become the golden example of synthetic lethality in cancer. In normal cells, PARP inhibition does not severely affect cell viability. Breast cancer patients with two dysfunctional copies of *BRCA1/2* are sensitive too PARP inhibition, specifically killing the tumor.

Looking at the underlying mechanism, it is clearly documented that one of the most common DNA aberrations in cells are single-strand breaks (SSB)[281]. If SSBs are left unrepaired, this could lead to genomic instability and SSBs are converted to double strand breaks (DSBs) during replication. In normal cells, BRCA1/2 is recruited to sites of double stranded breaks (DSB), where it promotes homologous recombination (HR) mediated repair, which ensures genomic integrity and prevents tumorigenesis, resulting in an alive cell[272]. People with germ-line mutations in *BRCA1/2* are at increased risk of developing breast or ovarian cancer[282]. Breast cancers could portray a situation in which both *BRCA1* or *2* genes are no longer actively present, either by one of the alleles affected by a mutation and the other one lost due to loss of heterozygosity (LOH), or by a homozygous mutation in both alleles of the *BRCA 1* or *2* gene.

Base excision repair (BER) is an important pathway for the repair of SSBs and

PARP1 is a critical component of this pathway[283]. PARP1 senses and binds to DNA breaks, which triggers poly(ADP) ribosylation of numerous nuclear proteins involved in DNA repair, including PARP1 itself[284]. When PARP1 is inhibited, DSB repair is not affected, but it causes failure of the SSB repair[285]. When SSBs are not efficiently repaired, the DNA replication fork may stall and result in the formation of a DSB[286]. Therefore, PARP1 inhibition increases the amount of DSBs. If either *BRCA1* or *BRCA2* is lost on both copies, inhibition of PARP1 results in the generation of replication-associated DNA lesions, which are no longer repaired, therefore leading to cell cycle arrest and/or cell death[278,280]. This results in a selectively synthetic lethal effect in cells without functional *BRCA1/2*, with minimal toxicity for the surrounding normal cells.

This is one of the synthetic lethal examples that successfully made the transition to the clinic. An additional DNA repair synthetic lethal combination forms between *BRCA2* and RAD52 human homolog (RAD52). In a study by Feng et al., it was determined that loss of RAD52 function is synthetically lethal with *BRCA2* deficiency[287]. When RAD52 is depleted, independently of *BRCA2* deficiencies, this significantly reduces HR. Nonetheless, when RAD52 inhibition is combined with *BRCA2* deficiencies, this results in extensive chromosome aberrations, especially chromatid-type aberrations[287]. In *BRCA2* deficient cells, when RAD52 is depleted there was a 2-10 time decrease of ionizing radiation-induced RAD51 foci and the frequency of spontaneous and double-strand break-induced HR increases, while *BRCA2* normal cells were virtually not affected[287]. RAD52 has thus shown to be an alternative repair pathway of HR and can function as a synthetic lethal target in BRCA2 deficient cells.

D.3 Synthetic lethality in combination with KRAS

Another example of a synthetic lethal combination is *KRAS* and GATA2. NSCLC is one of the most frequent cancers worldwide, with the *KRAS* pathway being mutated in about half of the cases. Kumar and colleagues showed that *RAS*-pathway mutant NSCLC cells depend on the transcription factor GATA2[288]. When GATA2 was inhibited in both NSCLC cells with or without *KRAS* mutations, the cells with mutations were severely reduced in their viability, while the ones without were unaffected.[288] In a pre-clinical model of *RAS*-driven NSCLC, inhibition of GATA2 drastically reduced tumor size and development[288]. In another study performed by Barbie et al., several mutant and wild-type *KRAS* cell lines underwent RNAi silencing of kinases and phosphatases, after which inhibition of TBK1 turned out to be displaying synthetic lethality with the *KRAS* oncogene[289]. In functional characterization of *TBK1*, a non-canonical IκB kinase, the

gene was established as a mediator of NF-κB signaling downstream of *KRAS*, thus providing the rationale behind its synthetic lethal interaction[289]. Furthermore *KRAS* forms a synthetic lethal connection with inhibition of serine-threonine kinase 33 (STK33) independent of cell origin, as shown in a large-scale shRNA screen[290].

E. Synthetic lethality in Ewing sarcoma

Synthetic lethal targeting could be a possibility in Ewing sarcoma. In a search for new targets in Ewing sarcoma, Potratz et al. performed a synthetic chemical enhancer screen, to find enhancers together with IGFR1R inhibitors in two childhood sarcomas, Ewing sarcoma and rhabdomyosarcoma (RMS)[291]. IGF1R inhibition seems to be of great interest as a new therapeutic target and remarkable responses to IGF1R-blocking antibodies were seen in some patients with advanced Ewing sarcoma and RMS, however disease progression and resistance is a common phenomenon[219,292,293]. To identify those genes that modulate the antitumor efficacy in combination with an IGF1R kinase inhibitor, Potratz et al. performed a drug enhancer screen, in which they did an siRNA screen targeted against genes in the IGFR1R pathway or related protein tyrosine kinases[291]. When macrophage-stimulating 1 receptor tyrosine kinase (MST1R) is knocked down, this enhances the activity of the IGF1R inhibitor and even restores the efficacy in highly drug-resistant cell lines[291]. It was found that loss of MST1R by RNAi blocks downstream ribosomal protein S6 (RPS6) activation[291].

Garnett et al. performed a large compound screen, screening a large panel of cancer cell lines with 130 drugs that were either under clinical or preclinical investigation[294]. In this study, it was revealed that Ewing sarcoma cells harboring the *EWS-FLI1* gene translocation were markedly sensitive for PARP inhibitors. Ewing sarcomas were found to be more sensitive to PARP inhibitors than cells from other tumor types. Additionally, Ewing sarcoma cell lines inhibited by a control siRNA in comparison to an siRNA against *EWS-FLI1* were shown to have decreased cell viability. Even though the biological function behind this mechanism was not revealed, this could theoretically be a synthetic lethal effect of the *EWS-FLI1* gene in combination with PARP inhibitors.

Summary and directions for synthetic lethality

- *Synthetic lethality, the phenomenon that two mutations together cause a cell to die, whereas both individual mutations have no effect, has stepped into the limelight as therapeutic target in cancer research over the last 15 years.*
- *Synthetic lethality can be due to two genes being targeted in the same pathway, but this does not necessarily have to be the case.*
- *A variety of methods can be used to identify synthetic lethal targets, with siRNA, shRNA and compound screens being most often used.*
- *Many examples of synthetic lethality have popped up over the last 10 years, with some that made the transition to the clinic successfully, such as BRCA1/2-PARP.*
- *A synthetic lethal chemical enhancer screen has provided a new target, MST1R that can be targeted to enhance the effect of IGF1R in Ewing sarcoma*

Synthetic lethality could be way to target Ewing sarcoma, with EWS-FLI1 as its primary event. In this thesis, searching for synthetic lethal genes in Ewing sarcoma will be one of the major topics.

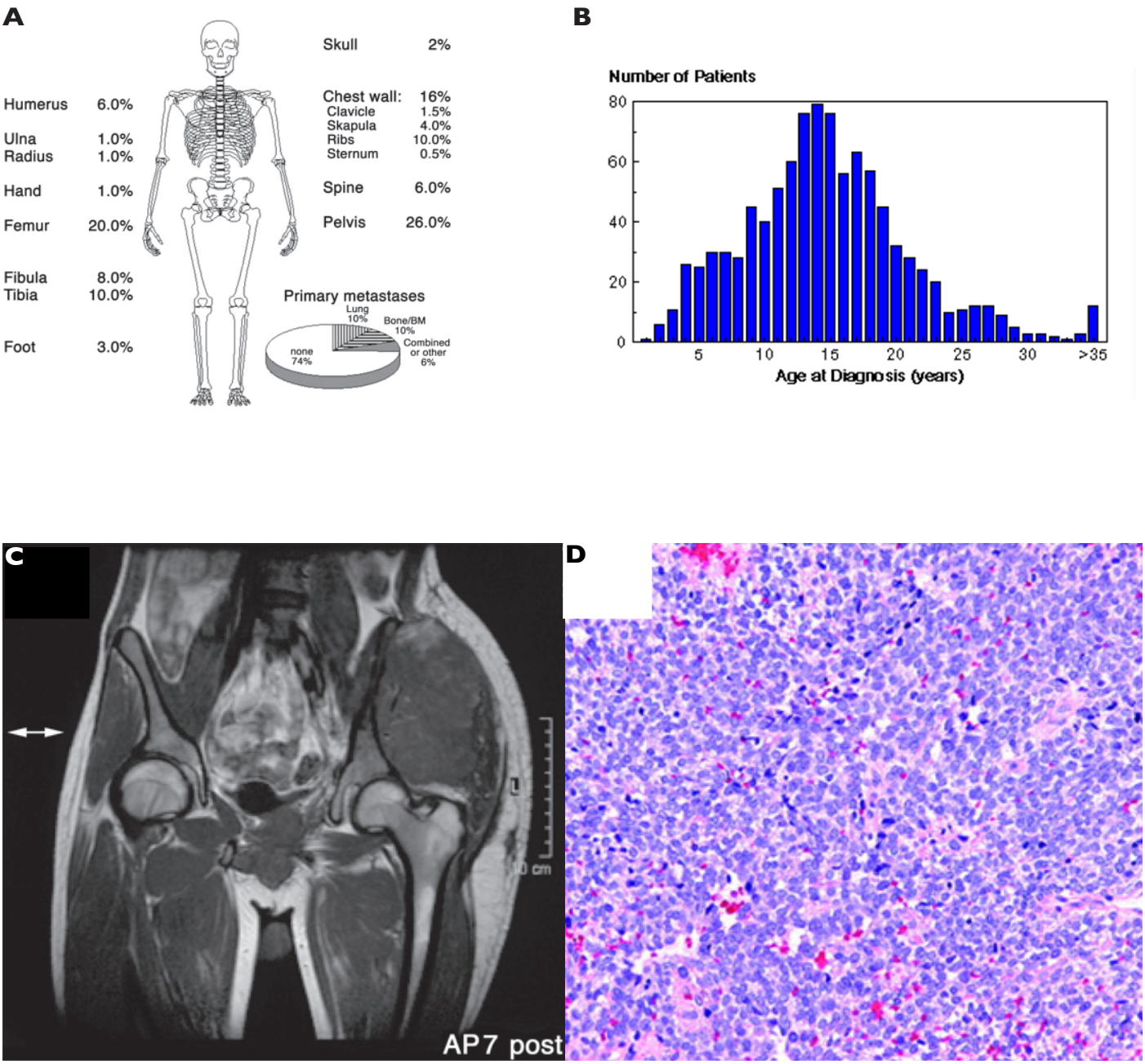

Figure 1. Clinical characteristics of Ewing' sarcoma. A) Location of Ewing' sarcoma. B) Age distribution at diagnosis of Ewing' sarcoma patients. C) Magnetic resonance image of a pelvic Ewing' sarcoma. D) Histological image of Ewing' sarcoma (HE staining). (Image adapted from Bernstein et al, The Oncologist, 2006 and http://www.cancerindex.org/ccw/faq/ewings.htm)

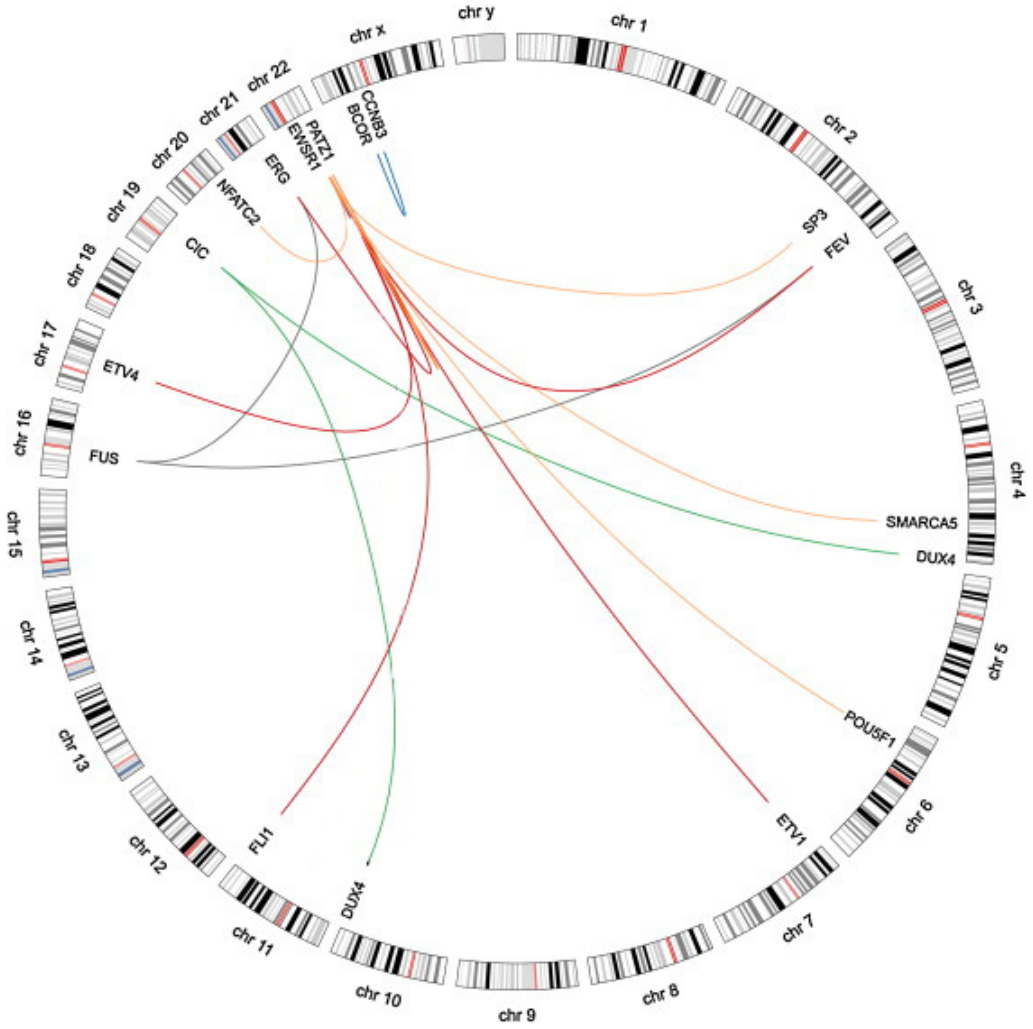

Figure 2. Fusion genes in Ewing' sarcoma and Ewing-like tumors. All currently described gene fusions in Ewing' sarcoma and Ewing-like tumors. (Figure adapted from Marino-Enriquez et al, Int J Biochem Cell Biol., 2014)

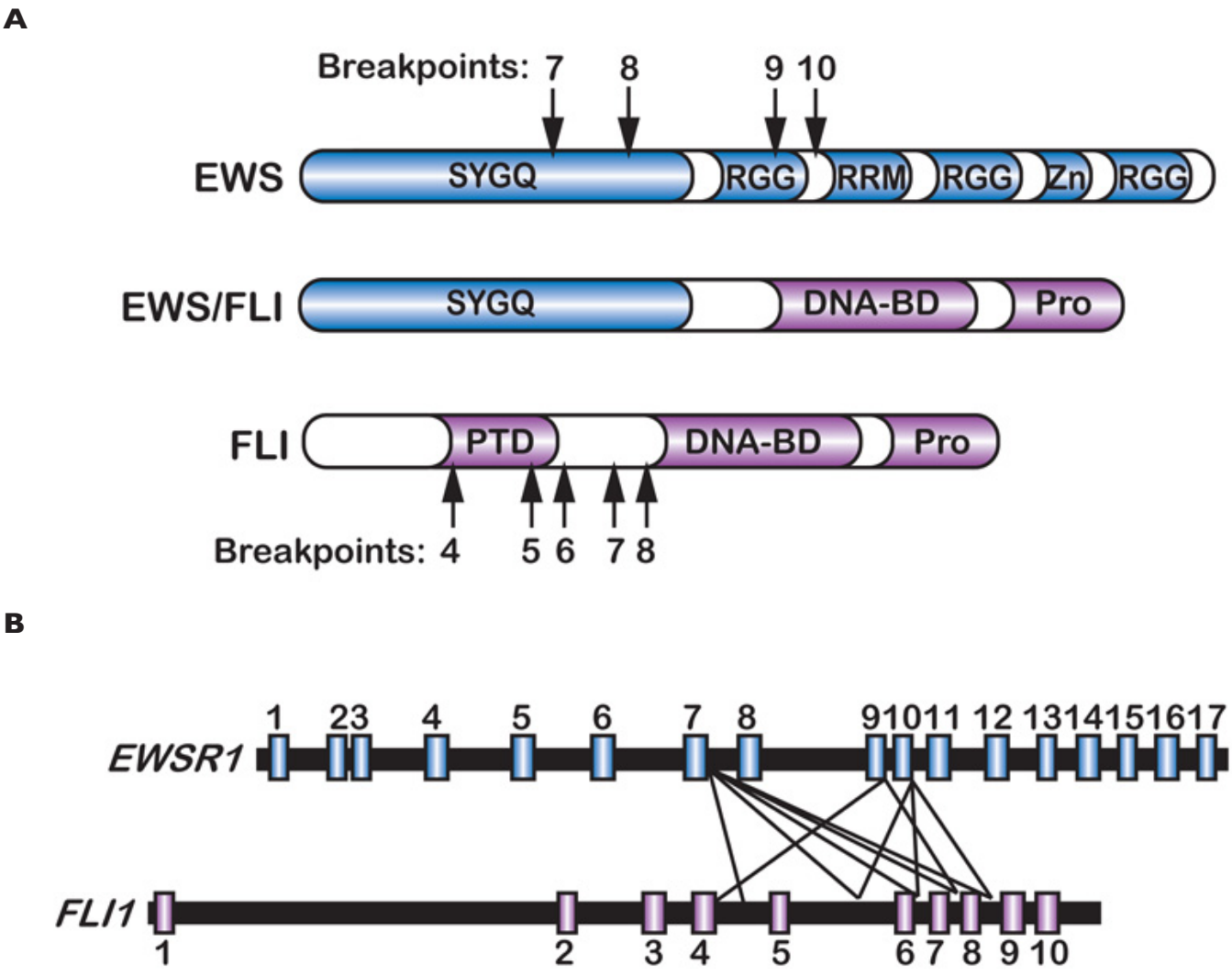

Figure 3. The *EWS-FLI1* gene fusion. A)The genomic domains of *EWSR1*, *FLI1*, and *EWS-FLI1* genes. The domains are serine-tyrosine-glycine-glutamine rich transactivation region (SYGQ), arginine-glycine-glycine rich regions (RGG), RNA-recognition motif (RRM), putative zinc finger (Zn), pointed domain (PTD), DNA binding domain (DNA-BD), proline-rich activation domain (Pro). Arrows indicate breakpoint, that lead to several fusion genes. B) Several fusion subtypes have been described, most commonly a translocation between exons 7 of *EWSR1* and exons 6 of *FLI1*. (Figure adapted from Sankar et al, Cancer Genet. 2011)

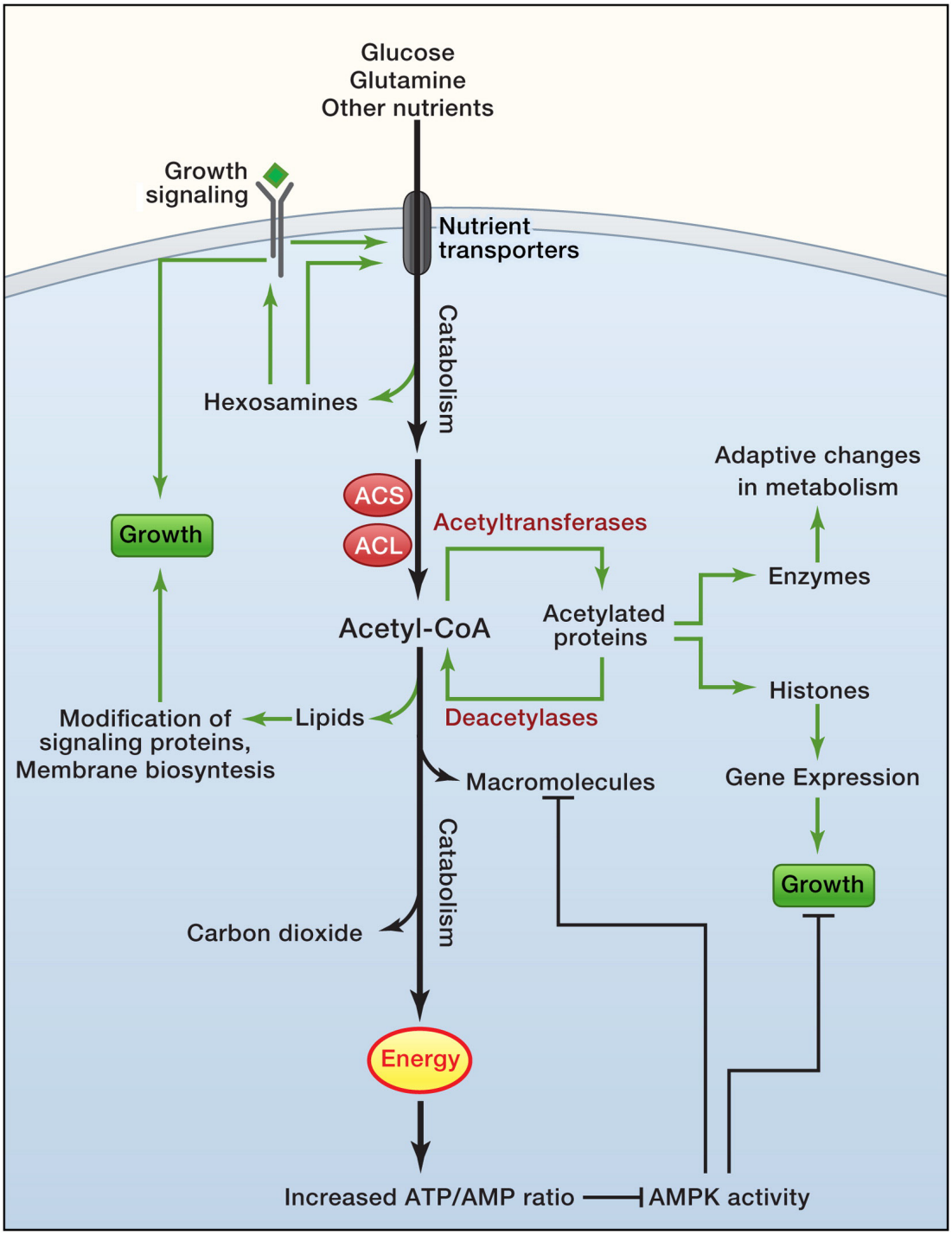

Figure 4. Cell growth and survival and the role of metabolism. Cell growth and proliferation are controlled by extracellular ligands, which bind to cell surface receptors and initiate signal transduction cascades, which eventually stimulating numerous cellular activities to enable growth and replicative division. Proper control of metabolism is essential for these effects. If a growth factor signal is given, the surface expression of glucose transporters and other nutrients is increased, which provide energy and metabolic precursors to produce macromolecules. If enough nutrients are present, other pathways stemming from core metabolism are induced to transmit growth signals. Acetyl-CoA generated by acetyl-CoA synthetases (ACS) and ATP-citrate lyase (ACL) provides substrate for the synthesis of lipids and other macromolecules, and for acetylation reactions to regulate gene expression and enzyme function. In order to allow the favorable energy state during cell proliferation, cells suppress AMPK, thereby allowing cells to take part in energy-consuming pathways and to progress through the cell cycle. Figure adapted from DeBerardinis and Thompson, Cell, 2012.

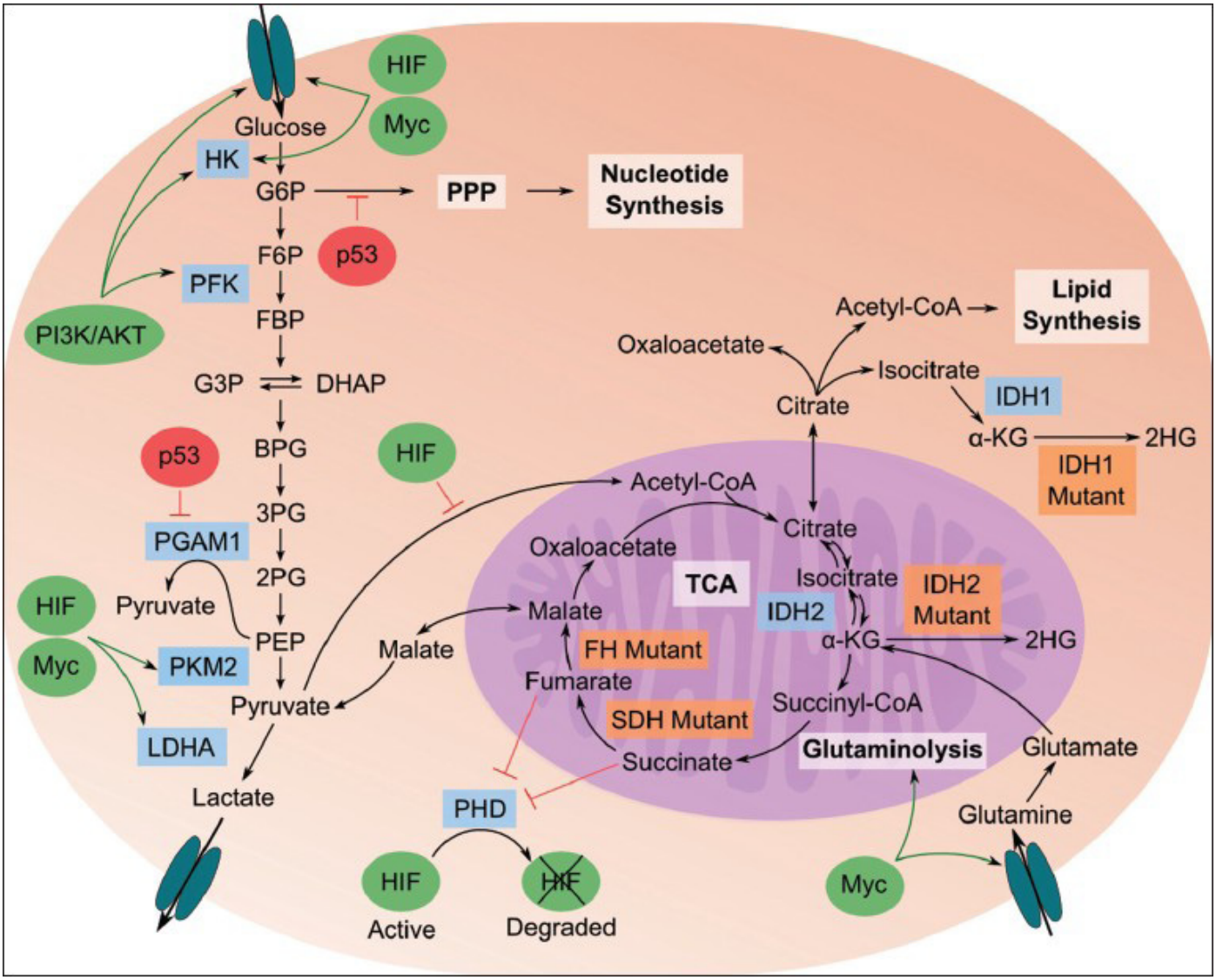

Figure 5: Tumor metabolism: Relationships between metabolites and genes in cancer cells. Glycolysis breaks down glucose into pyruvate, which is then turned to lactate, as flux through TCA cycle is down regulated in cancer cells. Pathways branching off of glycolysis, such as the pentose phosphate pathway, generate biochemical building blocks to sustain the high proliferative rate of cancer cells. Blue boxes are enzymes important in the metabolic transformation to support the cancerous phenotype; orange boxes are enzymes that are mutated in cancer cells. Green ovals are oncogenes that are up-regulated in cancer; red ovals are tumor suppressors that are down-regulated in cancer. Figure adapted from Vermeersch et al, Carcinog, 2013,

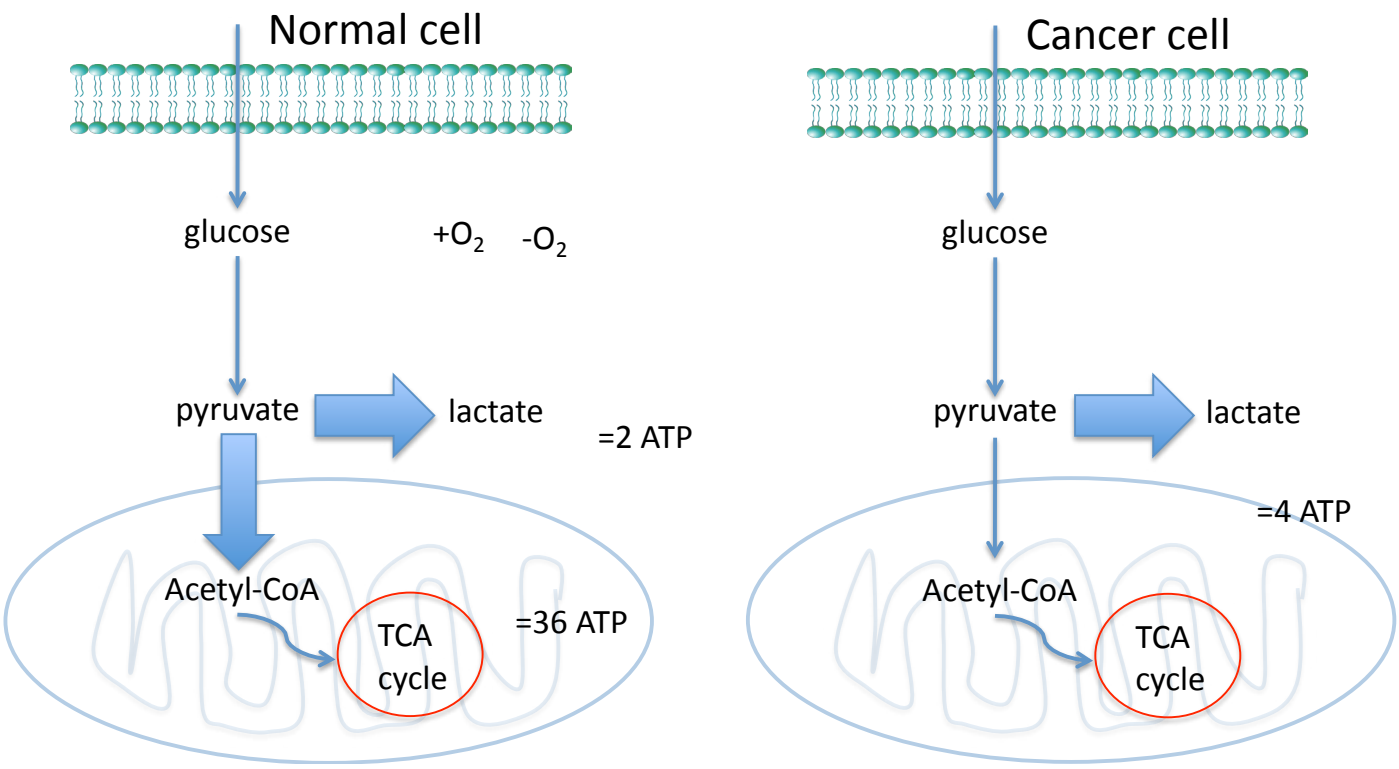

Figure 6. The Warburg effect. In normal cells, glucose is turned into pyruvate. When enough oxygen is present, the emphasis is on oxydative phosphorylation, and pyruvate enters the TCA cycle, generating 36 molecules of ATP. Under restrictive oxygen conditions, anaerobic glycosylation continues, and pyruvate is turned into lactate, generating 2 molecules of ATP. In tumor cells, the emphasis is on anaerobic glycolysation, despite the presence of oxygen, a phenomenon called the Warburg effect.

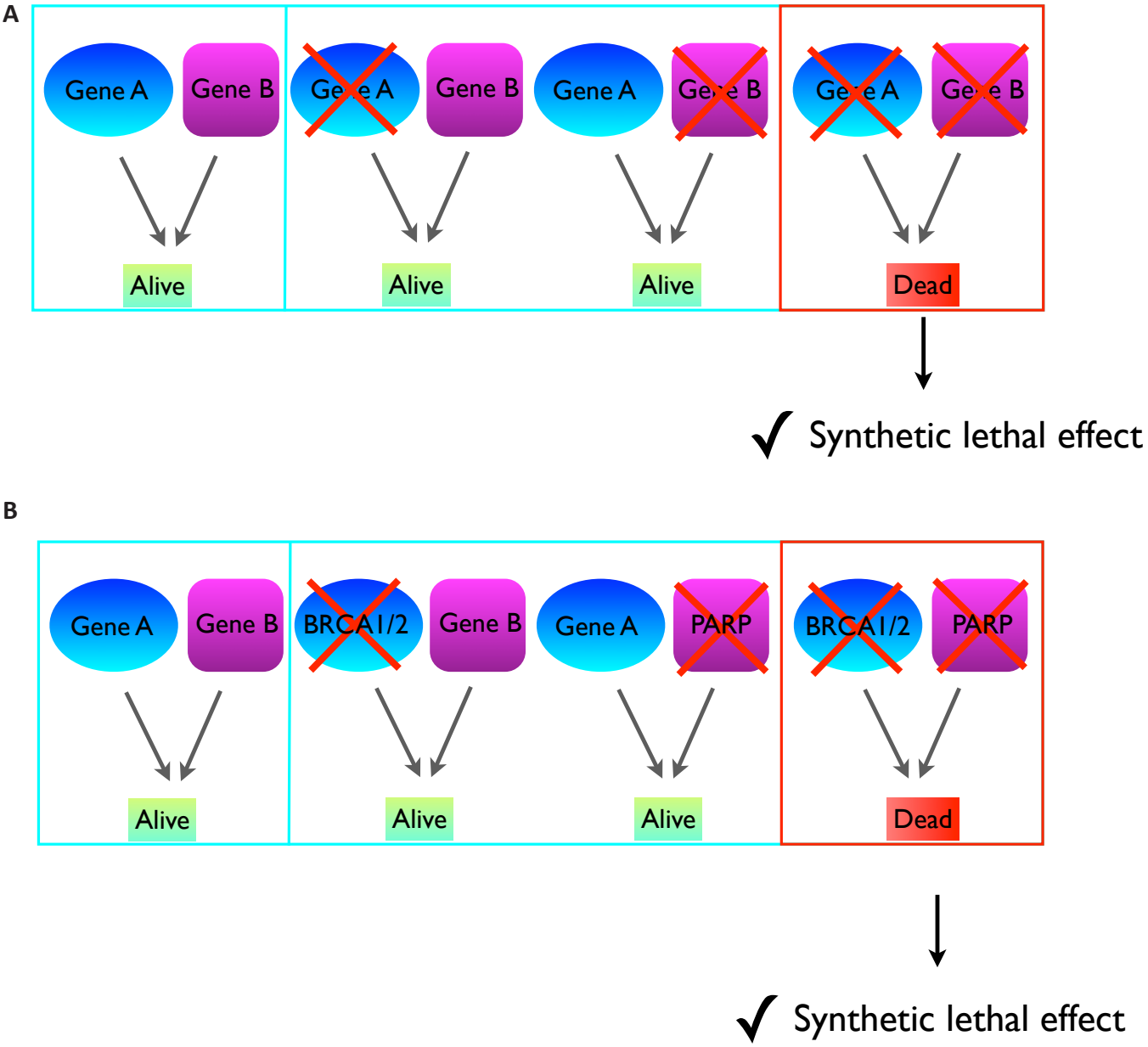

Figure 7. Synthetic lethality. A) The general principle of synthetic lethality. Mutations A or B alone do not affect cell survival, while both mutations at the same time lead to cell death. B) An example of a synthetic lethal interaction. In normal cells, *BRCA1/2* is recruited to sites of double stranded breaks (DSB), where it promotes HR mediated repair, resulting in an alive cell. PARP inhibition blocks the repair of single-strand breaks (SSBs), which if left unrepaired are converted to DSBs during replication. In breast cancer cells, patients often carry *BRCA1/2* mutations, and have lost the wild-type copy of *BRCA* due to loss of heterozygosity (LOH), which results in a viable cell. In normal cells, PARP inhibition does not severely affect cell viability. However, breast cancer cells, when inhibited for PARP, DSBs cannot be efficiently repaired, leading to cancer cell death and elimination of the tumor.

Results

I. The metabolic profiling of EWS-FLI1 in Ewing sarcoma

A. ***Abstract***

Ewing sarcoma, the second most commonly occurring pediatric bone tumor, is primarily characterized by a chromosomal translocation leading to the expression of a fusion protein involving the EWS RNA binding protein (*EWSR1*) and an ETS transcription factor (*FLI1*). EWS-FLI1 has previously been implicated in abnormal proliferation, invasion and tumorigenesis. As it is known that the cancer cell metabolism differs from normal cells, the question arises how EWS-FLI1 influences the Ewing sarcoma metabolism. To assess the effects of this oncogene in the Ewing sarcoma cell metabolism, we used a metabolomic approach in Ewing sarcoma cells in the presence or absence of EWS-FLI1. Several changes in the energy metabolism were observed throughout this study. Consistent changes recapitulating partially the Warburg effect were observed. Furthermore, levels of TCA intermediates, glycosylation precursors, fatty acid synthesis metabolites, glutathione metabolites and amino acids, especially changes in the tryptophan metabolic pathway, were altered upon EWS-FLI1 inhibition. The results in these different metabolic pathways were combined with expression data on the enzymes in these pathways, investigating the interplay between metabolics and genetics in Ewing sarcoma. The results indicate that EWS-FLI1 plays metabolic roles in the biosynthesis, redox signaling and energy metabolism, through a large variety of enzymes. These metabolic and enzymatic changes provide clues to the oncogenic transformation of Ewing sarcoma associated with an *EWS-FLI1* gene fusion.

B. Context

Ewing sarcoma, the second most commonly occurring pediatric bone tumor, is most commonly characterized by the presence of the fusion gene *EWS-FLI1*[7]. This fusion gene leads to the expression of an aberrant transcription factor. EWS-FLI1 has previously been implicated in abnormal proliferation, invasion and tumorigenesis[295,296]. *EWS-FLI1* is the major oncogene of Ewing sarcoma and act as a transcriptional activator/ repressor and modulates directly and indirectly its target genes[143,146]. Previously published proteomics and genomics data have clearly started to unravel the influence of EWS-FLI1 on transcriptomic cascades that may constitute the cancer pathogenesis of Ewing sarcoma.

Cancer, besides being a genetic disease, has been shown to have many differences in its' cellular metabolism in comparison to the metabolism of normal cells. The most well-known alteration is the Warburg effect, the idea that tumors rely rather on anaerobic glycolysis, even in the abundance of oxygen[149]. Some of the cancers' genetic modifications have found to promote this hallmark of cancer cells, metabolic reprogramming, such as up regulation of the expression of GLUT1, G6PD, TKTL1 enzymes in the glycolytic pathway or up regulation of expression of ACLY or FAS in fatty acid synthesis.[208,297,298] The oncogenic signaling and metabolic reprogramming are connected at several levels through a series of enzymatic reactions, however to expand this knowledge and connect these networks is not always intuitive.

Regarding Ewing sarcoma, a few observations could already link EWS-FLI1 with some metabolic aspects. First of all, EWS-FLI1 modulates the expression of a number of target genes, known to be implicated in the cancer cell metabolism, such as c-MYC.[299] c-MYC is a central regulator of not only cell proliferation, but also cancer cell metabolism, by influencing glycolytic activity by up regulating expression of glycolytic enzymes such as GLUT1, GLUT4, HK2, PFKM and ENO1.[300–304] c-MYC also plays a role to increase mitochondrial function, increasing the synthesis of Acetyl-CoA, thereby stimulating the (fatty acid) biosynthesis in the cancer cell[305,306]. Furthermore c-MYC appears to have a strong role in the glutamine regulation[307].

Interestingly, EWS-FLI1 has been shown to directly influence insulin-like growth factors receptor (IGF1R)[12,308]. Insulin and insulin-like growth factors (IGFs) are known as key regulators of energy metabolism and growth, particularly IGF1R, that influences

among others glucose uptake and cell growth. AKT and MAPK, two downstream members of the IGF1R pathway are important players in cell growth, influencing the tumor cell metabolism.

Additionally, glutathione S-transferase M4 (GSTM4), an EWS-FLI1 target, has been shown to be involved in Ewing sarcoma oncogenesis and therapeutic resistance[137]. Patients expressing low GSTM4 levels were better responders to chemotherapy and had better overall survival than patients having high levels.

These data suggest that EWS-FLI1 has an oncogenic component in regulating cellular metabolism, either directly or through downstream modulators. There is thus a major interest in getting a better understanding of the metabolic impact of EWS-FLI1. In order to thoroughly investigate the metabolism of Ewing sarcoma, we investigated the effects of EWS-FLI1 knockdown on the cellular metabolism using Ewing sarcoma cell lines and a comprehensive metabolomics platform. In this study, we identified a number of EWS-FLI1 dependent metabolic cascades that may contribute to Ewing sarcoma pathogenesis.

C. Material and methods

Cell lines and reagents

Ewing sarcoma cell lines, A673 and SK-N-MC, were grown in DMEM and RPMI 1640 respectively (PAA laboratories, GE Healthcare, Vélizy-Villacoublay, France), containing 10 % fetal bovine serum (FBS) (Eurobio, Courtaboeuf, France) and 1% P/S. The doxycycline inducible cell line A673-1C, previously generated in the lab by Tirode et al., was grown in DMEM containing 10% FBS, 1% FBS, Blasticidine (20 mg/ml) (Life technologies, Saint Aubin, France) and Zeocin (Life technologies, Saint Aubin, France) (200 mg/ml) (supplementary Figure 1)[18]. All cell lines contain a fusion transcript type 1 and were routinely checked for the translocation product. Cells were also checked for mycoplasma contamination. For the doxycycline-inducible silencing of the 1C cell line, doxycycline at a concentration of 1 µg/ml, exhibits strong inhibition of the *EWS-FLI1* fusion transcript. For siRNA mediated silencing of *EWS-FLI1*, cells were transfected in OptiMEM (Gibco, Life technologies, Saint Aubin, France) using RNAimax Lipofectamine (Life Technologies, Saint Aubin, France) twice with 15nM siRNA, with either an siRNA control or an siRNA against the fusion gene *EWS-FLI1* (Qiagen, Courtaboeuf, France).

Isolation of RNAs

Total RNAs were isolated using the NucleoSpin II RNA Reagent (Macherey Nagel, Hoerdt, France). RNAs from 1C were isolated 0,12, 24, 35, 48, 72, 168h after silencing with doxycycline. RNAs were isolated 4 days following transfection of A673 and SKNMC Ewing sarcoma cells with the specific *EWS-FLI1* siRNA (siEF1) or with the control siRNA (siCT).

Reverse transcription Quantitative PCR (RT-qPCR)

cDNAs were synthesized from 500 ng of RNA using the High-Capacity cDNA Reverse Transcription Kit (Applied Biosystems, Saint Aubi, France) RT kit. cDNA reverse transcription reactions were performed in 20 µl. cDNAs were diluted 1/10 and 9 µl of the diluted RT product was used for the qPCR. Gene expression was analyzed using SYBR PCR Master mix with an AB7500 Real-time PCR system (Applied Biosystems, Saint Aubi, France). Results were normalized to *GAPDH* and quantified by the ddCt-method. Primers are listed in Supplementary table 3.

Metabolomic Analysis.

For the metabolic analysis, cells were grown with or without doxycycline for the 1C clone. 1C cells were plated at day -7, after which cells were treated with doxycycline, at 168, 72, 48, 36, 24 and 12 hours before harvest. These time points were chosen to profile early, middle and late effects of *EWS-FLI1* inhibition. Cells were passed once, at 3 days before harvesting. For A673 and SKNMC, cells were transfected (d0) with an siRNA targeting *EWS-FLI1* or with a control siRNA and re-transfected in the same conditions at day 2. Cells were harvested at day 4 after the plating. For each condition, 5 biological replicates were performed. To harvest cells, medium was removed, monolayers were washed with PBS and Trypsin (PAA laboratories, GE Healthcare, Vélizy-Villacoublay, France) was added. Cells were incubated for 5 min at 37 °C until cells detached. Six volumes of medium were added to the Trypsin/ cell mix and suspended by gentle pipetting and titration. Cells were counted, 3.3 % of cells were used for RNA isolation, 6,6% of cells were used for protein lysate and the remaining cells per sample were spun down at 600 × g for 3 min in a polystyrene tube. Cells were washed once with PBS and then snap-frozen on liquid nitrogen and stored at −80 °C until analysis. Metabolomic profiling analysis of all samples was carried out in collaboration with Metabolon (Durham, NC, USA) as previously described, using liquid chromatography–mass spectrometry (LC-MS) and gas-chromatography mass spectrometry (GC-MS)[215,309–312]. The Metabolon library contains 14000 named and unnamed compounds[313]. In theory,

around metabolites 4000 could be identified currently, however, in most studies between 100-600 known metabolites are detected[314–317].

Statistical analysis

After identification and quantification of metabolites in the different conditions and replicates, quantification values were normalized to protein concentration from a Bradford assay. Metabolites were mapped to KEGG pathways[157]. Due to the limits of the level of detection, a number of metabolites (35 out of the total of 433 metabolites) were not detected in all samples of an experiment. Chemicals that were detected in less then 50% of samples of an experiment were not analyzed any further. If in the group of samples composed as one condition, being the total of 5 replicates for that group, metabolites were detected, but not in all samples, they were given the lowest value of detection for the missing values. For univariate statistics, a Welch's t test was performed to determine whether the average level of a given metabolite in one experimental condition was different from the average level of another condition. For each condition, a q value was determined, estimating the likelihood that a statistically significant comparison is a false discovery[318]. Multivariate statistics was performed in R, version 2.12.2[319]. In order to investigate whether the up regulation of metabolites in a certain class was specific, a Fisher test was performed. The input for the Fisher test was the number of significant up-regulated versus the number of unaltered metabolites in the specific pathway divided by the total number of significantly up-regulated metabolites versus the total number of unaltered metabolites outside of the pathway.

Transcriptomic Analysis.

Unpublished microarray data generated in the lab with siCT and siEF1 from A673 and SKNMC cells (generated by Thomas Grunewald) was received and analyzed for the alterations of enzymes upon inhibition of *EWS-FLI1*. The GeneChip microarray data in Thomas Grunewald's experiment were performed according to the Affymetrix GeneChip Expression Analysis Technical Manual (Affymetrix, Santa Clara, CA) using HGG- U133 plus arrays. Cells Data was extracted and plotted using the GraphPad Prism software.

D. Results

EWS-FLI1 impact on cellular metabolism of Ewing sarcoma cell lines.

To test whether EWS-FLI1 influences the cellular metabolism of Ewing sarcoma cells, we performed a time-series experiment to silence the fusion protein EWS-FLI1 in the 1C cell line by adding doxycycline (supplementary Figure 2). Lysates prepared from cells at similar growth phases were analyzed using two types of mass spectrometry, LC-MS/ MS and GC-MS. This analysis of the time series of 1C with different times of EWS-FLI1 inhibition revealed that a total of 253 named metabolites were altered upon inhibition (Supplementary table 1A). After normalization to protein concentration, the level of each metabolite was compared to the level at the starting point. To visualize the changes in metabolites between the different time points, we generated a heat map, showing a shift of metabolites between early and late time points (Figure 1A). Overall, upon inhibition of EWS-FLI1, more and more metabolites became significantly altered, thus changes in metabolites became more profound at later time points, particularly at 72 and 168 hours (Supplementary Figure 3). 1C dox cells with 72 hours of doxycycline treatment revealed 34 metabolites to be significantly up-regulated upon EWS-FLII inhibition and 36 significantly down-regulated. The following time point, 168 hours showed 89 metabolites that were significantly up-regulated upon EWS-FLI1 inhibition versus 60 down-regulated metabolites. The figure shows the remaining level of *EWS-FLI1* expression at the different time-points (Figure 1B).

To continue on these findings, we profiled 2 additional cell lines, A673 and SKNMC, in which we inhibited *EWS-FLI1* with an siRNA or a control siRNA (Figure 1C). Cells were prepared as for 1C and analysis revealed a total of 433 named metabolites (supplementary table 1B). Clustering showed a significant change in both cell lines upon inhibition of EWS-FLI1 (Figure 1D). In order to compare metabolites that were commonly up or down-regulated in Ewing sarcoma, 218 common metabolites in 1C, A673 and SKNMC were compared (1C vs 1C dox 168 hours, SKNMC siCT vs SKNMC siEF1, A673 siCT vs A673 siEF1) (Figure 1E, 1F). Both the overlap of the up-regulated as well as the down-regulated metabolites was proven to be significant (p-value of 0.0017 or $3.5x\ 10^{-7}$ respectively). A full list of the metabolites that were included for the analysis is provided in annex I and II.

We next used information from the above analyses of cell lysates to identify metabolic pathways affected by EWS-FLI1 expression. We selected KEGG sub pathways

that had significant and reproducible alteration in all cell lines, in several of the metabolites of the pathway. This analysis revealed that upon inhibition of EWS-FLI1, there were major changes in 1) glucose levels, 2) cysteine derivatives gamma-glutamylglutamate and Cysteine-glutathione-disulfide, 3) N- glycosylation precursors GDP-Fucose and N-acetylneuraminate 4) several fatty acid levels and 5) kynurenine levels. We then mapped these data to simplified versions of the pathway in which these metabolites play a role (Figure 2-6). In the next paragraphs, more detail will be given concerning these 5 altered pathways.

1. Kynurenine was identified as one of most up-regulated metabolites in the absence of EWS-FLI1 across all experiments.

Being one of the key elements of the tryptophan pathway, kynurenine, was significantly up-regulated in the absence of EWS-FLI1 protein expression (Figure 2A, 2B). Kynurenine is a metabolite of the amino acid L-tryptophan pathway, which by itself was not significantly altered by EWS-FLI1 expression (Figure 2C). Tryptophan is an essential amino acid that has previously been identified as a regulator in the immune response, as well as being involved in a number of cancers[320–322]. Kynurenine itself is degraded to three different metabolites, being kynurenate (unaltered by EWS-FLI1 expression), acetyl-CoA and nicotinamide adenine dinucleotide (NAD+) (Figure 2D), which were both up-regulated by EWS-FLI1 inhibition. The absence of tryptophan modulation, with the presence of modulation of kynurenine, implicated that EWS-FLI1 influences enzymes in the Tryptophan pathway. Tryptophan is typically metabolized to kynurenine by the enzyme tryptophan 2,3-dioxygenase (TDO2) but can also be degraded by the highly inducible enzyme indoleamine 2,3-dioxygenase (IDO1, IDO2), which is stimulated by pro-inflammatory cytokines such as interferon-γ and tumor necrosis factor-α[323–325]. To verify the implication of IDO and TDO2 in the observed modulation of kynurenine, we investigated the modulation of *IDO1*, *IDO2* and *TDO2*. Of these three, *IDO1* was not expressed (data not shown), whereas *IDO2* and *TDO2* were up-regulated upon inhibition of EWS-FLI1 (Figure 2E, F).

II. EWS-FLI1 influences the energy metabolism of Ewing sarcoma cells.

Changes in energy metabolism, were observed in all cell lines (Figure 3A). Changes in glucose levels, key molecule of the energy metabolism, were imminent upon inhibition of EWS-FLI1 (Figure 3B). A consistent up-regulation of glucose metabolism was seen in all cell lines. Derivatives of glucose, such as glucose-6-P and fructose 6-P (Figure 3C) were also elevated. In addition, various metabolites related to glucose

metabolism including glycolytic and pentose phosphate pathway (PPP) intermediates and cofactors such as NAD+ (Figure 2D). The pentose phosphate pathway is an alternative to glycolysis. Higher levels of additional disaccharides/trisaccharides were also observed. Finally, markers of the TCA cycle such as citrate (Figure 3D) and succinate were also elevated, showing a higher entrance of metabolites in the TCA cycle. Resulting from this, a minor increase of ATP was observed (Annex 1).

When investigating enzymatic levels that correlate with the changes of the level of glucose, we see that three classes of enzymes could be of interest, being glucose transporters, enzymes in the glycolysis pathway and enzymes coupling the PPP to the glycolysis pathways. Firstly, looking at glucose transporter, the class one transporters *GLUT1* was down-regulated upon EWS-FLI1 inhibition (Figure 3E). *GLUT6*, a gene that codes for the GLUT6 protein, a poorly described glucose transporter, has a motif that helps to retain the receptor intracellular, thereby preventing glucose transport[326–328]. *GLUT6* was up-regulated upon EWS-FLI1 inhibition (Figure 3F). Also, *ALDO* RNA expression, the connecting enzyme between the PPP and the glycolysis pathway, was down-regulated upon EWS-FLI1 inhibition (Figure 3G).

III. EWS-FLI1 influences protein N-Glycosylation.

Glucose provides key precursors for protein glycosylation (Figure 4A). In this study, elevated levels for several glycosylation precursors were apparent, including N-acetylneuraminate (Figure 4B), GDP-fucose (Figure 4C) and UDP-glucuronate (Figure 4D). UDP-galactose and UDP-glucose showed more subtle changes (Supplementary data 1).

Altered levels for these glycosylation precursors suggests that one element of the treatment response was to alter protein glycosylation a process important for proper protein folding as well as for function. Protein glycosylation is tightly regulated and altered by a large number of enzymes, of which at least 16 enzymes involved in the process have been identified so far[329]. The enzymes that modify N-glycosylation reside in the ER and are constituted of phosphoglucomutases, glucosidases, UDP-glucose:glycoprotein glucosyltransferases and mannosidases[330]. Altered enzyme expression upon EWS-FLI1 inhibition was investigated and both mannosidases such as *MAN* (Figure 4E), the glucosyltransferase *GALT* (Figure 4F) and the phosphoglucomutase *PGM* (Figure 4G) were altered.

IV. EWS-FLI1 influences the level of free fatty acids.

Cancer cells typically do not use fatty acids for energy production but instead conserve them for their increased biosynthesis and increased membrane production necessary for the increased cell growth. One of the most consistent changes in the dataset included accumulation of numerous medium-chain, long-chain, monounsaturated and polyunsaturated fatty acids with EWS-FLI1 inhibition, a metabolic signature overwhelmingly present with EWS-FLI1 silencing (Figure 5A). Fourteen out of twenty-five commonly altered metabolites were up-regulated fatty acids (Supplementary data 1). This overrepresentation of fatty acids was significant in all cell lines (Supplementary table 2). Examples of free fatty acids resulting from membrane and complex lipids are choline phosphate (Figure 5B), docosahexaenoate (Figure 5C) and eicosapentaenoate (Figure 5D). An increase in fatty acid levels can be caused by three groups of enzymes. First of all, glucose directs metabolites in the direction of fatty acid synthesis at the level of citrate, a reaction that requires the expression of enzyme *FASN* (Figure 5E), which is slightly decreased. Additionally, the levels of transcription of fatty acid synthesis enzymes could also be increased. The regulator that causes this is *SREBF1*, which is also reduced (Figure 5F)[331]. Fatty acid levels might also be increased by an increased rate of degradation, meaning more complex lipids or membrane lipids are transported and converted to simpler fatty acids by CPT1, which was the most apparent option from the metabolics data. EWS-FLI1 appears to have a strong influence on *CPT1* levels, significantly up regulating the enzyme CPT1 when EWS-FLI1 was inhibited (Figure 5G). This indicated that the up-regulation of simple fatty acids is most likely indeed due to a degradation of more complex lipids.

V. EW-FLI1 and its role in Glutathione metabolism.

The powerful regulator in cellular redox status, glutathione, plays an important role in the response to reactive oxygen species and oxidative stress in cancer. In our study, silencing of EWS-FLI1 expression in cells appears to influence glutathione metabolism at several levels (Figure 6A). EWS-FLI1 induces increased glutathione synthesis and greater oxidative stress as shown by elevated levels of the glutathione precursors methionine and cysteine, slightly increased reduced glutathione (GSH) and oxidized glutathione (GSSG) (Figure 6B).

Similarly, higher levels of the glutathione degradation/turnover products cysteinylglycine, along with increased γ-glutamyl amino acids (AA), such as for example gamma-glutamylglutamate (Figure 6C) were also observed when EWS-FLI1 was

inhibited. Increased glutathione production, turnover and oxidation was accompanied by higher levels of several metabolite markers of oxidative stress, including cysteine sulfinic acid, 7-beta-hydroxycholesterol and cysteine-glutathione disulfide (Figure 6D).

Many enzymes in the pathway are non-affected by EWS-FLI1. However, *CTH* expression, converting cystathionine to cysteine (Figure 6E) and *GSTM4*, deriving GSH to R-S-glutathione (Figure 6F) are up-regulated.

E. Discussion

EWS-FLI1 and energy metabolism.

The best-described metabolic aspect of cancer is changes in the energy status, most notably the Warburg effect, a term used to describe the preference for tumor to use anaerobic glycolysis even in the abundance of oxygen[149]. Here, we showed that EWS-FLI1 knockdown induces multiple changes in the cellular metabolome, particularly at the level of energy metabolism. Overall, the observed changes were consistent with an energy profile that moved from a cancer cell energy metabolism towards the energy metabolism of a more normal cell, based on the activity of the TCA cycle. Inhibition of EWS-FLI1 thus creates a strikingly partial reversion of the Warburg effect. Several molecules had a decreased level at day 7 of doxycycline treatment of 1C cells, or were increased respectively. A similar pattern was observed in A673 and SKNMC siEF1 cells in comparison to controls. Glucose, the key molecule of the energy pathway, was increased in all cell lines, indicating that less glucose is burned, also consistent with a partial reversal of the Warburg effect, due to the inhibition of the cancerous phenotype[332].

EWS-FLI1, which had previously been shown to be responsible for the oncogenic transformation of Ewing sarcoma, thus has shown to be directly linked to the rewiring of the energy metabolism of the cell, being directly implicated in the Warburg effect. *EWS-FLI1* hereby joins different oncogenes, such as *c-MYC* and *NFκB*, that have already been proven to play such a direct role in the Warburg effect[333–335]. EWS-FLI1 thus appears to acquire its target genes to the Warburg effect, as this cancer gene directly regulates metabolic enzymes and metabolites.

Although 4 to 25 fold changes of glucose levels in the different cell lines upon EWS-FLI1 were shown, the question arises why the TCA intermediates and ATP level are not increased at similar levels. A possible explanation could be the diminished cell growth after inhibition of EWS-FLI1. Indeed, 1C cells treated with doxycycline display reduced cell proliferation[18]. Due to this diminution of the increased cell proliferation observed in cancer, less glucose is needed, thus the levels of glucose are elevated. The rate of glucose utilization is coordinated with other pathways of energy generation and utilization, PPP and the TCA cycle[336]. With a diminution of the expression of glucose transporters, less glucose is imported into the cell. However, the diminution of *ALDO* levels, the connection between the PPP and glycolysis, is of lesser presence, thus less glucose is transported to the PPP. Alternatively, the increased levels of glucose can also

be explained by a (partial) “stalled” glucose metabolism and accumulation of excess metabolites. The static nature of these measurements makes directionality difficult to assess and these two possibilities will require further investigation.

Additionally, glycosylation precursors, linked to the glucose metabolism, are found to be elevated in EWS-FLI1 inhibited cells. N-linked glycosylation, part of the post-translational modifications, is indispensable for normal cellular function; it is a universal process that takes place in the endoplasmic reticulum (ER) and Golgi apparatus in all eukaryotes and is essential to survival[337]. One of the reasons behind is that this process is for some of the proteins to be folded, a sugar needs to be added to the chain[338,339]. Also, sometimes glycosylation leads to a more stable protein, as non-glycosylated proteins degrade faster[339]. Thirdly, glycosylation plays a role in cell-cell adhesion[339]. Glycosylation may play a role in Ewing sarcoma, as has previously been shown by Girnita et al[317]. N-linked glycosylation was shown to be essential for the translocation of IGF1R to the cell surface, IGF1R being a target of EWS-FLI1[308,342–344].

EWS-FLI1 and cellular redox status.

Two of the clearest changes were changes in both kynurenine and glutathione levels. Both are presumed to be interconnected and in connection with both redox status[345,346]. The up regulation of kynurenine indicates that EWS-FLI1 has a specific role in the metabolism of tryptophan, which could indicate both a paracrine and autocrine effect on the Ewing sarcoma cell[347].

Kynurenine, a derivative of tryptophan, is degraded by both IDO2 and TDO2, which in turn are stimulated by pro-inflammatory cytokines such as interferon-γ and tumor necrosis factor-α. In addition, elevations in the kynurenine metabolite 3-hydroxykynurenine *(KMO)*, which also serves as a marker of oxidative stress, were observed with EWS-FLI1 silencing. Taken together, these findings are suggestive of increased oxidative stress in Ewing sarcoma cells and an inflammatory response in upon silencing of EWS-FLI1 expression.

EWS-FLII and biosynthesis.

Some of the most noticeable changes of Ewing sarcoma cells after inhibition of EWS-FLI1 were the increased levels of free fatty acids. The elevations in free fatty acids may be reflective of increased synthesis, reduced fatty acid β-oxidation and/or

decreased incorporation into or increased release from phospholipids and other membrane and complex lipids. Alterations in synthesis and β-oxidation in Ewing sarcoma cells were not apparent from the data however, clear changes in membrane and complex lipids were observed with loss of EWS-FLI1 expression, suggesting that increases in free fatty acids may be attributable to changes in membrane turnover/ remodeling. Alterations in fatty acid metabolism are increasingly being recognized as being indicative metabolic markers in cancer cells. Fatty acids are present in several forms, either as saturated, unsaturated or as free fatty acids. They serve a variety of purposes in the cell, being important among others for energy storage, membrane proliferation and the generation of signaling molecules. They therefore are thus considered important players in the increased biosynthesis of cancer cells[348]. Our study has shown most likely the complex lipids and membrane lipids are broken down to simpler molecules, as shown by the metabolics data as well as the increase of *CPT1*, CPT1 conjugates fatty acids with carnitine to translocate them to the mitochondria, where the acylcarinitines undergo fatty acid oxidation[349]. Knowing that inhibiting EWS-FLI1 slows down proliferation and could lead to apoptosis, it could be thought that the accumulation of membrane phospholipid precursors and free fatty acids were no longer required to meet increased growth demands[18,350]. Thus, Ewing sarcoma seems to rely extensively on fatty acids for membrane formation. It could therefore be of interest to see whether limiting the supply of fatty acids or increasing the rate of fatty acid degradation can be of therapeutic benefit, as several pharmacological tools to manipulate fatty acid oxidation have recently been described, while keeping in mind that the fatty acid metabolism can be modulated in multiple points in the fatty acid pathway[351].

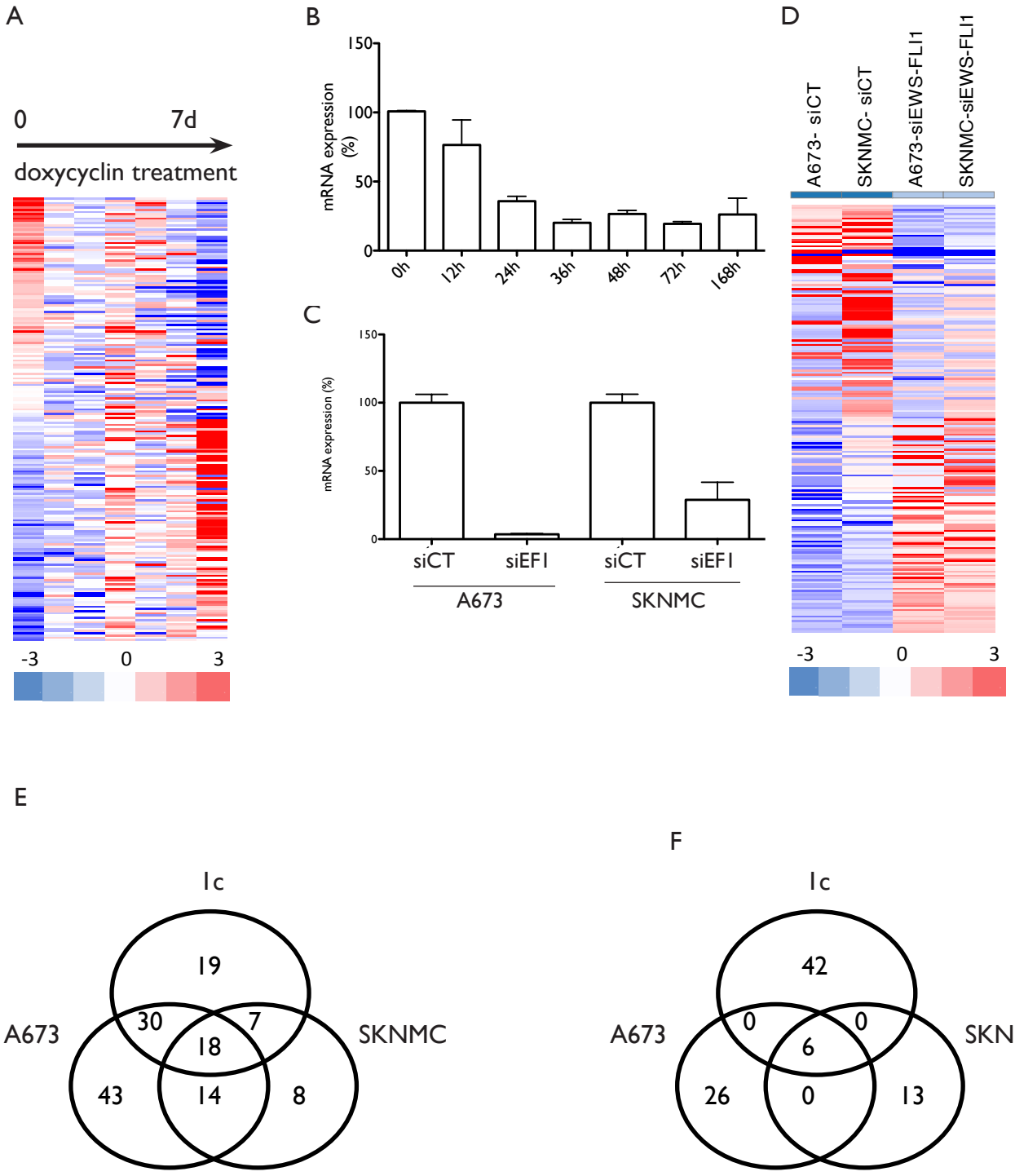

Figure 1. Metabolite profile of Ewing' sarcoma cell lines, inhibited by EWS-FLI1. A) Heat map showing 254 metabolites in lysates from five replicates from EWS-FLI1 doxycylin inducible cell line 1C in a time-series experiment for 7 days. A shift of metabolites was observed upon EWS-FLI1 inhibition that became more profound in later time points. B, C) Relative expression of *EWS-FLI1* in the 1C time series B) and the A673 and SKNMC inhibition C). D) Heat map showing 433 metabolites in lysates from five replicates from the Ewing' sarcoma cell lines A673 and SKNMC inhibited by siRNA for EWS-FLI1. E, F) Venn diagram comparing the 218 common metabolites in 3 different cell lines upon EWS-FLI1 inhibition. The venn diagrams indicate the number of metabolites that are significantly ($P<0.05$) upregulated E) or downregulated F). The overlap shows the common metabolites in all three cell lines. The highest common metabolites in the three cell lines are part of the kynurenine pathway, the glucose pathway, the cysteine glutathione pathway, the fatty acid synthesis pathway and the N-glycosylation pathway.

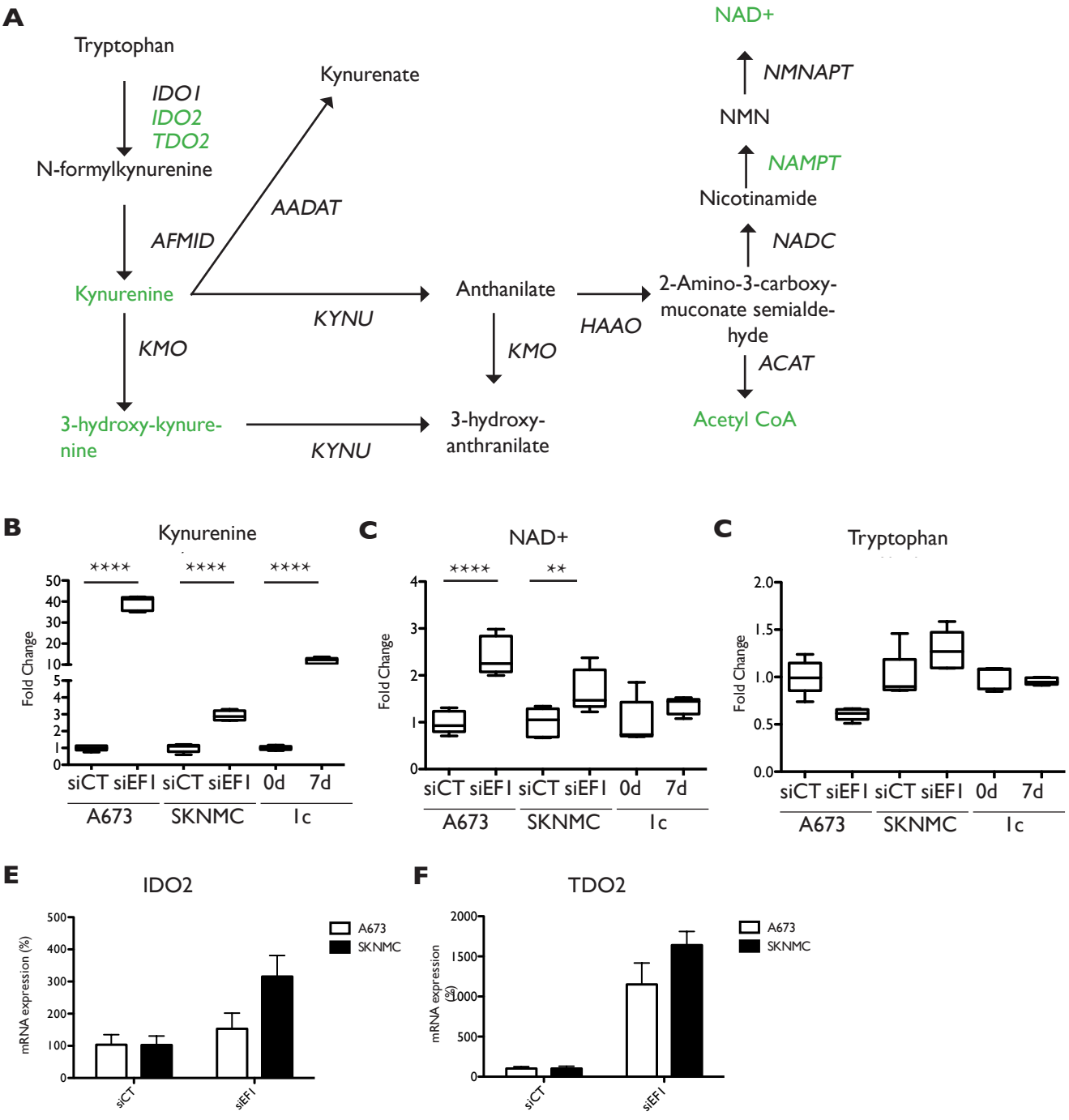

Figure 2. The influence of EWS-FLI1 on the tryptophan pathway. A) The kynurenine pathway; Tryptophan is metabolized to kynurenine, via N-Formylkynurenine, which is eventually degraded to kynurenate, Acetyl-CoA and NAD+. Enzymes and metabolites that are significantly upregulated upon EWS-FLI1 inhibition are shown in green. B) Kynurenine and C) NAD+ are upregulated upon inhibition of EWS-FLI1, whereas Tryptophan (D) is not significantly altered. The change of kynurenine is most correlated with changes of the enzymes (E) *IDO2* and (F)*TDO2*, which break down Tryptophan to Kynurenine.

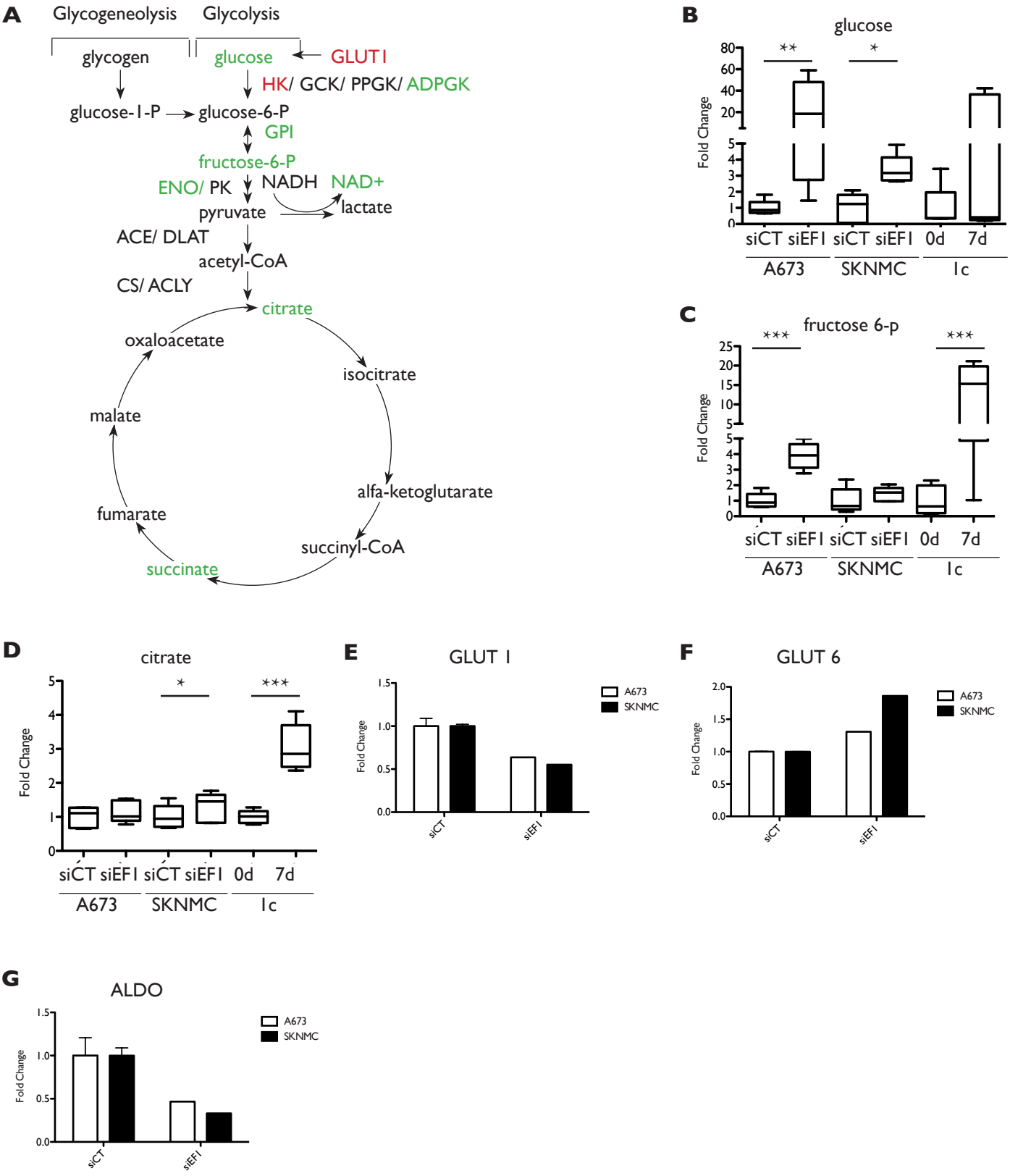

Figure 3: The influence of EWS-FLI1 on the glucose metabolism. A) EWS-FLI1 influences the energy production of Ewing's sarcoma cells. EWS-FLI1 upregulates several of the metabolites in the glycosysis pathway, such as B) Glucose, C) Fucose-6-P. Also markers of the TCA cycle such as D) citrate are upregulated. E) mRNA levels of *GLUT1*, a major glucose reporter is down regulated, whereas mRNA levels of F)*GLUT6*, an intracellular receptor that prevent glucose transpor a is upregulated. G) mRNA levels of *ALDO*, an enzyme connecting the PPP to the glycolysis pathway, is downregulated.

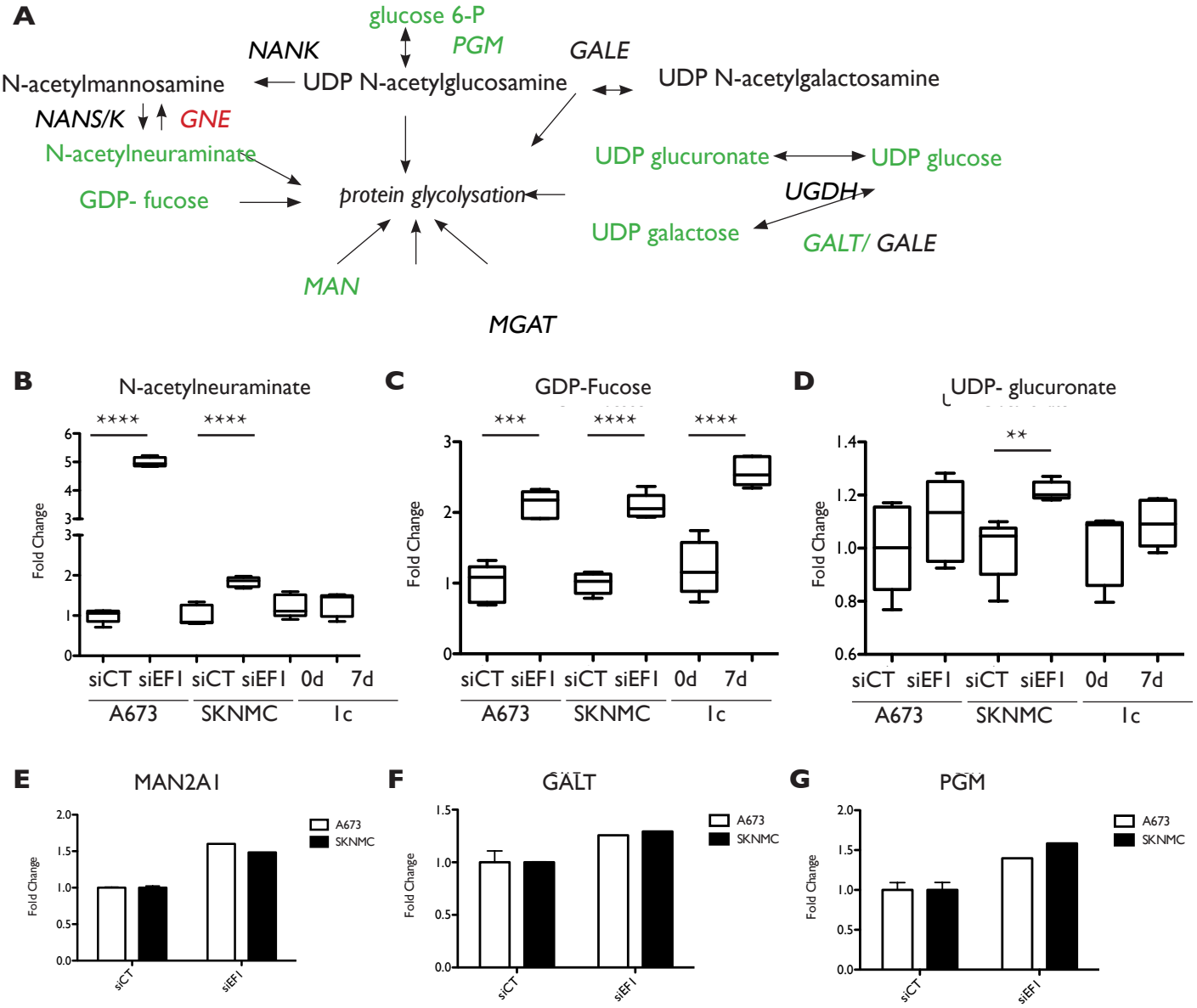

Figure 4. The influence of EWS-FLI1 on N-Glycosylation. A) An overview of the N-Glycosylation pathway. Glucose provides key precursors for protein glycosylation. Metabolites and enzymes that are upregulated by the inhibition of EWS-FLI1 are indicated in green. Several glycosylation precursors were increased, including B) N-acetylneuraminate, C) GDP-Fucose and D) UDP-Glucuronate. Expression of many enzymes are upregulated that play a part in protein glycosylation, such as E) *MAN2A1*, F) *GALT* and G) *PGM*.

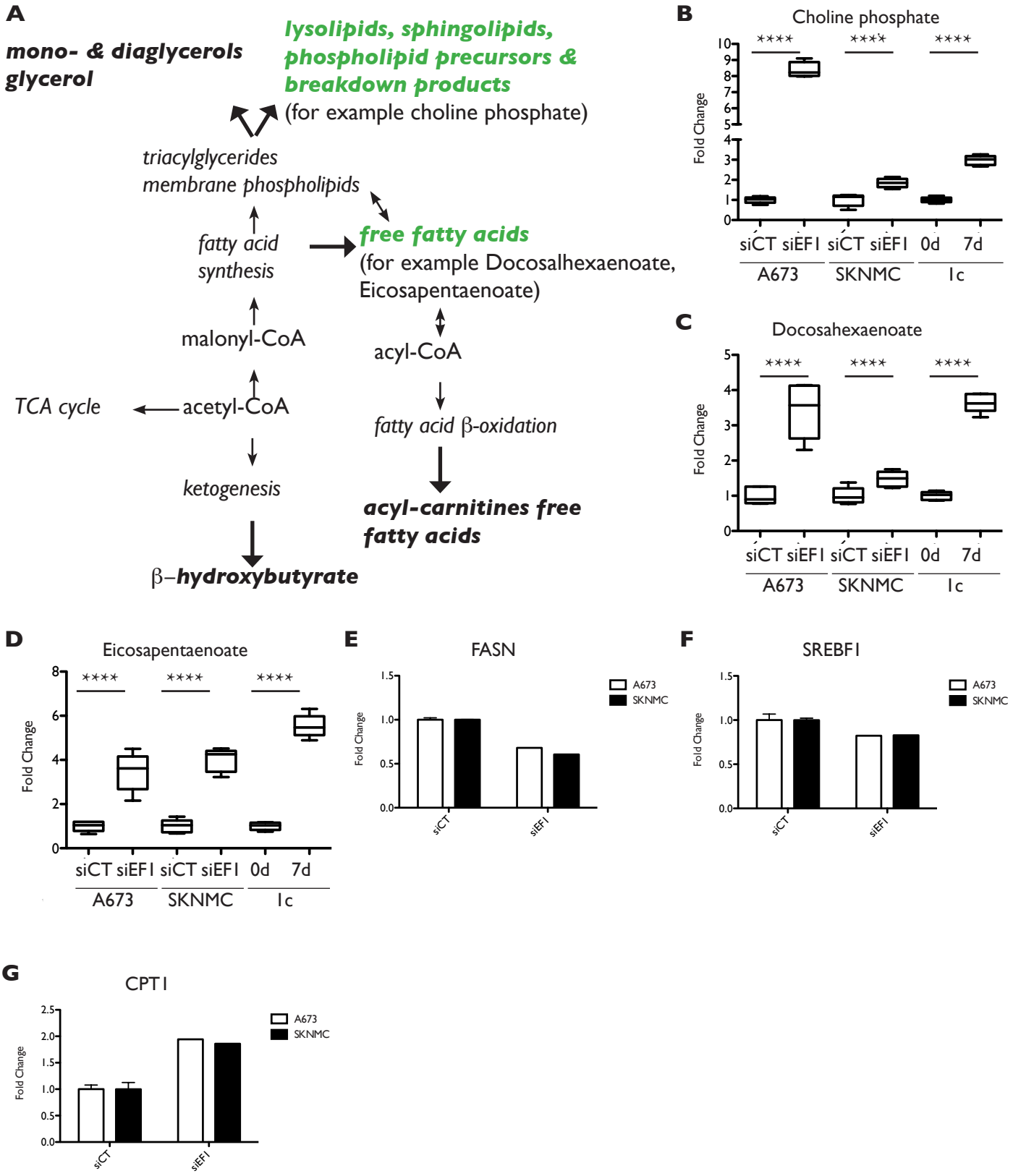

Figure 5: Fatty acid synthesis. Silencing of EWS-FLI1 expression in Ewing' sarcoma cells is associated with elevated levels of free fatty acids and elevated levels of lysolipids, sphingolipids and breakdown products.A) A simplified pahtway of the fatty acid pathway. Several free fatty acids, coming from complex lipids or membrane lipids, such as B) Choline phosphate, C) Docosahexaenoate and D) Eicosapentaenoate are shown. Several enzymes could be responsible for the changes in fatty acid levels; E) fatty acid synthesis expression (*FASN*) is decreased upon EWS-FLI1 inhibition, F) the levels of transcription of fatty acid synthesis enzymes (*SREBF1*) is also inhibited, however, F) up-regulation of simple fatty acids is most likely indeed due to a degradation of more complex lipids (*CPT1*).

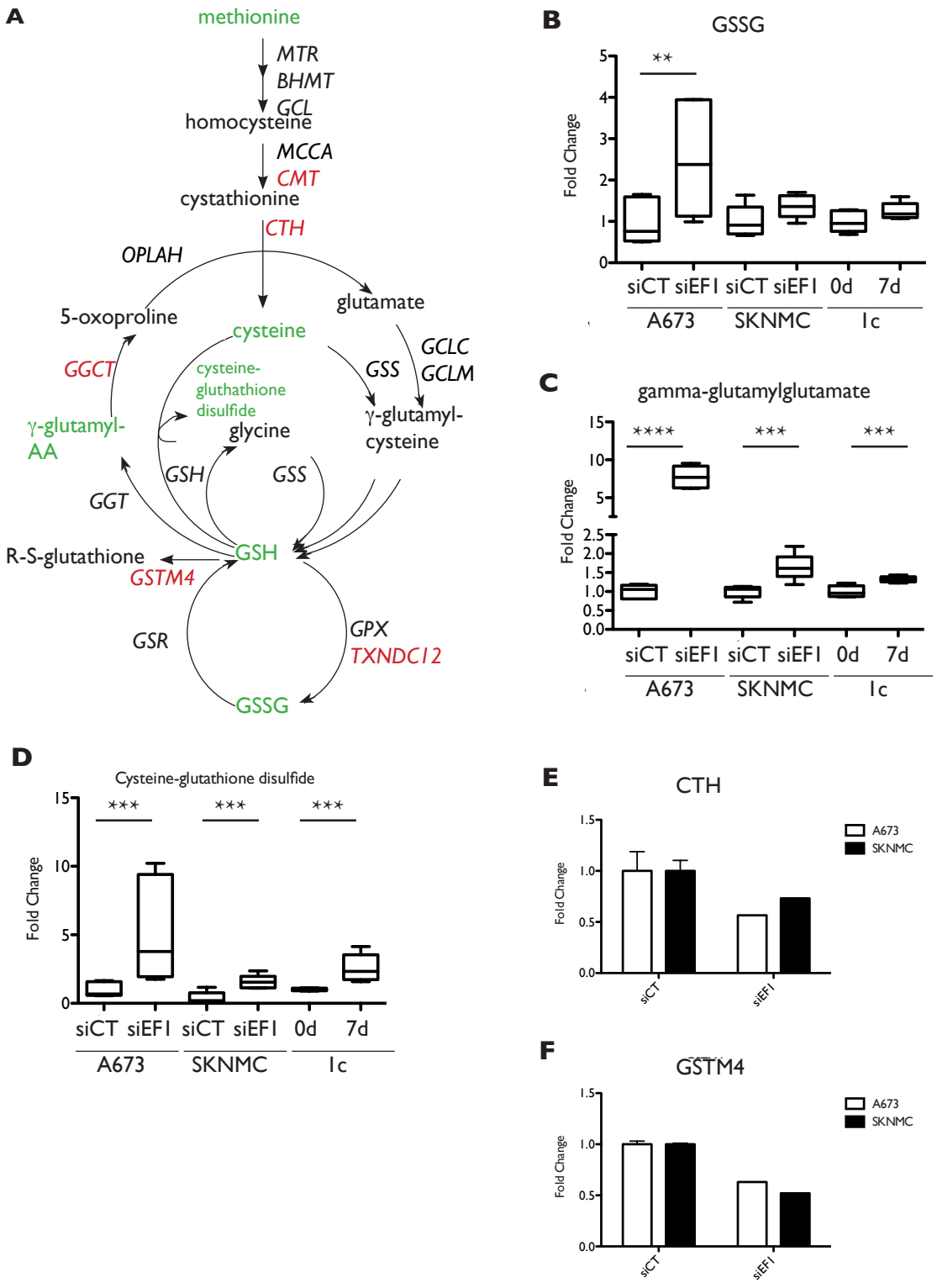

Figure 6: The glutathione pathway. A) Silencing of EF1 expression in Ewing' sarcoma cells appears to be associated with increased glutathione synthesis and turnover/recycling. B) Elevated levels of GSSG, glutathione degradation/ turn-over products such as C) gamma-glutamylglutamate and such as the biochemical marker of oxidative stress D) cysteine-glutathione-disulfide. E) EWS-FLI1 upregulates the expression of enzyme *CTH* and F) *GSTM4*.

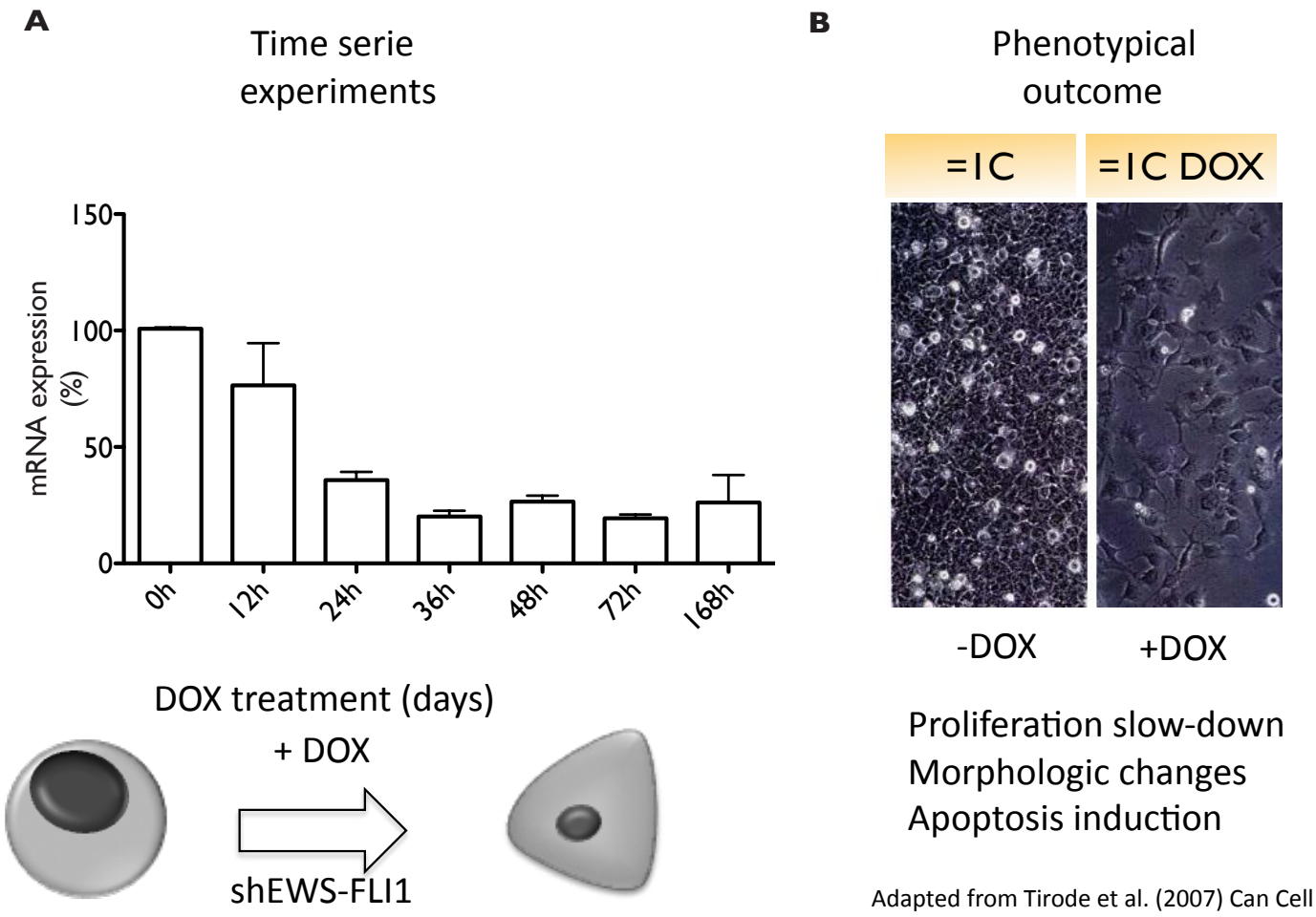

Supplementary figure 1. The doxycyline inducible cell line 1C. A) Upon treatment with doxycyline, the mRNA level of *EWS-FLI1* is diminished, B) proliferation slows down, the cells undergo morphological changes and there is a light induction of apoptosis.

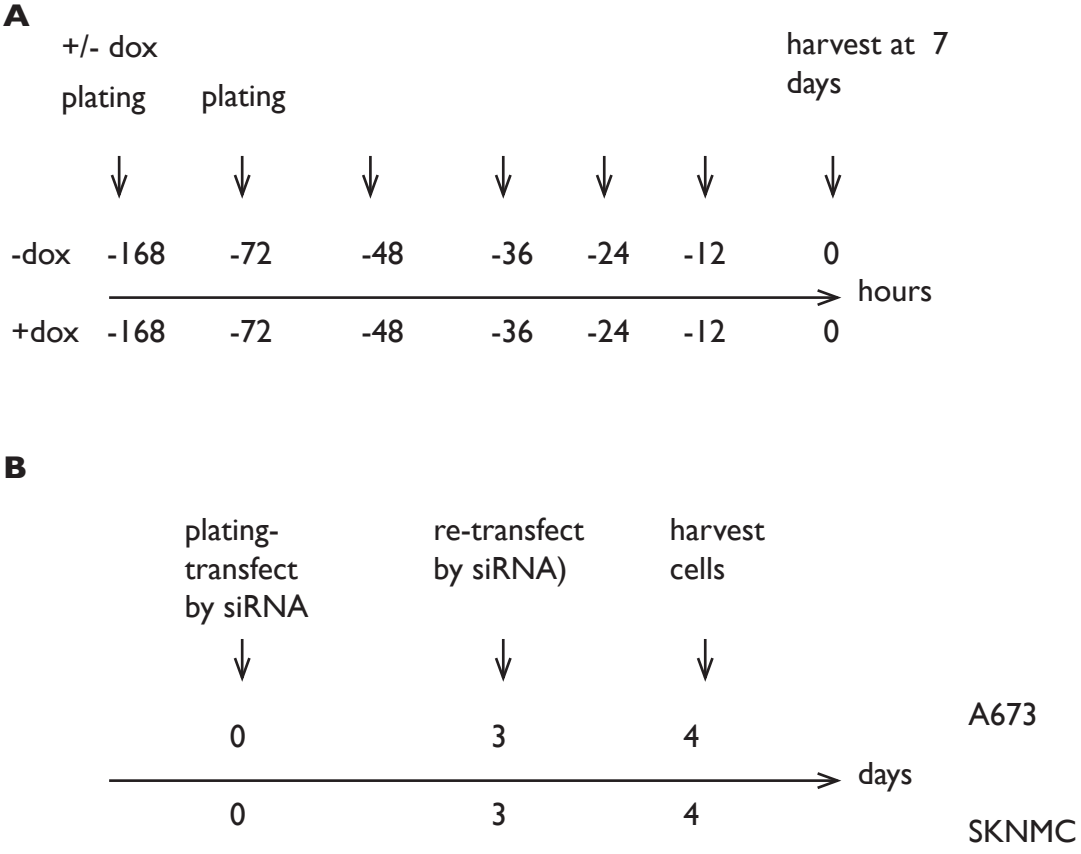

Supplementary figure 2. Schematic representations of the workflow of the metabolics experiments. A)1c cells where treated with doxycyclin to conditionally inhibit the expression of EWS-FLI1. 7 different time points were taken for analysis, each one containing 5 replicates. Arrows indicate doxycycline treatments in the upper part of the figure, or no treatment in the lower part of the figure B). A673 and SKNMC cells were plated, followed by a transfection with siRNA. 2 days later the cells were re-transfected, and harvested at day 4.

A

Welch's Two Sample t-Test -changes vs. control	**12h / 0h**	**24h / 0h**	**36h / 0h**	**48h / 0h**	**72h / 0h**	**168h / 0h**
Total number of biochemicals with $p \leq 0.05$	**32**	**46**	**44**	**37**	**70**	**149**
Biochemicals (↑|↓)	**8|24**	**10|36**	**32|12**	**18|19**	**34|36**	**89|60**
q-value (for $p \leq 0.05$)	0.20	0.21	0.16	0.24	0.06	0.01
Total number of biochemicals with $0.05 < p < 0.10$	21	19	31	23	28	23
Biochemicals (↑|↓)	7|14	7|12	20|11	10|13	12|16	14|9

*From a total of **253** named biochemicals*

B

Welch's Two Sample t-Test -changes vs. control	**Cell Line A673**	**Cell Line SKNMC**
	siEF1 / siCTR	**siEF1 / siCTR**
Total number of biochemicals with $p \leq 0.05$	**261**	**116**
Biochemicals (↑|↓)	**201|60**	**83|33**
q-value (for $p \leq 0.05$)	0.20	0.21
Total number of biochemicals with $0.05 < p < 0.10$	24	32
Biochemicals (↑|↓)	19|15	16|16

*From a total of **433** named biochemicals*

Supplementary table 1A and B. A) T-test of biochemicals altered in each time point in comparison to un-treated 1c cells. B). T-test of biochemicals altered in A673 and SKNMC cells, siEF1 vs siCT.

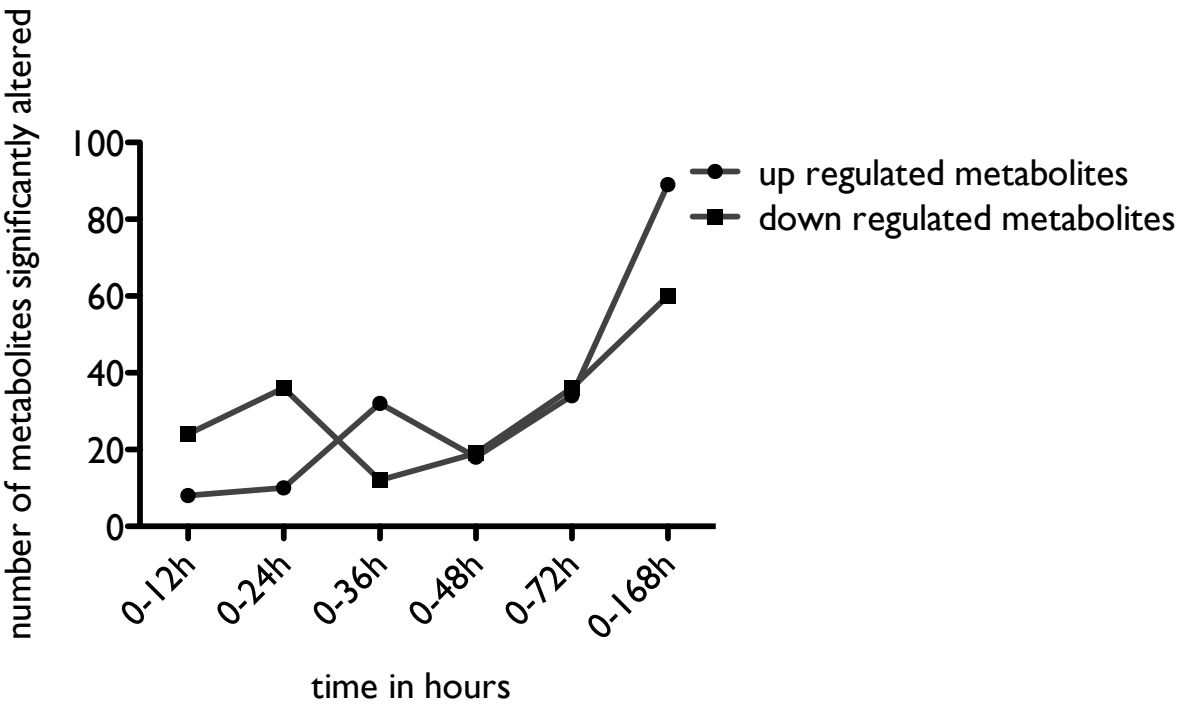

Supplementary figure 3. The number of metabolites that is altered over time upon inhibition of EWS-FLI1 in the 1C cell line. Changes at later time points become more profound.

Metabolite category	Cell line	significiant upregulated metabolites	Non-significant upregulated metabolites	p-value Fisher test
Amino Acids	A673	22	34	0.435
	SKNMC	10	46	0.701
	1C	8	44	**0.001**
Peptides	A673	8	1	**0.012**
	SKNMC	4	5	**0.086**
	1C	4	5	0.492
Fatty acids	A673	42	29	**0.003**
	SKNMC	20	41	**0.050**
	1C	48	23	**0.000**
Carbohydrates	A673	10	16	0.537
	SKNMC	6	20	0.795
	1C	4	22	**0.045**
Nucelotides	A673	14	16	0.844
	SKNMC	4	26	0.463
	1C	8	22	0.412

Supplementary table 2. Fisher test of the different metabolite categories

II. Searching for synthetic lethal genes in Ewing sarcoma: Identification of PKD1 as synthetic lethal target

A. Abstract

Ewing sarcoma, the second most commonly occurring pediatric bone tumor, is primarily characterized by a chromosomal translocation leading to the expression of a fusion protein involving the EWS RNA binding protein (*EWSR1*) and an ETS transcription factor (*FLI1*). Ewing sarcoma is aggressively treated with a combination of surgery and chemotherapy, but the overall survival rate of Ewing patients remains low (70-75%), particularly for metastatic cases (35%). In search for new therapeutic targets in Ewing sarcoma, we have identified genes whose inactivation could constitute a synthetic lethal mutation with the *EWS-FLI1* fusion gene. For that, we used a barcoded-pooled shRNA screening on the 1C Ewing cell line (tetracycline inducible shEWS-FLI1) in the presence or absence of doxycycline. A list of genes that negatively influence growth and survival Ewing sarcoma cells was identified. In addition, 4 synthetic lethal genes were identified, those being *PKD1*, *TRYX3*, *OR6C70* and *TXNL4A*. Further investigations were made for the *PKD1* gene in different Ewing sarcoma cell lines and show promise for further functional characterization to understand the mechanism behind this synthetic lethal effect.

B. Context

Ewing sarcoma, a sarcoma first described by Dr. James Ewing in 1921, is the second most commonly occurring pediatric bone tumor with a median peak incidence in the second decade of life. Ewing sarcoma primarily occurs in bone, especially in the pelvis, the diaphyseal regions of the long bones and bones of the chest wall, but a small fraction of primary tumors arises in extraskeletal soft tissue. Ewing sarcoma is associated with a chromosomal translocation leading to a fusion gene between the EWS RNA binding protein and an ETS transcription factor. In about 85% of the cases, the translocation is an *EWS-FLI1* gene fusion, leading to the EWS-FLI1 fusion protein. The chimeric protein acts as an aberrant transcription factor and is thought to induce transformation through its de-or dysregulation of cell growth and differentiation. This oncogene is expected to aberrantly regulate hundreds of genes, which may finally contribute to transformation and tumor growths and/or metastasis.

Ewing sarcoma is treated by multimodal regimens consisting of local surgery, radiotherapy and intensive chemotherapy. Currently, the average 5-year survival rate of patients with localized disease is approximately 70-75%[2–4]. Nevertheless, the long-term survival for patients with metastatic, refractory or relapsed disease is significantly reduced, being around 35%[5,6]. Metastatic disease thus poses a challenge, as relapse is frequent despite the aggressive treatment. These challenges thus indicate the need for novel therapeutic targets. In recent years, the search for a better therapeutic target for Ewing sarcoma as for many other cancers has focused on the development of personalized therapy, driven by the premise that it will increase therapeutic efficacy and reduce toxicity. However, the development of drugs for these targets that selectively kills tumor cells, without causing damage to the normal cells of the body remains challenging. Given its essential role in the biology of Ewing sarcoma, inhibition of its oncogene *EWS-FLI1* would appear to be a perfect for targeted therapy. However the inhibition of transcription factors appear to be very challenging, therefore, several studies have focused on instead targeting downstream effectors of EWS-FLI1 in Ewing sarcoma. Examples of such studies are the inhibition of PRKCβ or the inhibition of IGF1R[142,308].

Several targeted therapies based on this principle were in clinical trials, such as Figitumumab an anti-IGF1R antibody[352,353]. Some patients have shown remarkable responses to these IGF1R-blocking antibodies however, as for most single agent targeted

therapies, disease progression and resistance is also a common phenomenon observed in these trials.

An alternative approach that has been suggested to find new therapeutic targets is the concept of synthetic lethality, the idea that mutations in two genes combined are lethal, whereas a mutation in only one of the genes is not[354]. Examples of successful synthetic lethal interactions are PARP inhibition in *BRCA1/2* breast cancers, or GATA inhibition in mutated *KRAS* NSCLC[278–280,288]. To systematically study disease related genes essential for cell survival and proliferation in the Ewing sarcoma context and to identify synthetic lethal genes that are specific to Ewing sarcoma cells harboring the *EWS-FLI1* fusion gene, we performed a functional shRNA screen. The purpose of this screen was not only to identify essential genes for cell survival and proliferation, but also to identify synthetic lethal genes in the context of Ewing sarcoma.

C. Materials and Methods

Cell lines

The doxycycline inducible cell line A673-1C, previously generated in the lab by Tirode et al., was grown in DMEM containing 10% FBS (Eurobio, Courtaboeuf, France), 1% P/S, Blasticidine (Life technologies, Saint Aubin, France) (20 mg/ml) and Zeocin (Life technologies, Saint Aubin, France) (200 mg/ml)[18]. For the doxycycline-inducible silencing of the 1C cell line, doxycycline was used at a concentration of 1 µg/ml, exhibiting strong inhibition of EWS-FLI1. Ewing sarcoma cell lines, A673 and SK-N-MC, were grown in DMEM and RPMI 160 respectively (PAA laboratories, GE Healthcare, Vélizy-Villacoublay, France) containing 10 % FBS (Eurobio, Courtaboeuf, France) and 1% P/S. During the shRNA screen, cells were grown in 5-layer flasks (Millipore, Darmstadt, Germany).

Lentiviral production

An shRNA library, consisting of 5400 disease related genes (Cellecta Human Library 2), was purchased from Cellecta (Mountain View, CA, USA). Lentiviral stocks were prepared using the 293T packaging cell line. Cells were plated over three days without antibiotics so that they were 70% confluent at the time of transfection. Lentiviral packaging plasmids consisting of a mixture of VSV-G, pPAX, (Addgene, Cambridge, MA, USA) were mixed with the plasmids from the shRNA library and used to transfect 293T cells using calcium phosphate Clonetech kit (CalPhos™ Mammalian Transfection Kit, Saint-Quentin-en-Yvelines Cedex France) according to the manufacturer's protocol. Virus-containing supernatants were collected from cell cultures at 72 h post-transfection, filtered and stored at −80 °C. The titer was determined by puromycin selection at 1 x 10'7 infectious units/ml. Virus was only used after one freeze-thaw cycle.

Pooled shRNA screen

1C cells were thawed, grown and split into two parts. 1C and 1C dox cells were plated and grown 7 days before the start of the screen. A total of 20 x 10'6 target cells for eight replicates for both conditions were seeded in 10 cm diameter plates. 12 hours after plating, the medium was replaced for fresh medium containing 1 µg/ml polybrene, to select shRNA-harboring cells. Both conditions were infected with the pool of 27500 viruses at a multiplicity of infection (MOI) of 0.3. Cells were left in culture to be transducted overnight. 12 hours after transduction, the medium was replaced for new medium containing 1 µg/ml puromycin. 24 hours after transduction, cells were trypsinized, the total of cells on different plates for one replicate transduction were

pooled and passed into a 5 layer T150 flasks.

Cells of the 3 replicates of both conditions were harvested by centrifugation, washed once in PBS and stored at -80°C for subsequent DNA purification and used as reference time points, the other 5 replicates continued to be in culture. For subsequent passages, cells were passed at confluence, approximately twice a week. For every passage a minimum of 27 x 10'6 cells was left in culture, representing each shRNA 1000 times, while the remaining cells were harvested.

After 10 doublings, all cells were harvested, a total of 100 x 10'7 cells. Final harvests and starting harvest of the infected cells were used for analysis. Genomic DNA was isolated; shRNAs were amplified, followed by high-throughput sequencing (Illumina) as deconvolution method, as described previously[355].

shRNA scoring

The barcodes were converted to genes using a bar code Analyzer and deconvoluter key from Cellecta (http://www.decipherproject.net/software/). Most of the 5400 genes were represented by at least 5 shRNAs (range 4-6 shRNAs, excluding control genes). After analysis, 418 shRNAs were deleted from analysis, as the sequence of the shRNA was redundant. Control shRNAs target Actin 1 (*ACTA1*), β-actin (*ACTB*), Glyceraldehyde 3-phosphate dehydrogenase (*GAPDH*), Luciferase (Luc), polo-like kinase 1 (*PLK1*), DNA-directed RNA polymerase II subunit (*POLR2B*), Retinoblastoma-Related Protein 2 (*RBL2*), RING-box protein 1 (*RBX1*), Eukaryotic translation initiation factor 3 subunit A (*EIF3A*) and Kinesin family member 11 (*KIF11*). Both unsupervised and consensus clustering of the shRNA depletion and enrichment profiles determined replicate reproducibility. To determine the genes most important for gene proliferation and survival, as well as synthetic lethal genes, genes were selected by p-value and fold change. Cut-off values were 0.01 and 1.5 respectively. In order for a gene to be selected, the gene should at least carry 2 or more shRNA that confer the required phenotype.

DAVID analysis

Gene ontology functional annotation analysis was performed using DAVID[356,357]. The input was the selected essential gene list, while using the whole gene list as background. The analysis was performed with an ease of 0.001, a Bonferroni correction and a minimum count of 5.

Plasmid transfection

Individual *PKD1* shRNAs clones for validation were purchased from Cellecta (Mountain view, CA) in pRSI16-U6-(sh)-HTS6-UbiC-TagRFP-2A-Puro, Cellecta205360961|NM_000296.3|PKD1|12358 (shRNA # 1), Cellecta205360961|NM_000296.3|PKD1|12359 (shRNA # 2) and Cellecta205360961|NM_000296.3|PKD1|12360 (shRNA #3). Cells were seeded and left overnight to adhere, for 60-80% of confluence, at the time of transfection. shRNAs were transfected short time using JetPrime transfection buffer and reagent according to the manufactures' protocol (JetPrime, Polypus, Strasbourg, France).

Isolation of RNAs

Total RNAs were isolated using the Nucleospin Total RNA isolation kit (Macherey Nagel, Hoerdt, Germany). RNAs were isolated at harvest points to ensure the down regulation of *EWS-FLI1* throughout the screen. To validate down regulation of *PKD1*, total RNAs were harvested 3 days after transfection.

Reverse transcription Quantitative PCR (RT-qPCR)

cDNAs were synthesized from 500 ng of RNA using the High-Capacity cDNA Reverse Transcription Kit RT kit (Applied Biosystems, Life Technologies, Saint Aubi, France). Reverse transcriptase reactions were performed in 20 µl. cDNAs were diluted 1/10 and 9 µl of diluted RT product was used for the qPCR. Gene expression was analyzed using SYBR PCR Master mix with an AB7500 Real-time PCR system (Applied Biosystems, Life Technologies, Saint Aubi, France). Results were normalized to *GAPDH* and quantified by the ddCt-method. Primers are listed in Supplementary Methods.

Cell counting

In order to address cell number and viability, cells were transfected and selected with puromycin for 96 hours. Cells were counted in a Beckman vi-Cell XR cell viability analyzer in a total volume of 1 ml.

Transcriptomic Analysis.

Previously published data showing the modulation of genes after EWSR1-FLI1 inhibition using the 1C model published by Tirode et al were downloaded and analyzed to study gene alterations[18].

D. Results

Pooled screen identifies genes essential for cell growth and survival.

Ewing sarcoma 1C cells were split, after which one part was treated for 7 days with doxycycline, to conditionally inhibit and stabilize the expression of EWS-FLI1. After 7 days, the cells were plated, left for 12 hours to adhere, infected at an MOI of 0.3 with the library of 27500 shRNAs covering 5400 genes. 200 copies of each shRNA were infected for each condition in each replicate. A total of 8 replicates per condition were infected, 3 replicates for each start point, called $1C^{start}$ and 1C dox^{start} cells, 5 replicates for the final time point, $1C^{end}$ and 1C dox^{end}. 24 hours after infection, cells were selected by puromycin and cultured in the continuous presence or absence of doxycycline, for a total of 10 doublings (Figure 1A). $1C^{start}$ and 1C dox^{start} cells that were used as a starting point control were harvested at 3 days after infection. The two different groups, $1C^{end}$ and 1C dox^{end}, were harvested after these 10 doublings. 1C and 1C dox do not portray the same rate of proliferation, therefore both conditions were passed independently of one another at confluence[18].

After proliferation, the shRNAs were isolated, amplified and quantified. The entire of the 27000 shRNAs that had been infected into the different conditions could be retrieved in the $1C^{start}$ and 1C dox^{start} replicates, verifying that the infection had been successful. Reproducibility of short hairpin RNA (shRNA) enrichment and depletion profiles was evaluated across the experimental replicates, as a quality control. The $1C^{end}$, 1C dox^{end} and $1C^{start}$ and 1C dox^{start} replicates clustered closely by both unsupervised and consensus clustering of shRNA depletion and enrichment profiles, attesting to the robustness of the screens (supplementary Figure 3). As $1C^{start}$ and 1C dox^{start} clustered consistently together and no differences were observed between both conditions, they were pooled according to this cluster analysis and thus considered as one group that will be referred to as $1C^{start}$. Since lentiviral shRNA integrates into the genome of a target cell, if a given shRNA decreases cell viability, the relative abundance of that shRNA will decrease over this period, therefore the shRNA can no longer be identified and will thus “drop-out” of the results. Following this analysis, we can thus identify shRNAs that “drop out” specifically when carrying an *EWS-FLI1* gene fusion ($1C^{end}$) versus cells that are inhibited for EWS-FLI1 (1C dox^{end}).

Comparisons between the shRNA representations at the end of the experiment versus the start of the experiment and between the different treatment arms were performed. This led to a rank of each gene, based upon the ranking of shRNA sets determined by the full list of 27K shRNAs. Positive and negative control genes in the screen were verified and proven to be inhibited versus non-affected, thus providing an internal control of the screen. This study has resulted in the identification of a number of genes essential to the growth and survival phenotype in Ewing sarcoma cells, thus identifying essential genes for $1C^{end}$ and 1C dox^{end}, as well as genes essential for $1C^{end}$ or 1C dox^{end} alone. Selection criteria that were used for the identification of genes essential in both conditions were a Fold Change (FC) of 2.5 between $1C^{start}$ and $1C^{end}$ or 1C dox^{end} and a p-value equal to or lower then 0.01. In order for a gene to be selected, at least two shRNAs needed to portray the phenotype. Firstly, a group of genes was identified that was proven to be essential for both 1C and 1C dox, constituting of 789 genes (Figure 1B). A comprehensive list of the 789 ranked genes, along with annotation for the shRNA clones, is provided in annex III. A functional analysis was performed for these commonly essential genes identified in the screen using DAVID, to further specify the nature of the different groups of genes[356,358]. The DAVID analysis was performed using the whole infected gene list as background whereas the identified essential genes were given as input. This gene ontology analysis revealed a strong enrichment in spliceosome genes, genes connected to the ribosome, genes involved in GPCR signaling as well as genes involved in mRNA processing (Table 1).

Pooled screen identifies specific for 1C and 1C dox.

To identify candidate genes that were specific to either 1C or 1C dox, 2 comparisons were made, being between$1C^{start}$ and $1C^{end}$ and between $1C^{end}$ and 1C dox^{end} or between $1C^{start}$ and 1C dox^{end} and 1C dox^{end} and $1C^{end}$ respectively. For the genes specific to 1C, shRNAs were selected that had a 2.5 FC between$1C^{start}$ and $1C^{end}$, with a p-value equal to or lower then 0.01. For the second comparison, $1C^{end}$ and 1C dox^{end}, shRNAs were selected with a FC of 2.5 and a p-value equal to or lower then 0.05. 282 shRNAs were specifically killed in 1C and not 1C dox, thus portraying a synthetic lethal phenotype, but only genes were selected that had 2 shRNAs against the gene. In total, the screen thus identified 4 genes that are synthetic lethal (kill $1C^{end}$ but not 1Cdox^{end}, Figure 1B, grey section). For genes specific to 1C dox, the same comparisons were made, a 2.5 FC between $1C^{start}$ and 1C dox^{end}, with a p-value equal to or lower then 0.01 and a 2.5 FC between $1C^{end}$ and 1C dox^{end} and a p-value equal to or lower then 0.05. 668 shRNAs were selected, resulting in 21 genes that are specific to 1C dox. A list of genes specific

to 1C dox is provided in annex IV.

***PKD1* is identified as synthetic lethal candidate gene.**

The 4 genes that were selected as candidate synthetic lethal genes, polycystic kidney disease 1 (autosomal dominant) (*PKD1*), olfactory receptor, family 6, subfamily C, member 70 (*OR6C70*), trypsin X3 (*TRYX3*) and thioredoxin-like 4A (*TXNL4A*) each had 2 shRNAs against the phenotype (Figure 1C). These four genes were not particularly linked to each other, belonging to different classes (Figure 2A): the Transient Receptor Potential Polycystic (*TRPP*) family, the olfactory gene family, the protease family and a gene involved in pre-mRNA splicing respectively. In order to select the genes for validation, genes were investigated for function, expression in Ewing sarcoma and the absence of modulation by EWS-FLI1. The results are indicated in Figure 2. *PKD1*, coding for a glycoprotein primarily identified in polycystic kidney disease, was chosen for further validation, as it was expressed in Ewing sarcoma, non-modulated by EWS-FLI1 and literature covering the gene was available.

***PKD1* is validated as synthetic lethal candidate gene.**

3 *PKD1* shRNA were selected for validation. Cells were plated, left to adhere for 24 hours, after which they were double transiently transfected, with a combination of an shRNA targeting *EWS-FLI1* (shEF1) and a control non-targeting sequence (shCT) or shEF1 and an shRNA targeting *PKD1* (shPKD1). This approach was chosen as transfection with an shPKD1 in Ewing sarcoma cells is lethal and thus results in a decrease in RNA quality, whereas it is not in shEF1 transfected cells. RNA was harvested 3 days after transfection. The level of knockdown of *PKD1* was verified by RT-QPCR, indicating that the shRNAs against *PKD1* significantly knocked down *PKD1* mRNA levels (Figure 3A)

Validation experiments for the *PKD1* synthetic lethal gene were carried out in A673, SKNMC and EW24 cells. These three Ewing cell lines were transiently transfected with shPKD1 and shCT or shEF1. These cells were grown for four days and counted at 4 days after transfection. shPKD1 cells with EWS-FLI1 expression, were significantly decreased in cell number in comparison to the cells that were inhibited for EWS-FLI1 using all 3 shRNAs (Figure 3B). When cells did not express EWS-FLI1, knockdown of *PKD1* did not result in a significant loss of viable cells.

E. Discussion

The performed high-throughput shRNA screen in Ewing sarcoma has resulted in 3 categories of genes, being genes essential to both 1C and 1C dox, genes specific to 1C dox but not to 1C and genes that are specific to 1C but not to 1C dox, the latter considered to be synthetic lethal genes. The group of essential genes was expected to contain genes that encode proteins with basic cellular functions, such as genes that for DNA replication, genes involved into translation and genes involved in transport processes[359–361]. Not surprisingly, many of the genes that were in this group were related to spliceosome, ribosome, RNA splicing and processing and RNA metabolic processes. Next to this, a group of specific to 1C dox as well as a group specific to 1C, the so-called synthetic lethal genes. In comparison to the synthetic lethal gene group, the group of genes specific to 1C dox is bigger. This could be explained by the fact that 1C dox cells undergo morphological changes, a slow down of proliferation and show some apoptosis[18]. It could therefore be thought that these cells are somewhat more sensitive for inhibition of specific genes in comparison to 1C cells.

PKD1 was identified as the causative gene of Autosomal polycystic kidney disease.[362] PC-1 is involved directly and indirectly on several signaling pathways that are involved in cellular growth and differentiation, such as wingless-type MMTV integration site family (WNT), Janus kinase/ Signal Transducers and Activators of Transcription (JAK/STAT), nuclear factor of activated T-cells (NFAT), mTOR, PI3K, MAPK and AKT pathways.[363–367] PC-1 has been shown to phosphorylate AKT, leading to up regulation of downstream targets of AKT, a pathway commonly up-regulated in cancer[368]. Therefore, PC-1 inhibition could be selectively killing cells due to the inhibition of the AKT pathway. Further functional validation is needed to clarify which pathways are underlying the effect and how to best exploit this phenotype.

In summary, we have performed a high-throughput shRNA screen that identified *PKD1* as a synthetic lethal target in Ewing sarcoma. It was validated in several Ewing sarcoma cell lines, suggesting that selective targeting of PC-1 might be effective and selective against Ewing sarcoma cells.

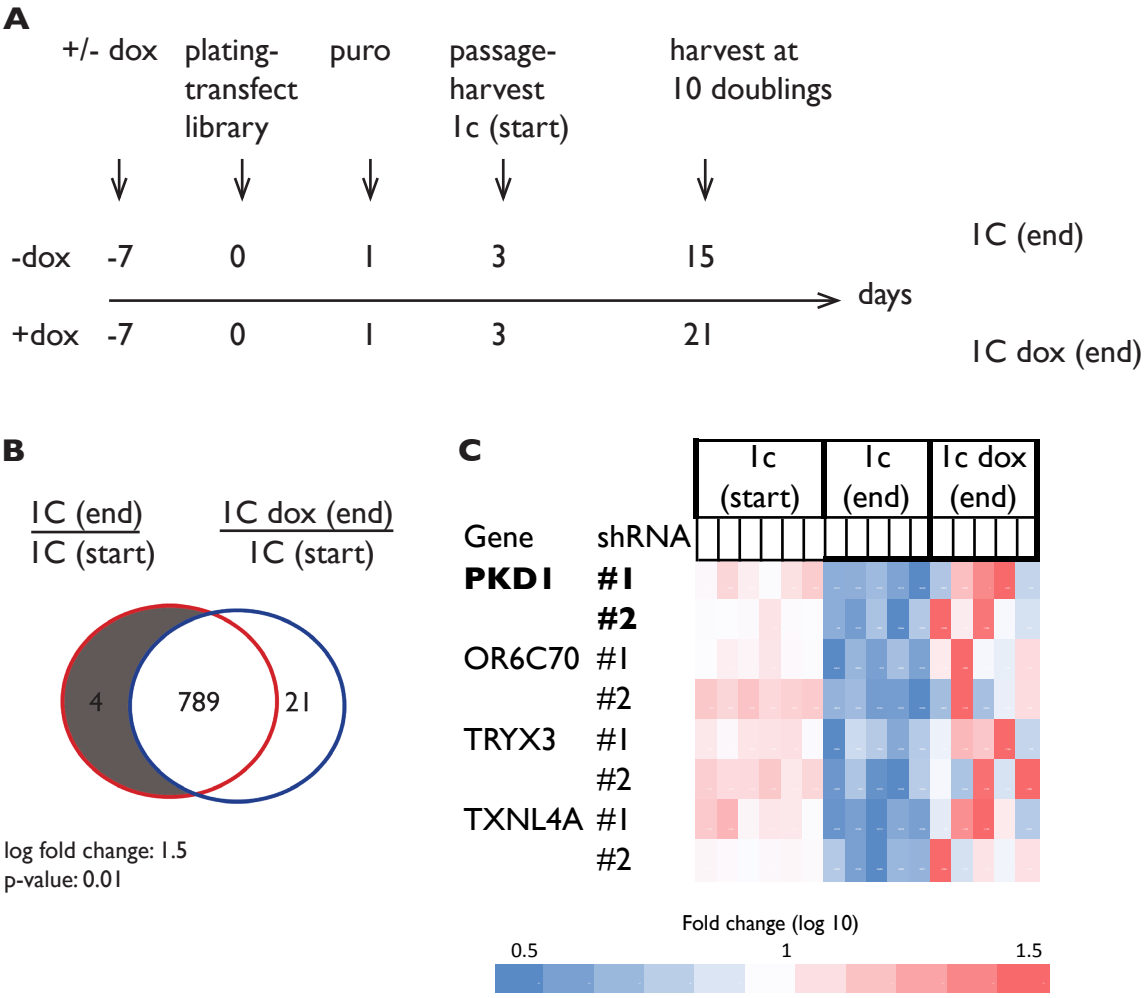

Figure 1. PKD1 is identified as candidate synthetic lethal gene in a pooled shRNA screen A) Schematic representations of the workflow of the shRNA screen experiments. 1c cells with or without dox were infected, and grown to 10 doublings after puromycin selection. B) Venn diagram representing the lethal genes of 1c and 1c dox cells. The overlap represents commonly essential genes. The grey part of the venn diagram represents the synthetic lethal candidate genes. C) 4 candidate synthetic lethal genes were identified, having at least 2 shRNAs that confer the synthetic lethal phenotype. *PKD1*, highlighted in bold, was selected for validation by individual shRNA experiments. The relative log fold scale indicates the differences in cell growth

Category	Term	Count	P-Value	Fold Enrichment	Bonferroni	Benjamini
SP_PIR_KEYWORDS	ribosome	15	9.90E-09	5.4	4.40E-06	2.20E-06
GOTERM_CC_FAT	cytosolic ribosome	15	3.10E-08	5.1	1.40E-05	6.90E-06
KEGG_PATHWAY	Ribosome	16	5.50E-09	5	5.40E-07	2.70E-07
GOTERM_CC_FAT	cytosolic small ribosomal subunit	10	3.00E-05	4.8	1.30E-02	1.50E-03
KEGG_PATHWAY	Spliceosome	22	2.00E-10	4.3	1.90E-08	1.90E-08
GOTERM_BP_FAT	translational elongation	16	2.50E-07	4.3	5.00E-04	2.50E-04
UP_SEQ_FEATURE	zinc finger region:C4-type	9	4.80E-04	4.1	6.30E-01	6.30E-01
SP_PIR_KEYWORDS	Spliceosome	19	8.60E-08	3.9	3.90E-05	7.70E-06
GOTERM_CC_FAT	ribosomal subunit	16	1.60E-06	3.9	6.90E-04	1.20E-04
GOTERM_BP_FAT	rRNA processing	12	6.10E-05	3.8	1.20E-01	1.50E-02
GOTERM_BP_FAT	rRNA metabolic process	12	6.10E-05	3.8	1.20E-01	1.50E-02
GOTERM_MF_FAT	structural constituent of ribosome	16	4.00E-06	3.7	2.60E-03	1.30E-03
GOTERM_CC_FAT	small ribosomal subunit	11	2.00E-04	3.7	8.40E-02	7.90E-03
GOTERM_CC_FAT	spliceosome	20	2.60E-07	3.6	1.10E-04	2.80E-05
GOTERM_CC_FAT	cytosolic part	19	5.40E-07	3.6	2.40E-04	4.70E-05
GOTERM_CC_FAT	ribosome	21	2.10E-07	3.5	9.20E-05	3.10E-05
SP_PIR_KEYWORDS	ribosomal protein	18	2.80E-06	3.4	1.30E-03	1.80E-04
GOTERM_BP_FAT	ribosome biogenesis	13	1.40E-04	3.4	2.40E-01	2.70E-02
GOTERM_BP_FAT	ribonucleoprotein complex biogenesis	22	3.30E-07	3.3	6.70E-04	2.20E-04
GOTERM_CC_FAT	ribonucleoprotein complex	59	4.90E-17	3.1	2.10E-14	2.10E-14
SP_PIR_KEYWORDS	ribonucleoprotein	28	1.90E-08	3.1	8.40E-06	2.80E-06
SP_PIR_KEYWORDS	protein biosynthesis	20	5.90E-06	3	2.60E-03	3.30E-04
SP_PIR_KEYWORDS	mrna splicing	29	7.00E-08	2.9	3.10E-05	7.80E-06
GOTERM_BP_FAT	RNA splicing, via transesterification reactions	18	6.40E-05	2.8	1.20E-01	1.40E-02
GOTERM_BP_FAT	RNA splicing, via transesterification reactions with bulged adenosine as nucleophile	18	6.40E-05	2.8	1.20E-01	1.40E-02
GOTERM_BP_FAT	nuclear mRNA splicing, via spliceosome	18	6.40E-05	2.8	1.20E-01	1.40E-02
GOTERM_BP_FAT	translation	26	1.60E-06	2.7	3.30E-03	8.20E-04
SP_PIR_KEYWORDS	mrna processing	31	7.20E-07	2.6	3.20E-04	5.40E-05
GOTERM_BP_FAT	RNA splicing	32	2.30E-06	2.4	4.60E-03	7.70E-04
GOTERM_BP_FAT	mRNA processing	33	3.50E-06	2.3	7.10E-03	1.00E-03
GOTERM_BP_FAT	RNA processing	51	1.60E-08	2.2	3.20E-05	3.20E-05
GOTERM_BP_FAT	mRNA metabolic process	38	2.10E-06	2.2	4.10E-03	8.30E-04
INTERPRO	Nucleotide-binding, alpha-beta plait	24	3.50E-04	2.2	3.10E-01	3.10E-01
GOTERM_MF_FAT	RNA binding	55	9.10E-08	2.1	6.00E-05	6.00E-05
INTERPRO	RNA recognition motif, RNP-1	22	8.80E-04	2.1	6.20E-01	3.80E-01
SP_PIR_KEYWORDS	rna-binding	43	1.60E-05	1.9	7.30E-03	8.20E-04
GOTERM_CC_FAT	cytosol	70	7.80E-06	1.7	3.40E-03	4.90E-04
SP_PIR_KEYWORDS	acetylation	163	3.90E-11	1.6	1.70E-08	1.70E-08
GOTERM_CC_FAT	nuclear lumen	82	8.00E-05	1.5	3.40E-02	3.50E-03
GOTERM_CC_FAT	organelle lumen	96	2.50E-04	1.4	1.00E-01	9.20E-03
GOTERM_CC_FAT	intracellular organelle lumen	95	3.00E-04	1.4	1.20E-01	9.90E-03
GOTERM_CC_FAT	membrane-enclosed lumen	96	6.60E-04	1.4	2.50E-01	2.00E-02
GOTERM_CC_FAT	non-membrane-bounded organelle	147	2.80E-05	1.3	1.20E-02	1.50E-03
GOTERM_CC_FAT	intracellular non-membrane-bounded organelle	147	2.80E-05	1.3	1.20E-02	1.50E-03

Table 1. DAVID analysis for the essential genes of 1C and 1C dox.

A

Gene name	Full name	Info	Modulation EWS-FLI1
PKD1 (5310)	Polycystic kidney disease 1 (autosomal dominant)	This gene encodes a member of the polycystin protein family. The encoded glycoprotein contains a large N-terminal extracellular region, multiple transmembrane domains and a cytoplasmic C-tail. It is an integral membrane protein that functions as a regulator of calcium permeable cation channels and intracellular calcium homoeostasis. It is also involved in cell-cell/matrix interactions and may modulate G-protein-coupled signal-transduction pathways. It plays a role in renal tubular development, and mutations in this gene cause autosomal dominant polycystic kidney disease type 1 (ADPKD1).	No
OR6C70 (390327)	Olfactory Receptor, Family 6, Subfamily C, Member 70	Olfactory receptors interact with odorant molecules in the nose, to initiate a neuronal response that triggers the perception of a smell. The olfactory receptor proteins are members of a large family of G-protein-coupled receptors (GPCR) arising from single coding-exon genes. Olfactory receptors share a 7-transmembrane domain structure with many neurotransmitter and hormone receptors and are responsible for the recognition and G protein-mediated transduction of odorant signals. The olfactory receptor gene family is the largest in thegenome.	No
TRYX3 (136541)	Protease, Serine, 58	This gene encodes a member of the trypsin family of serine proteases. This gene and several related trypsinogen genes are localized to the T cell receptor beta locus on chromosome 7. This gene was previously described as a trypsinogen-like pseudogene, but it is now thought to be a protein-coding gene.	No
TXNL4A	Thioredoxin-like 4A	Essential role in pre-mRNA splicing as component of the U5 snRNP and U4/U6-U5 tri-snRNP complexes that are involved in spliceosome assembly.	Induced by EWS-FLI1 in 1C

B

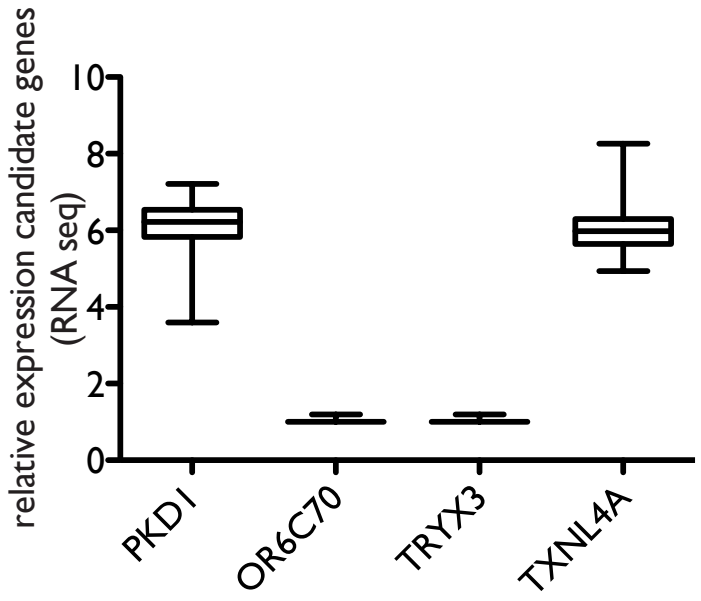

Figure 2. A summary of the synthetic lethal candidate genes. A) A summary of the 4 different synthetic lethal genes with their functions and modulation by EWS-FLI1. B) relative expression of the candidate genes in Ewing' sarcoma

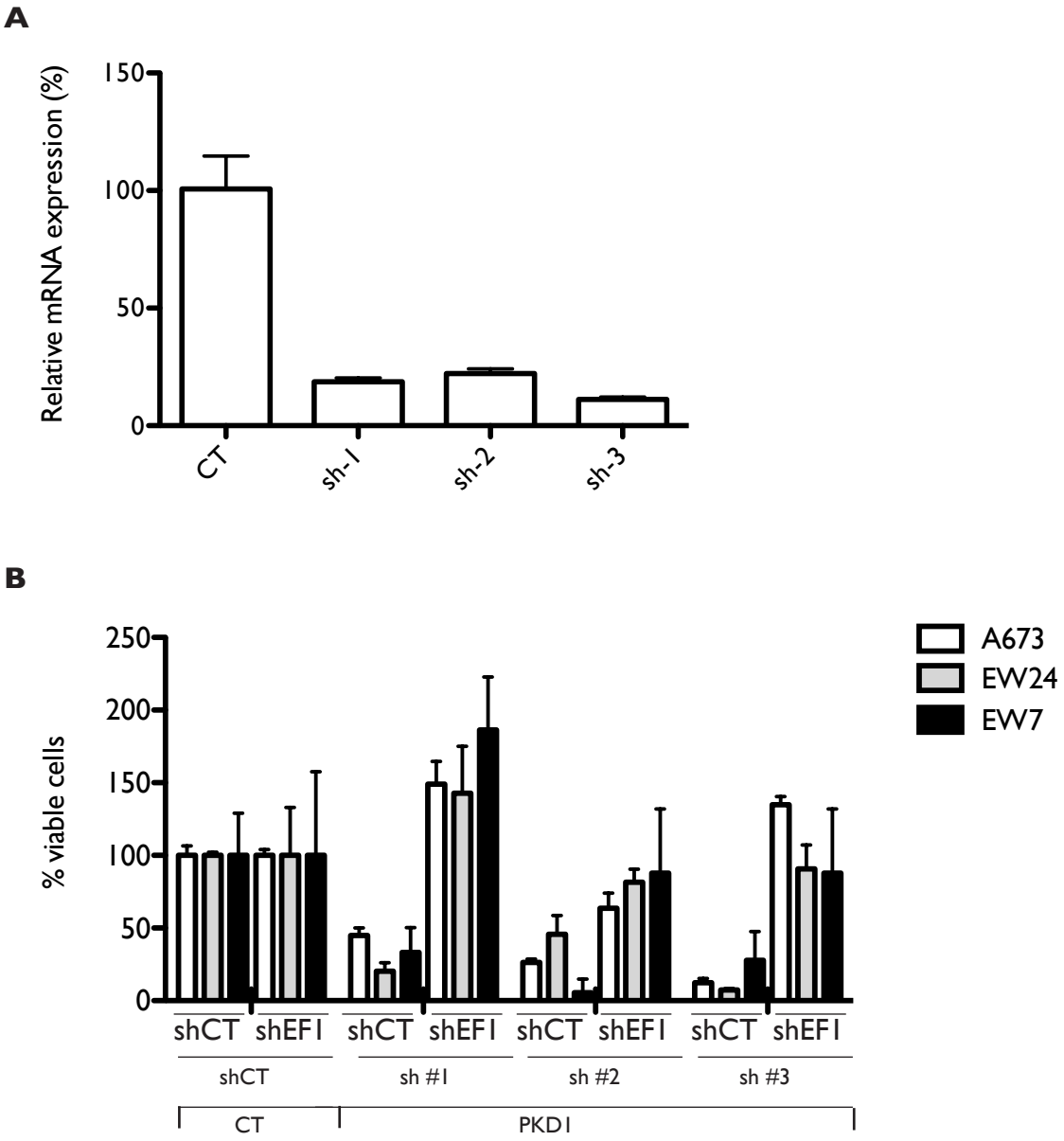

Figure 3. Validation of target gene suppression for *PKD1* as candidate synthetic lethal gene. A) Remaining *PKD1* mRNA expression 36h in A673 shEF1- transfected cells after knockdown of shPKD1 in comparison to shCT. B)The percentage of viable cells 4 days after knockdown of PC-1 in sh-CT transfected cells in comparison to sh-EF1 transfected cells in A673 cells (left), EW24 cells (middle) and EW7 (right).

Name gene	Forward primer	Reverse primer
GAPDH	CTTCAACAGCGACACCCACT	GTGGTCCAGGGGTCTTACTC
EWS-FLI1	GAGGCCAGAATTCATGTTATTGC	GCCAAGCTCCAAGTCAATATAGC
PKD1	GTACAACGAGTCCTTCCCG	TCAGGTTCTCGAAGGCATTAG

Supplementary table 1: Primer sequences

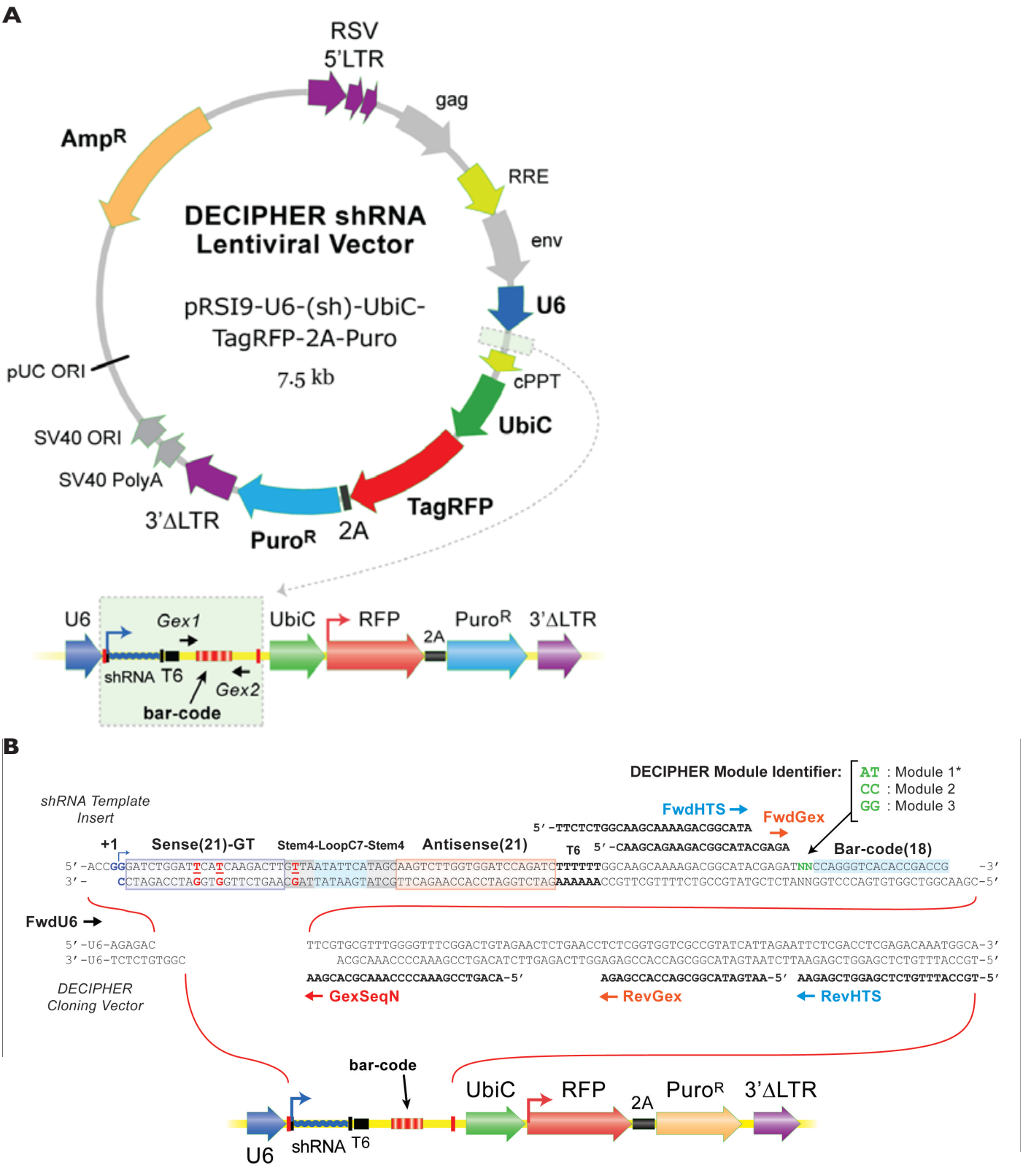

Supplementary figure 1. The Cellecta Lentiviral vector with the individual elements. A) The Cellecta vector with the different promotors, the RFP tag, the Puro resistace, the shRNS and barcode. B) The expression cassette in detail, with the shRNA and barcode.

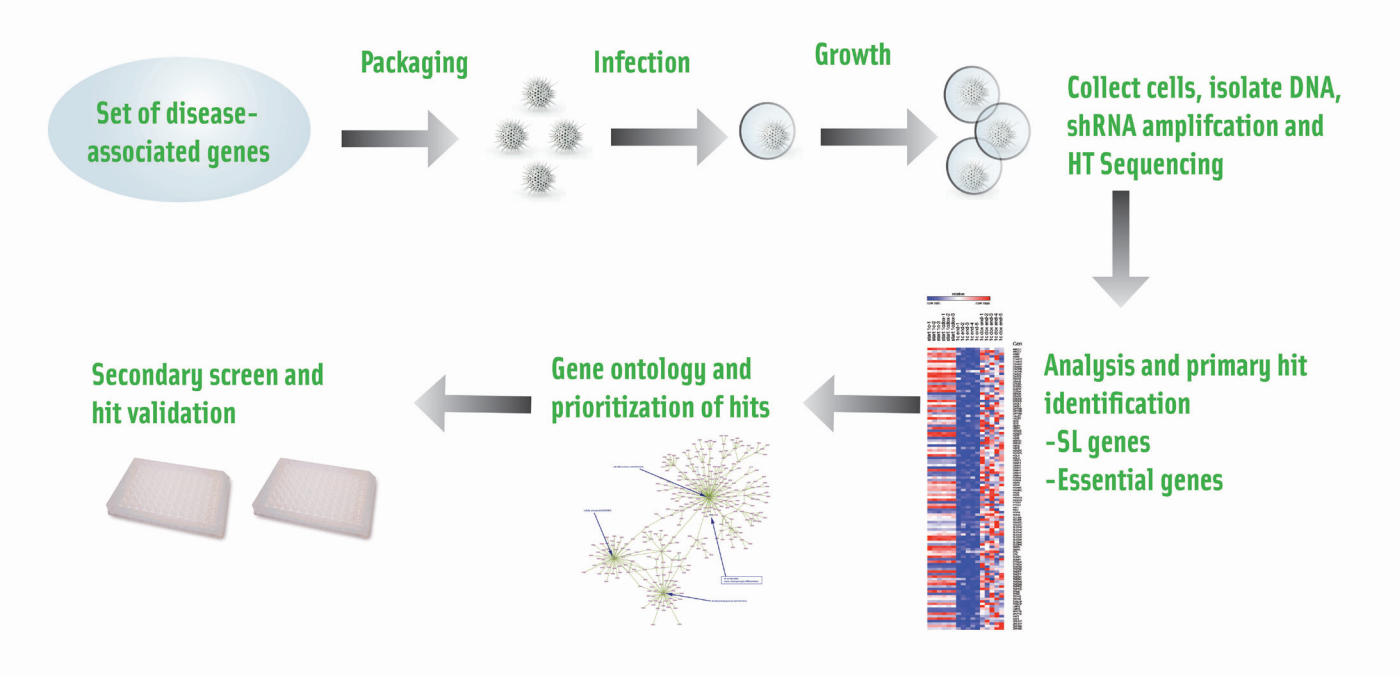

Supplementary figure 2. Overview of the workflow of the shRNA screen

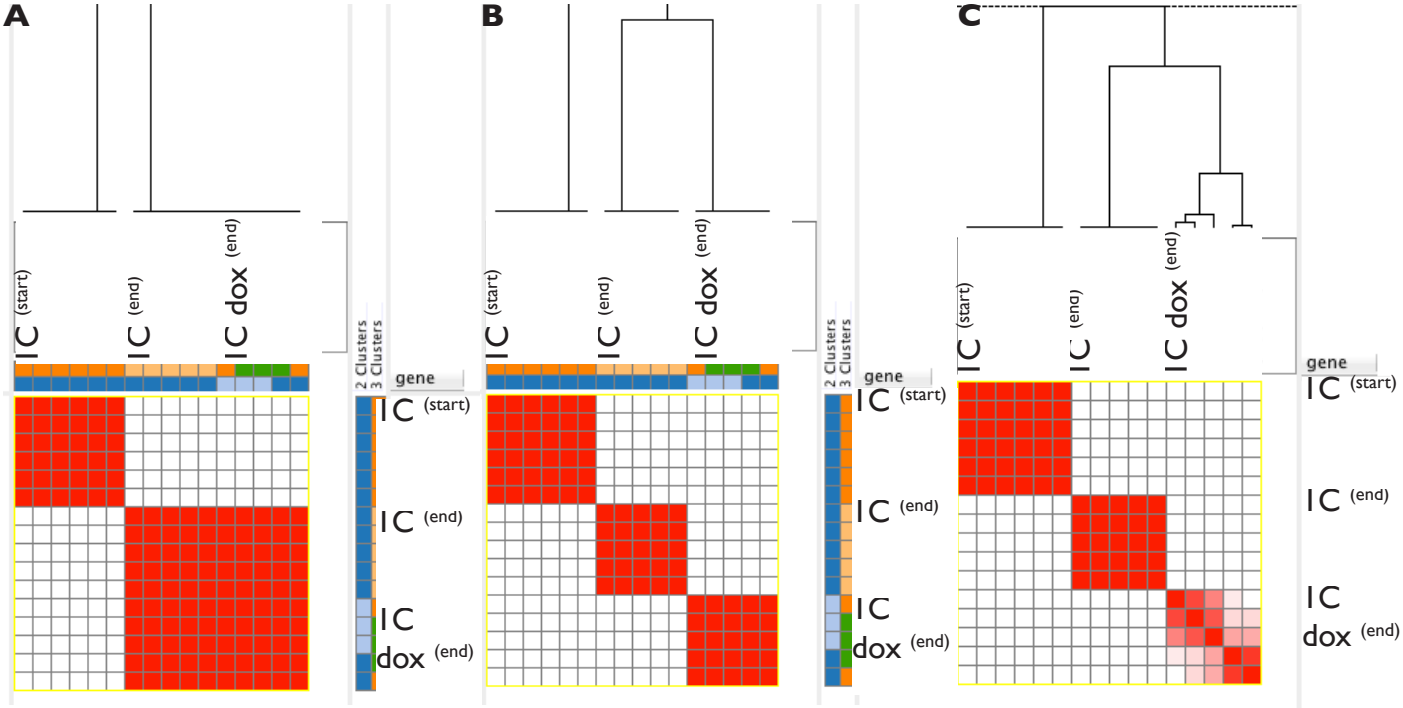

Supplementary figure 3. Cluster plots for the different conditions, to determine the robustness of the data. The analysis was performed in GENE-E. The input for the cluster plots was the normalized reads for the the different groups, $1C^{start}$, $1C^{end}$ and 1C dox^{end}. The blocks represent the different replicates of the group, being 6 replicates for $1C^{start}$ versus 5 replicates for $1C^{end}$ or 1C dox^{end}. A) Consensus clustering on 2 clusters shows a clear separation between $1C^{start}$ versus $1C^{end}$ and 1C dox^{end}. B) Clustering on 3 clusters shows a separation between $1C^{start}$, $1C^{end}$ and 1C dox^{end}. C) Clustering by 5 clusters continues to show a clear separation between $1C^{start}$, $1C^{end}$ and 1C dox^{end}.

Discussion

A. A better understanding of cancer metabolics: what does it signify for Ewing sarcoma?

The EWS-FLI1 fusion protein in Ewing sarcoma acts as a transcriptional regulator to modulate a large network of target genes expression and ongoing EWS-FLI1 expression which is required for maintenance of transformation[12,126,133,143,369]. Although the role of EWS-FLI1 in transcriptional regulation is well documented, little is understood about the role of EWS-FLI1 in the metabolism of Ewing sarcoma. This dissertation focuses on getting a better understanding of the metabolism of Ewing sarcoma to more precisely understand the metabolics of this cancer in general and the metabolic regulation of EWS-FLI1 in particular by using a GC-MS and LC-MS-MS approach.

The global metabolic analysis performed has identified twenty-four commonly changed metabolites in different pathways, implicated in processes such as energy metabolism, the tryptophan pathway, N-glycosylation, fatty acid synthesis and glutathione metabolism. This study has specifically implicated the regulation of EWS-FLI1 on the metabolite kynurenine, a derivative of the amino acid tryptophan.

A better understanding of the specific cancer cell metabolics is relevant on two counts:

1) oncogenic transformation processes are complex and molecular mechanisms that underlie metabolic reprogramming of cancer cells are complex. Together with alterations at a genomic level and oncogenic signaling, this of course coincides with changes at a metabolic level. The interaction between both is highly dynamic and influential. As recent years have shown a strong EWS-FLI1 signature on a genomic level, the integration of metabolics data could thus improves our knowledge and understanding of this childhood tumor[370]. More specifically, the metabolites in the tryptophan pathway that are influenced by EWS-FLI1 appear to play a role in metastasis and immune invasion and response to treatment, described in part B.

2) Metabolics could have an influence on treatment response. In a paper by Scotlandi, they identified genes related to treatment response to chemotherapy[371]. After the identification of a set of genes, they performed a gene ontology analysis, identifying pathways that were altered upon response to chemotherapy. Seven of the 12 pathways that were identified related to metabolism (glutathione, cyanoamino acid, taurine and hypotaurine, arachidonic acid, pyruvate metabolism) or biosynthesis (monoterpenoid or fatty acid biosynthesis). The

others were related to gap junction or to pathways related to the nervous system development and functions. Some of these pathways may be altered in response to chemotherapy in all cancer types; some may be (in)directly linked to or supported by the *EWS-FLI1* oncogene. In this project, some of these pathways, such as the glutathione pathway and fatty acid biosynthesis, have been observed as altered upon EWS-FLI1 inhibition in Ewing sarcoma.

A number of questions will remain after this project. As many metabolites have been significantly increased upon EWS-FLI1 inhibition, the question arises whether this effect is a true valid up regulation of the specific pathway or a stalling of the already present metabolites upon the decreased cell proliferation. The method we used does not have the possibility to differentiate between both hypotheses, as the metabolites are measured at one specific time, not taking in account the dynamic flux in the cellular model underlying the metabolic changes. In the course of my PhD, several dynamic methods have emerged for probing transients in cellular metabolism, being one dynamic metabolic flux analysis (MFA)[372]. MFA measures the flow of carbon through intracellular biochemical pathways of a cancer cell, thereby dynamically measuring the metabolite level of different pathways. This could be a nice addition to the existing current method, to further continue our understanding of the metabolics behind EWS-FLI1.

B. The influence of kynurenine on Ewing sarcoma

Kynurenine, a derivative of the amino acid tryptophan, was identified as being majorly up-regulated upon inhibition of EWS-FLI1. Kynurenine could be of importance for treatment response and resistance in Ewing sarcoma. The current work has led to a hypothesis concerning the involvement of kynurenine in the Ewing sarcoma cell.

During my thesis, Georges-Alain Franzetti, a fellow PhD student, did a proteomics study after inhibition of the fustion protein, to identify proteins that are altered upon EWS-FLI1 inhibition. One of the major pathways that his work has identified is the aryl hydrocarbon receptor (AHR) pathway, a pathway in which several proteins were altered (Figure 1A). The AHR itself is repressed by EWS-FLI1. Kynurenine has been identified as an endogenous ligand of the AHR, linking both project together[347].

AHR is a ligand-dependent basic helix-loop-helix-Per-ARNT-Sim (PAS)-containing transcription factor that responds to a variety of exogenous and endogenous chemicals with the induction/repression of expression of series of genes that influence a wide spectrum of biological and toxic effects in a variety of species and tissues[373–376]. When AHR is not ligand bound, it is located in the cytoplasm, in a chaperone complex with HSP90, AIP, p23 and c-SRC[377–379] (Figure 1B). After AHR binds to a ligand, it disassociates from its chaperones and undergoes a conformational change that exposes its nuclear localization signal (NLS), which then is responsible for the translocation to the nucleus[380]. Here, it forms a heterodimer with aryl hydrocarbon receptor nuclear translocator (ARNT). The heterodimer then binds to a dioxin-responsive element, through which it influences a large quantity of genes involved in carcinogen and drug metabolism.

AHR has been implicated in different cellular processes, such as tumorigenesis, inflammation, embryogenesis, cell motility and migration, inflammation and transformation. Deregulation of these physiological processes is known to contribute to events such as tumor initiation, promotion and progression[381]. Additionally, AHR has been considered a major regulator of xenobiotic-induced carcinogenesis, thereby contributing to treatment resistance.

Kynurenine could potentially be involved in drug metabolism through its interaction with the AHR. In this hypothesis, kynurenine levels are elevated in cells with lower EWS-FLI1 expression. AHR is simultaneously up-regulated in those cells.

When kynurenine binds to AHR, it thus dissociates from its chaperones, translocates from the cytosol to the nucleus, where it binds to ARNT. Here it interacts with specific sequences in target genes to control their transcriptional activity, such as phase I and II xenobiotic enzymes and estrogen signaling pathways. Phase I and II xenobiotic metabolic were to be up-regulated upon EWS-FLI1 binding (Figure 1C). This opens up new exiting future research opportunities in the interaction between metabolics and genetics.

This theory seems somewhat paradoxical, as Ewing sarcoma cells are characterized by a high expression of EWS-FLI1. However, more and more it becomes known that the level of expression of protein biomarkers in a tumor is not equal, but rather a diversity existing at different genetic and epigenetic levels[382–384]. When continuing a bit on this idea, it could be hypothesized that fluctuations at the level of oncogene expression can differentiate between different tumor cells. One could hypothesize then that it is those cells that have a low expression of EWS-FLI1 that are eventually responsible for its influence on treatment resistance. In these cells, the up regulation of kynurenine can activate AHR, which by consequence induces those phase I and II enzymes, thereby playing a role in the elimination and detoxification of xenobiotics[385].

This hypothesis could be verified by introducing a GFP-AHR receptor in the cell, after which cells are inhibited for EWS-FLI1. If the increase in kynurenine and the increase AHR expression is sufficient upon EWS-FLI1 inhibition, kynurenine will bind to the AHR, translocating to the nucleus, a change that could be verified by fluorescent microscopy, or separating the different cellular fractions, the nucleus and cytosol for western blot.

A second hypothesis on how kynurenine contributes to tumorigenesis concerns the immune system. Kynurenine is a regulator of antitumor immune responses via the AHR. Tryptophan is degraded to kynurenine via two enzymes, being TDO2 and IDO. Both IDO and TDO2 are capable of suppressing tumor immunity and promoting immune evasion, due to the depletion of tryptophan and the formation of kynurenine[347,386–388]. Depletion of tryptophan in the local microenvironment results in the activation of the general control nonderepressible 2 (GCN2) kinase, a serine/threonine-protein kinase that senses amino acid deficiency through binding to uncharged transfer RNA (tRNA) and tolerance of T cells[389] . The increased amount of kynurenine binds the AHR in tumor cells and T cells, that once activated results in tolerance in T cells and leads to enhanced clonogenic survival and motility in tumor cells[347,390] .

IDO, *TDO2* and *AHR* are up-regulated when EWS-FLI1 is inhibited. It is in this situation that one could hypothesize that there is an increased immune suppression and enhanced motility in tumor cells. In fact, it was previously shown that inhibition of EWS-FLI1 expression increased cell migration of Ewing sarcoma cells[69]. In this working hypothesis, it is thus possible to imagine that cells in the tumor with lower EWS-FLI1 expression are the ones that migrate out of the tumor and metastasize, an effect supported by the up regulation of kynurenine levels. Several IDO and TDO2 inhibitors have recently been described[391]. It would therefore be possible to treat cells that are inhibited for EWS-FLI1 with an inhibitor, in order to verify that their migration diminishes, therefore giving the perspective that this could be an added therapy in order to avoid metastasis of Ewing sarcoma cells.

A

AHR pathway	Proteins down-regulated by EWS-FLI1
Chaperone proteins AHR	HSP90AB1, HSP90B1, HSPB1
Phase I xenobiotic metabolic enzymes	ALDH7A1
Phase II xenobiotic metabolic enzymes	NQO2, GSTM2, GSTP1
AHR and cell cycle progression	MCM7
Estrogen signaling	CTSD
Cell cycle inhibition	CDK6

B

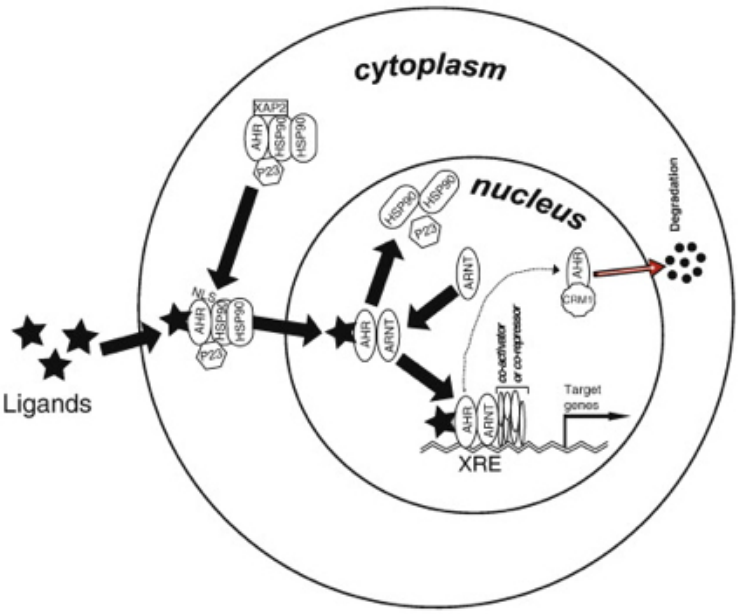

C

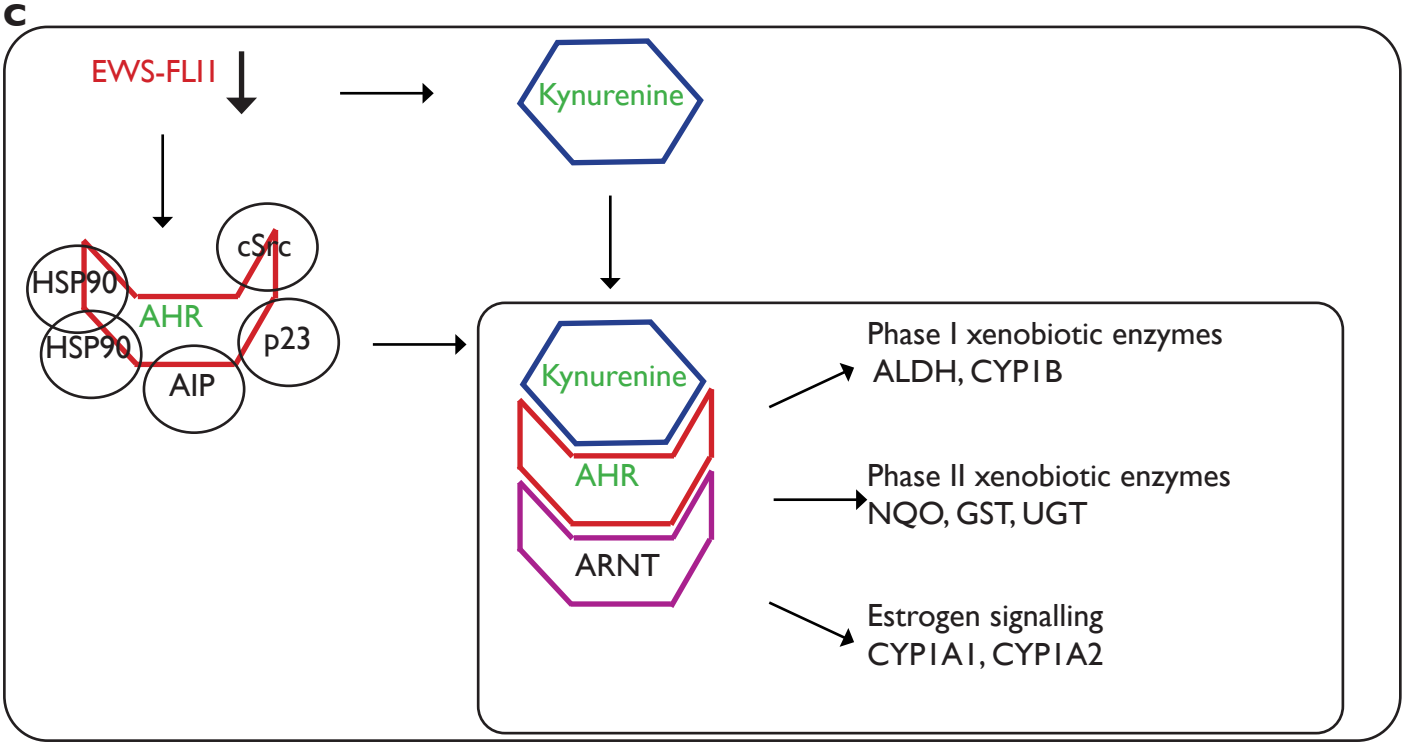

Figure 1: Possible mechanism of resistance in Ewing sarcoma. A) Proteins upregulated upon EWS-FLI1 inhibiting relating to the AHR pathway. B) Functional target regulation of AHR (figure adapted from Feng et al, 2013). C) Possible mechansism of resistance. Cells with lower levels of EWS-FLI1 upregulate kynurenine levels, a derivative of tryptophan. Cells with lower levels of EWS-FLI1 have higher levels of AHR. Upon ligand binding of kynurenine to AHR, it dissociates from its chaperones, translocates from the cytosol to the nucleus, where it binds to ARNT. Here it interacts with specific sequences in target genes to control their transcriptional activity, such as phase I and II xenobiotic enzymes, and estrogen signalling pathways.

C. The search for synthetic lethal genes: balance and perspectives

Ewing sarcoma, the second most commonly occurring pediatric bone tumor is commonly characterized by an *EWS-FLI1* gene fusion[7]. The current treatment of Ewing sarcoma patients consists of chemotherapy, localized surgery and radiation. Although the overall survival for patients is high, the long-term survival for patients with metastatic, disease is significantly reduced being around 35%; patients with relapsed or recurrent tumors show a cumulative survival of less then 10%[1,5,6]. There is thus a high interest to find new, more specific and efficient targets in the treatment of Ewing sarcoma. In recent years, the concept of synthetic lethality has been introduced as a way to find new therapeutic targets in cancer.

Within the framework of my thesis, I have been interested in the search of these synthetic lethal genes in Ewing sarcoma. At the moment I started my thesis, several possibilities had become available in order to discover synthetic lethal genes, such as siRNA and shRNA screens, that could either be performed in arrayed or pooled format, or compound based screenings. Numerous promising results have been published using pooled shRNA screens which have identified genes essential for growth and related phenotypes in different cancer cells[392–395]. This experimental technique started being used as a way to discover synthetic lethal genes, for instance in an shRNA screen performed by Luo et al., who discovered multiple synthetic lethal interactions with the *RAS* oncogene[396]. Several siRNA medium or large scale approaches has also resulted in the identification of synthetic lethal targets, such as in the study performed by Sarthy et al., who equally identified interactions of the *RAS* oncogene[397]. In the Ewing sarcoma field, a targeted small to medium scale kinase siRNA screen has identified MSTR1R inhibition as modifiers of IGF1R[291].

Due to the accessibility of shRNA libraries, which allows for a non-targeted screening of many genes in parallel, we decided to pursue a high-throughput shRNA screen to identify new genes that have a synthetic lethal interaction with EWS-FLI1 in Ewing sarcoma. In this experimental setup, I took a library of more than 5400 disease related genes, which were screened for cell survival and proliferation. The approach that was used is thus non-targeted, meaning that no pre-selection has been made in order to target specific pathways that were already known in the Ewing sarcoma context. The screen has revealed 4 synthetic lethal targets, as well as a group of 789 genes that was found to be essential for both Ewing sarcoma cells, as well as Ewing sarcoma cells that had undergone inhibition of EWS-FLI1.

In the duration of my thesis, several other high-throughput shRNAs have been published, identifying different groups of essential genes in the cancer context. The most extensive investigation of essential genes for cancer growth and survival has been a study by Cheung et al., where more then 11000 genes in 102 cancer cell lines were screened[355]. The majority of the cell lines they used for the paper where of ovarian, colon and pancreatic cancer origin and thus they identified several cancer specific genes, however, they also identified a group of genes that were identified in a large group of cell lines, named "commonly essential genes." High scoring genes in their analysis are *PAX8*, *CCNE1*, *KRAS*, *SOX9* and *RPTOR*[355]. None of these genes was included in our list of screened genes therefore comparison was not possible. This also brought out two of the weaknesses in our screening, as we screened only disease related genes and very few signaling pathways. In the future, it might be beneficial to strengthen this part and screen another group of genes that contain a strong enrichment in cell signaling pathways, but also genes that target cell surface markers, extracellular matrix genes and DNA binding genes. Moreover, in our screening, we only made use of the 1C model, but the screening of Cheung et al. have again shown that inter-cell line variation cannot be neglected, therefore, our approach would have profited from the inclusion of (an) additional cell line model(s).

Furthermore, during my thesis, a study profiling 500 different kinases in Ewing sarcoma has been reported by Arora et al., however they did not investigate a synthetic lethal aspect[398]. The validated 3 genes in the Arora paper were polo-like kinase 1 (*PLK1*), serine threonine kinase 10 (*STK10*) and tyrosine kinase, non- receptor, 2 (*TNK2*)[398]. PLK1 is a mitotic regulator with a diverse range of biologic functions throughout the cell cycle[399,400]. PLK1 inhibition has been considered as a strategy in the treatment of solid tumors and has shown to specifically inhibit *KRAS* mutated tumors[396,401,402]. However, in the findings of Arora et al., it was considered a global lethal gene as it also reduced proliferation of normal fibroblast cells. Our group of 789 lethal genes was compared to this previously published data from Arora et al. and not surprisingly, in our data, *PLK1* was also identified as one of the strongest lethal genes, in both $1C^{end}$ and 1C dox^{end} [398]. These findings indicate that in the Ewing sarcoma context, targeting PLK1 might not be of interest, as it does not specifically inhibit EWS-FLI1 driven cells.

The purpose of my thesis project was to identify candidate synthetic lethal genes, of which 4, *TXNL4A, ORC670, TRYX3* and *PKD1*, have been identified. The newly identified synthetic lethal genes were not previously known in the Ewing sarcoma

literature, thus verifying that large-scale screens have the potential to identify unexpected targets. No common pathway was found to be synthetic lethal as the 4 synthetic lethal genes, are part of different gene families with clearly distinct functions. Only *PKD1* has previously been described in an oncogenic context, the other three genes have not previously been reported as being essential in cancer.

Overall, the scientific progress has provided some additional tools for the functional characterization of the human genome, that are worth considering for further study to identify new (synthetic lethal) targets in the Ewing sarcoma context. Genome-scale RNAi screens have allowed for systematic loss-of-function genomics. However, in order to look at the other side of the spectrum, gain-of-function studies have long not been available for systematic analysis. Recently, several libraries of open reading frames (ORFs) or cDNAs have been published[403,404]. One could imagine over-expressing a gene in the Ewing sarcoma that specifically kills cells harboring the *EWS-FLI1* gene fusion. Therefore, this possibility could be a future perspective in Ewing sarcoma research.

D. *PKD1*: new angle for Ewing sarcoma treatment?

PKD1, a gene that is part of the TRP family and encodes for PC-1, was found to portray a synthetic lethal phenotype when inhibited in Ewing sarcoma. Validation in 3 Ewing sarcoma cell lines, all carrying an EWS-FLI1 gene fusion, demonstrated that knockdown caused a significant decrease in cell number, compared to control transfected cells. PC-1 is a very large glycoprotein that is characterized by a large N-terminus extracellular region, several transmembrane domains as well as a cytoplasmic tail[362,405]. PC-1 is defined as a signaling receptor involved in cell-cell or cell-matrix interactions, however, other functions have also been attributed to PC-1[406–409]. PC-1 has known interactions with the tuberous sclerosis 1 (TSC) complex, Signal Transducers and Activators of Transcription (STAT) proteins, the NFAT pathway, the WNT pathway and glucose signaling (Figure 2A)[367,410]. PC-1 interacts in that the C-terminus binds to and regulates the activity of crucial signaling molecules. This cytoplasmic tail of PC-1 has been shown to bind and activate G proteins, thereby activating c-Jun and AP-1 in a G protein-dependent fashion[411–414].

In order to further characterize the synthetic lethal effect of *PKD1* inhibition in EWS-FLI1, there is a need to understand why PC-1 inhibition kills Ewing sarcoma cells. In the course of my thesis, one of the other members of the laboratory of Olivier Delattre, Franck Tirode, generated RNAseq data on 30 cell lines. Correlation analysis was done using this RNA-seq data from the lab, correlating the expression *PKD1* in Ewing sarcoma with known *PKD1* interacting genes (Figure 2B). *PKD1* was shown to be correlated with *AKT*, *MAPK* and *TSC2* and anti-correlated with *GSK-3*β.

One of the hypotheses behind the synthetic lethal effect of PC-1 inhibition in Ewing sarcoma could be related with the interaction of PC-1 and AKT. The PI3K–AKT pathway has been known to be vital to the growth and survival of cancer cells. PC-1 expression has previously been shown to result in phosphorylation of AKT[368]. Phosphorylation of AKT leads to its activation and activated AKT can then go on to activate or deactivate its myriad substrates (e.g. mTOR) via its kinase activity. A possible hypothesis for the cell death observed in Ewing could thus be that upon inhibition of PC-1, leads to down-regulation of the phosphorylation of AKT, thereby no longer activating its downstream targets, thus creating a decrease in cell growth and survival. As expression of *PKD1* was shown to be correlated with *AKT* in the panel of Ewing sarcoma cell lines and Ewing sarcoma cells showed high expression of *AKT*. It therefore could be thought that in

Ewing sarcoma, low PC-1 leads to low AKT, thus decreasing the growth and survival of cancer cells, whereas cells that do not have high AKT levels (the EWS-FLI1 low/ negative cells), are not as sensitive for PKD1 inhibition, therefore being less prone to show an effect on the growth and survival levels.

PC-1 has previously been shown to inhibit GSK-3β, thereby modulating WNT signaling[415]. In the RNA-seq data, *PKD1* expression was indeed shown to be anti-correlated with *GSK-3*β expression. In non-proliferating cells, GSK-3β is active, while during cellular responses it is inhibited. Substrates of GSK-3β therefore tend to be dephosphorylated, functionally inhibiting them[416]. GSK-3β interacts with a large number of proteins, who have a role in a wide spectrum of cellular processes, such as translation, transcription, proliferation, metabolism, cytoskeletal regulation, cell proliferation and apoptosis[367,417]. The role of GSK-3β in cancer remains somewhat controversial in that it may function as a ‘‘tumor suppressor” for certain types of tumors, but promotes growth and development for some others. GSK3β binds to and phosphorylates several proteins in the WNT pathway and is instrumental to the down regulation of β-catenin[399,400]. Therefore it could be hypothesized that inhibition of PC-1 up-regulates GSK-3β, thereby up regulating the canonical WNT pathway, down regulating proliferation, transcription and translation.

In summary, there are several possible hypotheses explaining the effect of PC-1 inhibition. In order to start determining the cell biology underlying this effect, we first need to determine the expression level of *PKD1* target genes, in order to get a first hint towards the understanding of this synthetic lethal effect. Currently, no PC-1 inhibitors are described, limiting the inhibition of PC-1 to using si and shRNAs.

A

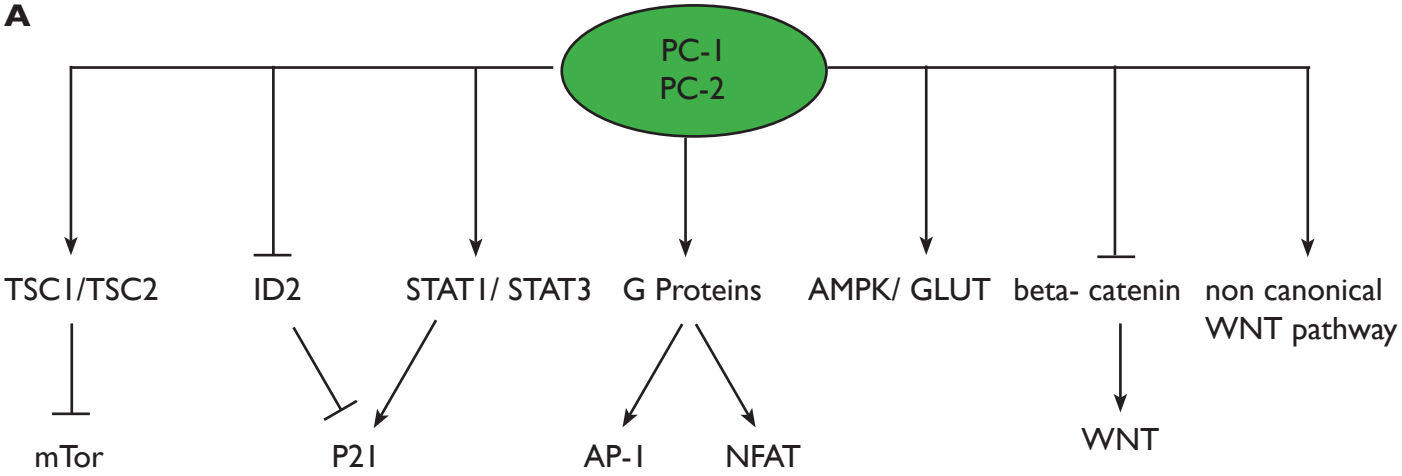

B

coeff corr	PKD1	GSK3B	TSC1	TSC2	MAPK	AKT	PI3K	STAT1	ID2	CDKN1A	SLC2A1	SLC2A4	RUNX2	RCAN1	JAK1	DACT1	MTOR	NFATC1	NFATC2	NFATC3
PKD1		-0.51	0.32	0.74	0.53	0.60	0.23	-0.07	0.25	0.23	-0.25	0.35	0.33	0.21	0.26	0.16	-0.10	0.03	0.35	-0.33
GSK3B	-0.51		0.11	-0.72	-0.49	-0.33	-0.14	0.39	-0.10	-0.33	0.44	-0.25	-0.27	0.01	-0.04	-0.05	0.46	-0.21	-0.21	0.30
TSC1	0.32	0.11		0.13	0.03	0.16	0.21	0.35	0.29	-0.08	-0.07	0.11	-0.10	0.01	0.41	0.09	0.25	-0.11	-0.05	-0.04
TSC2	0.74	-0.72	0.13		0.62	0.48	0.28	-0.32	0.05	0.20	-0.41	0.38	0.23	0.07	-0.02	0.16	-0.37	0.13	0.26	-0.49
MAPK	0.53	-0.49	0.03	0.62		0.34	0.33	-0.21	0.27	0.39	-0.16	0.38	0.33	0.18	0.22	0.12	-0.44	0.03	0.35	-0.19
AKT	0.60	-0.33	0.16	0.48	0.34		0.17	0.12	0.11	0.26	-0.23	0.06	0.49	0.33	0.19	0.35	-0.06	0.27	0.28	-0.26
PI3K	0.23	-0.14	0.21	0.28	0.33	0.17		0.10	0.31	0.19	-0.08	0.30	0.20	0.18	0.23	0.10	-0.39	-0.08	0.26	0.04
STAT1	-0.07	0.39	0.35	-0.32	-0.21	0.12	0.10		0.23	0.11	0.00	-0.05	0.15	0.14	0.37	0.30	0.22	-0.08	0.23	0.07
ID2	0.25	-0.10	0.29	0.05	0.27	0.11	0.31	0.23		0.34	-0.08	0.34	-0.03	0.06	0.54	0.10	-0.15	-0.15	0.36	0.03
CDKN1A	0.23	-0.33	-0.08	0.20	0.39	0.26	0.19	0.11	0.34		-0.26	0.34	0.51	0.24	0.45	0.31	-0.50	0.21	0.53	-0.13
SLC2A1	-0.25	0.44	-0.07	-0.41	-0.16	-0.23	-0.08	0.00	-0.08	-0.26		-0.04	-0.20	0.05	-0.21	-0.07	0.43	-0.18	-0.05	0.11
SLC2A4	0.35	-0.25	0.11	0.38	0.38	0.06	0.30	-0.05	0.34	0.34	-0.04		0.03	0.20	0.17	0.08	-0.28	-0.05	0.44	-0.08
RUNX2	0.33	-0.27	-0.10	0.23	0.33	0.49	0.20	0.15	-0.03	0.51	-0.20	0.03		0.44	0.10	0.54	-0.31	0.38	0.35	-0.22
RCAN1	0.21	0.01	0.01	0.07	0.18	0.33	0.18	0.14	0.06	0.24	0.05	0.20	0.44		0.01	0.44	0.05	0.30	0.36	-0.15
JAK1	0.26	-0.04	0.41	-0.02	0.22	0.19	0.23	0.37	0.54	0.45	-0.21	0.17	0.10	0.01		-0.09	-0.16	-0.21	0.34	0.15
DACT1	0.16	-0.05	0.09	0.16	0.12	0.35	0.10	0.30	0.10	0.31	-0.07	0.08	0.54	0.44	-0.09		-0.01	0.23	0.35	-0.15
MTOR	-0.10	0.46	0.25	-0.37	-0.44	-0.06	-0.39	0.22	-0.15	-0.50	0.43	-0.28	-0.31	0.05	-0.16	-0.01		-0.03	-0.35	0.13
NFATC1	0.03	-0.21	-0.11	0.13	0.03	0.27	-0.08	-0.08	-0.15	0.21	-0.18	-0.05	0.38	0.30	-0.21	0.23	-0.03		0.10	-0.29
NFATC2	0.35	-0.21	-0.05	0.26	0.35	0.28	0.26	0.23	0.36	0.53	-0.05	0.44	0.35	0.36	0.34	0.35	-0.35	0.10		-0.06
NFATC3	-0.33	0.30	-0.04	-0.49	-0.19	-0.26	0.04	0.07	0.03	-0.13	0.11	-0.08	-0.22	-0.15	0.15	-0.15	0.13	-0.29	-0.06	

Figure 2: The possible pathways through which PKD1 can confer synthetic lethality. A) PKD1 affect mutliple signalling pathways. Figure adapted from Chapin and Caplan, JCB, 2010). B) Correlation analysis using previously generated RNA-seq data from the lab, determining the expression of a large panel of genes in Ewing cell lines, revealed a significant positive correlation between *PKD1* and *AKT* and an anticorrelation between GSK3b.

E. General conclusion

Ewing sarcoma is characterized by a chromosomal translocation, most often *EWS-FLI1*. The research dwelled upon in this thesis has been focused on two different parts of this fusion gene; a metabolic role of EWS-FLI1 in Ewing sarcoma and using the concept of synthetic lethality to find genes that confer a synthetic lethal phenotype in combination of EWS-FLI1.

In a combined approach of inhibiting EWS-FLI1 and a global metabolic screen, it was possible to demonstrate different metabolic pathways that are influenced by this oncogene. Among these newly identified different metabolic pathways that are influenced by EWS-FLI1, kynurenine pathway, the glucose pathway, glycosylation pathways, free fatty acids and the glutathione pathway have been of particular interest. The results in the different metabolic pathways of interest were combined with expression data on the enzymes in these pathways, in order to get a better understanding of the mechanisms of cancer-specific metabolic reprogramming.

In terms of using synthetic lethality, this research has aimed at the identification of novel therapeutic targets. In using a pooled shRNA screen approach and an inducible *EWS-FLI1* Ewing sarcoma model, four candidate synthetic lethal genes were identified, after which one was validated in additional Ewing sarcoma cell lines. This last part suggests that selective targeting of PC-1 might be selectively effective against Ewing sarcoma cells.

References

1. Gurney, J., Swensen, A. & Bulterys, M. in *Cancer Incid. Surviv. Child. Adolesc. United States SEER Program 1975-1995* (eds. Ries, L. A. G. *et al.*) 99–110 (National Cancer Institute, SEER Program. NIH Pub., 1999).
2. Bacci, G. *et al.* Pattern of relapse in 290 patients with nonmetastatic Ewing's sarcoma family tumors treated at a single institution with adjuvant and neoadjuvant chemotherapy between 1972 and 1999. *Eur. J. Surg. Oncol. J. Eur. Soc. Surg. Oncol. Br. Assoc. Surg. Oncol.* **32,** 974–979 (2006).
3. Esiashvili, N., Goodman, M. & Marcus, R. B., Jr. Changes in incidence and survival of Ewing sarcoma patients over the past 3 decades: surveillance epidemiology and end results data. *J. Pediatr. Hematol. Oncol.* **30,** 425–430 (2008).
4. Gupta, A. A. *et al.* Clinical outcome of children and adults with localized Ewing sarcoma: impact of chemotherapy dose and timing of local therapy. *Cancer* **116,** 3189–3194 (2010).
5. Ladenstein, R. *et al.* Primary disseminated multifocal Ewing sarcoma: results of the Euro-EWING 99 trial. *J. Clin. Oncol. Off. J. Am. Soc. Clin. Oncol.* **28,** 3284–3291 (2010).
6. Paulussen, M. *et al.* Ewing's tumors with primary lung metastases: survival analysis of 114 (European Intergroup) Cooperative Ewing's Sarcoma Studies patients. *J. Clin. Oncol. Off. J. Am. Soc. Clin. Oncol.* **16,** 3044–3052 (1998).
7. Delattre, O. *et al.* Gene fusion with an ETS DNA-binding domain caused by chromosome translocation in human tumours. *Nature* **359,** 162–165 (1992).
8. Sorensen, P. H. *et al.* A second Ewing's sarcoma translocation, t(21;22), fuses the EWS gene to another ETS-family transcription factor, ERG. *Nat Genet* **6,** 146–51. (1994).
9. Peter, M. *et al.* A new member of the ETS family fused to EWS in Ewing tumors. *Oncogene* **14,** 1159–64. (1997).
10. Jeon, I. S. *et al.* A variant Ewing's sarcoma translocation (7;22) fuses the EWS gene to the ETS gene ETV1. *Oncogene* **10,** 1229–34. (1995).
11. Thompson, A. D., Teitell, M. A., Arvand, A. & Denny, C. T. Divergent Ewing's sarcoma EWS/ETS fusions confer a common tumorigenic phenotype on NIH3T3 cells. *Oncogene* **18,** 5506–13. (1999).
12. Prieur, A., Tirode, F., Cohen, P. & Delattre, O. EWS/FLI-1 silencing and gene profiling of Ewing cells reveal downstream oncogenic pathways and a crucial role for repression of insulin-like growth factor binding protein 3. *Mol Cell Biol* **24,** 7275–83 (2004).
13. May, W. A. *et al.* The Ewing's sarcoma EWS/FLI-1 fusion gene encodes a more potent transcriptional activator and is a more powerful transforming gene than FLI-1. *Mol Cell Biol* **13,** 7393–8 (1993).
14. Ward, P. S. & Thompson, C. B. Metabolic reprogramming: a cancer hallmark even Warburg did not anticipate. *Cancer Cell* **21,** 297–308 (2012).
15. Warburg, O. H., Posener, K. & Negelein, E. Uber den Stoffwechsel der Carcinomzelle. *Biochem J* **152,** 209–344 (1924).
16. Hanahan, D. & Weinberg, R. A. Hallmarks of cancer: the next generation. *Cell* **144,** 646–674 (2011).
17. Herrero-Martín, D. *et al.* Stable interference of EWS–FLI1 in an Ewing sarcoma cell line impairs IGF-1/IGF-1R signalling and reveals TOPK as a new target. *Br. J. Cancer* **101,** 80–90 (2009).
18. Tirode, F. *et al.* Mesenchymal stem cell features of Ewing tumors. *Cancer Cell* **11,** 421–429 (2007).
19. Unknown. Medicine: cancer crusade. *Time Mag.* (1931).
20. Ewing, J. Diffuse endothelioma of bone. *Proc New York Pathol Soc* **21,** 17–24 (1921).

21. Lin, P. P., Wang, Y. & Lozano, G. Mesenchymal stem cells and the origin of Ewing's sarcoma. *Sarcoma* **2011,** (2011).
22. Oberling, C. Les réticulosarcomes et les réticulo-endothéliosarcomes de la moelle osseuse (sarcome d'Ewing). *Bull Ass Fr Cancer* **17,** 259–263 (1928).
23. Bernstein, M. *et al.* Ewing's sarcoma family of tumors: current management. *Oncologist* **11,** 503–519 (2006).
24. Aurias, A., Rimbaut, C., Buffe, D., Dubousset, J. & Mazabraud, A. [Translocation of chromosome 22 in Ewing's sarcoma]. *Comptes Rendus Seances Acad. Sci.* **296,** 1105–7 (1983).
25. Aurias, A., Rimbaut, C., Buffe, D., Zucker, J. M. & Mazabraud, A. Translocation involving chromosome 22 in Ewing's sarcoma. A cytogenetic study of four fresh tumors. *Cancer Genet. Cytogenet.* **12,** 21–5 (1984).
26. Angervall, L. & Enzinger, F. M. Extraskeletal neoplasm resembling Ewing's sarcoma. *Cancer* **36,** 240–251 (1975).
27. Askin, F. B., Rosai, J., Sibley, R. K., Dehner, L. P. & McAlister, W. H. Malignant small cell tumor of the thoracopulmonary region in childhood: a distinctive clinicopathologic entity of uncertain histogenesis. *Cancer* **43,** 2438–2451 (1979).
28. Jaffe, R. *et al.* The neuroectodermal tumor of bone. *Am. J. Surg. Pathol.* **8,** 885–898 (1984).
29. Ushigome, S., Machinami, R. & Sorensen, P. in *Pathol. Genet. Tumours Soft Tissue Bone* (eds. Fletcher, C. D. M., Unni, K. K. & Mertens, F.) 298–300 (IARC Press, 2002).
30. Jawad, M. U. *et al.* Ewing sarcoma demonstrates racial disparities in incidence-related and sex-related differences in outcome. *Cancer* **115,** 3526–3536 (2009).
31. *WHO Classification of Tumours of Soft Tissue and Bone. Fourth Edition*. **5,** (IARC Press, 2013).
32. Hutter, R. V., Francis, K. C. & Foote, F. W. Ewing's Sarcoma in Siblings: Report of the Second Known Occurrence. *Am. J. Surg.* **107,** 598–603 (1964).
33. Joyce, M. J. *et al.* Ewing's sarcoma in female siblings. A clinical report and review of the literature. *Cancer* **53,** 1959–62 (1984).
34. Hartley, A. L. *et al.* Cancer incidence in the families of children with Ewing's tumor. *J. Natl. Cancer Inst.* **83,** 955–956 (1991).
35. Linden, G. & Dunn, J. E. Ewing's sarcoma in Negroes. *Lancet* **1,** 1171 (1970).
36. Jensen, R. D. & Drake, R. M. Rarity of Ewing's tumour in Negroes. *Lancet* **1,** 777 (1970).
37. Li, F. P., Tu, J. T., Liu, F. S. & Shiang, E. L. Rarity of Ewing's sarcoma in China. *Lancet* **1,** 1255 (1980).
38. Worch, J. *et al.* Racial differences in the incidence of mesenchymal tumors associated with EWSR1 translocation. *Cancer Epidemiol Biomarkers Prev* **20,** 449–53 (2011).
39. Potratz, J., Dirksen, U., Jürgens, H. & Craft, A. Ewing sarcoma: clinical state-of-the-art. *Pediatr. Hematol. Oncol.* **29,** 1–11 (2012).
40. Widhe, B. & Widhe, T. Initial symptoms and clinical features in osteosarcoma and Ewing sarcoma. *J. Bone Joint Surg. Am.* **82,** 667–674 (2000).
41. Sneppen, O. & Hansen, L. M. Presenting symptoms and treatment delay in osteosarcoma and Ewing's sarcoma. *Acta Radiol. Oncol.* **23,** 159–162 (1984).
42. Craft, A. W. Challenges in the management of bone tumors--1996. *Ann. N. Y. Acad. Sci.* **824,** 167–179 (1997).
43. Ferrari, S. *et al.* Ewing's sarcoma of bone: relation between clinical characteristics and staging. *Oncol. Rep.* **8,** 553–556 (2001).
44. De Alava, E. & Gerald, W. L. Molecular biology of the Ewing's sarcoma/primitive neuroectodermal tumor family. *J Clin Oncol* **18,** 204–13. (2000).

45. Kovar, H. *et al.* Overexpression of the pseudoautosomal gene MIC2 in Ewing's sarcoma and peripheral primitive neuroectodermal tumor. *Oncogene* **5,** 1067–70. (1990).
46. Baldini, E. H. *et al.* Adults with Ewing's sarcoma/primitive neuroectodermal tumor: adverse effect of older age and primary extraosseous disease on outcome. *Ann. Surg.* **230,** 79–86 (1999).
47. El Weshi, A. *et al.* Extraskeletal Ewing's sarcoma family of tumours in adults: analysis of 57 patients from a single institution. *Clin. Oncol. R. Coll. Radiol. Gt. Br.* **22,** 374–381 (2010).
48. Cotterill, S. J. *et al.* Prognostic factors in Ewing's tumor of bone: analysis of 975 patients from the European Intergroup Cooperative Ewing's Sarcoma Study Group. *J Clin Oncol* **18,** 3108–14. (2000).
49. Paulussen, M. *et al.* Localized Ewing tumor of bone: final results of the cooperative Ewing's Sarcoma Study CESS 86. *J. Clin. Oncol. Off. J. Am. Soc. Clin. Oncol.* **19,** 1818–1829 (2001).
50. Bacci, G. *et al.* Prognostic factors in nonmetastatic Ewing's sarcoma of bone treated with adjuvant chemotherapy: analysis of 359 patients at the Istituto Ortopedico Rizzoli. *J. Clin. Oncol. Off. J. Am. Soc. Clin. Oncol.* **18,** 4–11 (2000).
51. Zucman, J. *et al.* Combinatorial generation of variable fusion proteins in the Ewing family of tumours. *EMBO J.* **12,** 4481–4487 (1993).
52. Zucman, J. *et al.* Cloning and characterization of the Ewing's sarcoma and peripheral neuroepithelioma t(11;22) translocation breakpoints. *Genes. Chromosomes Cancer* **5,** 271–7. (1992).
53. Zoubek, A. *et al.* Does expression of different EWS chimeric transcripts define clinically distinct risk groups of Ewing tumor patients? *J Clin Oncol* **14,** 1245–51. (1996).
54. De Alava, E. *et al.* EWS-FLI1 fusion transcript structure is an independent determinant of prognosis in Ewing's sarcoma. *J Clin Oncol* **16,** 1248–55. (1998).
55. Zoubek, A. *et al.* Variability of EWS chimaeric transcripts in Ewing tumours: a comparison of clinical and molecular data. *Br. J. Cancer* **70,** 908–913 (1994).
56. Le Deley, M. C. *et al.* Impact of EWS-ETS fusion type on disease progression in Ewing's sarcoma/peripheral primitive neuroectodermal tumor: prospective results from the cooperative Euro-E.W.I.N.G. 99 trial. *J Clin Oncol* **28,** 1982–8 (2010).
57. Urano, F., Umezawa, A., Hong, W., Kikuchi, H. & Hata, J. A novel chimera gene between EWS and E1A-F, encoding the adenovirus E1A enhancer-binding protein, in extraosseous Ewing's sarcoma. *Biochem Biophys Res Commun* **219,** 608–12. (1996).
58. Mastrangelo, T. *et al.* A novel zinc finger gene is fused to EWS in small round cell tumor. *Oncogene* **19,** 3799–804. (2000).
59. Sankar, S. & Lessnick, S. L. Promiscuous partnerships in Ewing's sarcoma. *Cancer Genet.* **204,** 351–365 (2011).
60. Shing, D. C. *et al.* FUS/ERG gene fusions in Ewing's tumors. *Cancer Res.* **63,** 4568–4576 (2003).
61. Ng, T. L. *et al.* Ewing sarcoma with novel translocation t(216) producing an in-frame fusion of FUS and FEV. *J Mol Diagn* (2007).
62. Szuhai, K. *et al.* The NFATc2 gene is involved in a novel cloned translocation in a Ewing sarcoma variant that couples its function in immunology to oncology. *Clin. Cancer Res.* **15,** 2259–2268 (2009).
63. Wang, L. *et al.* Undifferentiated small round cell sarcomas with rare EWS gene fusions: identification of a novel EWS-SP3 fusion and of additional cases with the EWS-ETV1 and EWS-FEV fusions. *J. Mol. Diagn. JMD* **9,** 498–509 (2007).
64. Yamaguchi, S. *et al.* EWSR1 is fused to POU5F1 in a bone tumor with translocation

t(6;22)(p21;q12). *Genes. Chromosomes Cancer* **43,** 217–222 (2005).
65. Sumegi, J. *et al.* A novel t(4;22)(q31;q12) produces an EWSR1-SMARCA5 fusion in extraskeletal Ewing sarcoma/primitive neuroectodermal tumor. *Mod. Pathol. Off. J. United States Can. Acad. Pathol. Inc* **24,** 333–342 (2011).
66. Pierron, G. *et al.* A new subtype of bone sarcoma defined by BCOR-CCNB3 gene fusion. *Nat. Genet.* **44,** 461–466 (2012).
67. Richkind, K. E., Romansky, S. G. & Finklestein, J. Z. t(4;19)(q35;q13.1): A recurrent change in primitive mesenchymal tumors? *Cancer Genet. Cytogenet.* **87,** 71–74 (1996).
68. Specht, K. *et al.* Distinct transcriptional signature and immunoprofile of CIC-DUX4 fusion-positive round cell tumors compared to EWSR1-rearranged ewing sarcomas: Further evidence toward distinct pathologic entities. *Genes. Chromosomes Cancer* (2014). doi:10.1002/gcc.22172
69. Chaturvedi, A., Hoffman, L. M., Welm, A. L., Lessnick, S. L. & Beckerle, M. C. The EWS/FLI oncogene drives changes in cellular morphology, adhesion, and migration in Ewing sarcoma. *Genes Cancer* **3,** 102–116 (2012).
70. Lynn, M. *et al.* High-resolution genome-wide copy-number analyses identify localized copy-number alterations in Ewing sarcoma. *Diagn. Mol. Pathol. Am. J. Surg. Pathol. Part B* **22,** 76–84 (2013).
71. Armengol, G. *et al.* Recurrent gains of 1q, 8 and 12 in the Ewing family of tumours by comparative genomic hybridization. *Br. J. Cancer* **75,** 1403–9 (1997).
72. Hattinger, C. M., Rumpler, S., Kovar, H. & Ambros, P. F. Fine-mapping of cytogenetically undetectable EWS/ERG fusions on DNA fibers of Ewing tumors. *Cytogenet Cell Genet* **93,** 29–35 (2001).
73. Fejes, A. P. *et al.* FindPeaks 3.1: a tool for identifying areas of enrichment from massively parallel short-read sequencing technology. *Bioinforma. Oxf. Engl.* **24,** 1729–30 (2008).
74. Kullendorff, C. M. *et al.* Cytogenetic aberrations in Ewing sarcoma: are secondary changes associated with clinical outcome? *Med Pediatr Oncol* **32,** 79–83. (1999).
75. Tarkkanen, M. *et al.* Clinical correlations of genetic changes by comparative genomic hybridization in Ewing sarcoma and related tumors. *Cancer Genet. Cytogenet.* **114,** 35–41 (1999).
76. Brisset, S. *et al.* CGH analysis of secondary genetic changes in Ewing tumors: correlation with metastatic disease in a series of 43 cases. *Cancer Genet Cytogenet* **130,** 57–61 (2001).
77. Ozaki, T. *et al.* Genetic imbalances revealed by comparative genomic hybridization in Ewing tumors. *Genes. Chromosomes Cancer* **32,** 164–71 (2001).
78. Hattinger, C. M. *et al.* Prognostic impact of chromosomal aberrations in Ewing tumours. *Br. J. Cancer* **86,** 1763–1769 (2002).
79. Kovar, H. *et al.* Narrow spectrum of infrequent p53 mutations and absence of MDM2 amplification in Ewing tumours. *Oncogene* **8,** 2683–90. (1993).
80. Huang, H. Y. *et al.* Ewing sarcomas with p53 mutation or p16/p14ARF homozygous deletion: a highly lethal subset associated with poor chemoresponse. *J Clin Oncol* **23,** 548–58 (2005).
81. De Alava, E. *et al.* Prognostic impact of P53 status in Ewing sarcoma. *Cancer* **89,** 783–92. (2000).
82. Nunn, M. F., Seeburg, P. H., Moscovici, C. & Duesberg, P. H. Tripartite structure of the avian erythroblastosis virus E26 transforming gene. *Nature* **306,** 391–395 (1983).
83. Leprince, D. *et al.* A putative second cell-derived oncogene of the avian leukaemia retrovirus E26. *Nature* **306,** 395–397 (1983).
84. Sharrocks, A. D. The ETS-domain transcription factor family. *Nat. Rev. Mol. Cell Biol.* **2,** 827–837 (2001).

85. Hollenhorst, P. C., McIntosh, L. P. & Graves, B. J. Genomic and biochemical insights into the specificity of ETS transcription factors. *Annu. Rev. Biochem.* **80,** 437–471 (2011).
86. Sharrocks, A. D., Brown, A. L., Ling, Y. & Yates, P. R. The ETS-domain transcription factor family. *Int. J. Biochem. Cell Biol.* **29,** 1371–1387 (1997).
87. Graves, B. J. & Petersen, J. M. Specificity within the ets family of transcription factors. *Adv. Cancer Res.* **75,** 1–55 (1998).
88. Klämbt, C. The Drosophila gene pointed encodes two ETS-like proteins which are involved in the development of the midline glial cells. *Dev. Camb. Engl.* **117,** 163–176 (1993).
89. Lacronique, V. *et al.* A TEL-JAK2 fusion protein with constitutive kinase activity in human leukemia. *Science* **278,** 1309–1312 (1997).
90. Kim, C. A. *et al.* Polymerization of the SAM domain of TEL in leukemogenesis and transcriptional repression. *EMBO J.* **20,** 4173–4182 (2001).
91. Baker, D. A., Mille-Baker, B., Wainwright, S. M., Ish-Horowicz, D. & Dibb, N. J. Mae mediates MAP kinase phosphorylation of Ets transcription factors in Drosophila. *Nature* **411,** 330–334 (2001).
92. Fenrick, R. *et al.* Both TEL and AML-1 contribute repression domains to the t(1221) fusion protein. *Mol Cell Biol* **19,** 6566–74. (1999).
93. Rao, V. N., Ohno, T., Prasad, D. D., Bhattacharya, G. & Reddy, E. S. Analysis of the DNA-binding and transcriptional activation functions of human Fli-1 protein. *Oncogene* **8,** 2167–2173 (1993).
94. Mavrothalassitis, G. & Ghysdael, J. Proteins of the ETS family with transcriptional repressor activity. *Oncogene* **19,** 6524–6532 (2000).
95. Ghysdael, J. & Boureux, A. in *Oncog. Transcr. Regul.* (eds. Yaniv, M. & Ghysdael, J.) 29–88 (Birkhäuser, 1997).
96. Li, R., Pei, H. & Watson, D. K. Regulation of Ets function by protein - protein interactions. *Oncogene* **19,** 6514–6523 (2000).
97. Imler, J. L., Schatz, C., Wasylyk, C., Chatton, B. & Wasylyk, B. A Harvey-ras responsive transcription element is also responsive to a tumour-promoter and to serum. *Nature* **332,** 275–278 (1988).
98. Bradford, A. P. *et al.* The Pit-1 homeodomain and beta-domain interact with Ets-1 and modulate synergistic activation of the rat prolactin promoter. *J. Biol. Chem.* **275,** 3100–3106 (2000).
99. Yordy, J. S. & Muise-Helmericks, R. C. Signal transduction and the Ets family of transcription factors. *Oncogene* **19,** 6503–6513 (2000).
100. Seth, A. & Watson, D. K. ETS transcription factors and their emerging roles in human cancer. *Eur. J. Cancer Oxf. Engl. 1990* **41,** 2462–2478 (2005).
101. Hassler, M. & Richmond, T. J. The B-box dominates SAP-1-SRF interactions in the structure of the ternary complex. *EMBO J.* **20,** 3018–3028 (2001).
102. Zinszner, H., Albalat, R. & Ron, D. A novel effector domain from the RNA-binding protein TLS or EWS is required for oncogenic transformation by CHOP. *Genes Dev* **8,** 2513–26. (1994).
103. Morohoshi, F., Arai, K., Takahashi, E. I., Tanigami, A. & Ohki, M. Cloning and mapping of a human RBP56 gene encoding a putative RNA binding protein similar to FUS/TLS and EWS proteins. *Genomics* **38,** 51–7. (1996).
104. Andersson, M. K. *et al.* The multifunctional FUS, EWS and TAF15 proto-oncoproteins show cell type-specific expression patterns and involvement in cell spreading and stress response. *BMC Cell Biol.* **9,** 37 (2008).
105. Tan, A. Y. & Manley, J. L. The TET family of proteins: functions and roles in disease. *J. Mol. Cell Biol.* **1,** 82–92 (2009).
106. Lee, K. A. W. Ewings family oncoproteins: drunk, disorderly and in search of partners.

Cell Res. **17,** 286–288 (2007).
107. Burd, C. G. & Dreyfuss, G. Conserved structures and diversity of functions of RNA-binding proteins. *Science* **265,** 615–621 (1994).
108. Iko, Y. *et al.* Domain architectures and characterization of an RNA-binding protein, TLS. *J. Biol. Chem.* **279,** 44834–44840 (2004).
109. Bertolotti, A. *et al.* EWS, but not EWS-FLI-1, is associated with both TFIID and RNA polymerase II: interactions between two members of the TET family, EWS and hTAFII68, and subunits of TFIID and RNA polymerase II complexes. *Mol Cell Biol* **18,** 1489–97. (1998).
110. Petermann, R. *et al.* Oncogenic EWS-Fli1 interacts with hsRPB7, a subunit of human RNA polymerase II. *Oncogene* **17,** 603–10. (1998).
111. Alliegro, M. C. & Alliegro, M. A. A nuclear protein regulated during the transition from active to quiescent phenotype in cultured endothelial cells. *Dev Biol* **174,** 288–97. (1996).
112. Araya, N. *et al.* Cooperative interaction of EWS with CREB-binding protein selectively activates hepatocyte nuclear factor 4-mediated transcription. *J Biol Chem* **278,** 5427–32 (2003).
113. Tan, A. Y. & Manley, J. L. TLS inhibits RNA polymerase III transcription. *Mol. Cell. Biol.* **30,** 186–196 (2010).
114. Yang, L., Embree, L. J., Tsai, S. & Hickstein, D. D. Oncoprotein TLS interacts with serine-arginine proteins involved in RNA splicing. *J Biol Chem* **273,** 27761–4. (1998).
115. Yang, L., Embree, L. J. & Hickstein, D. D. TLS-ERG leukemia fusion protein inhibits RNA splicing mediated by serine-arginine proteins. *Mol Cell Biol* **20,** 3345–54. (2000).
116. Lerga, A. *et al.* Identification of a RNA binding specificity for the potential splicing factor TLS. *J Biol Chem* **11,** 10 (2000).
117. Guipaud, O. *et al.* An in vitro enzymatic assay coupled to proteomics analysis reveals a new DNA processing activity for Ewing sarcoma and TAF(II)68 proteins. *Proteomics* **6,** 5962–5972 (2006).
118. May, W. A. *et al.* Ewing sarcoma 11;22 translocation produces a chimeric transcription factor that requires the DNA-binding domain encoded by FLI1 for transformation. *Proc. Natl. Acad. Sci. U. S. A.* **90,** 5752–5756 (1993).
119. Lessnick, S. L., Braun, B. S., Denny, C. T. & May, W. A. Multiple domains mediate transformation by the Ewing's sarcoma EWS/FLI-1 fusion gene. *Oncogene* **10,** 423–31. (1995).
120. Hahm, K. B. Repression of the gene encoding the TGF-beta type II receptor is a major target of the EWS-FLI1 oncoprotein. *Nat Genet* **23,** 481. (1999).
121. Nakatani, F. *et al.* Identification of p21WAF1/CIP1 as a direct target of EWS-Fli1 oncogenic fusion protein. *J Biol Chem* **278,** 15105–15 (2003).
122. Ohno, T., Rao, V. N. & Reddy, E. S. EWS/Fli-1 chimeric protein is a transcriptional activator. *Cancer Res* **53,** 5859–63 (1993).
123. Ben-David, Y., Giddens, E. B., Letwin, K. & Bernstein, A. Erythroleukemia induction by Friend murine leukemia virus: insertional activation of a new member of the ets gene family, Fli-1, closely linked to c-ets-1. *Genes Dev.* **5,** 908–918 (1991).
124. Guillon, N. *et al.* The oncogenic EWS-FLI1 protein binds in vivo GGAA microsatellite sequences with potential transcriptional activation function. *PLoS ONE* **4,** e4932 (2009).
125. Gangwal, K. *et al.* Microsatellites as EWS/FLI response elements in Ewing's sarcoma. *Proc. Natl. Acad. Sci. U. S. A.* **105,** 10149–54 (2008).
126. Smith, R. *et al.* Expression profiling of EWS/FLI identifies NKX2.2 as a critical target gene in Ewing's sarcoma. *Cancer Cell* **9,** 405–16 (2006).
127. Aman, P. *et al.* Expression patterns of the human sarcoma-associated genes FUS and EWS and the genomic structure of FUS. *Genomics* **37,** 1–8. (1996).
128. Turc-Carel, C., Philip, I., Berger, M. P., Philip, T. & Lenoir, G. M. Chromosome study of Ewing's sarcoma (ES) cell lines. Consistency of a reciprocal translocation t(11;22)(q24;q12).

Cancer Genet. Cytogenet. **12,** 1–19 (1984).
129. Toomey, E. C., Schiffman, J. D. & Lessnick, S. L. Recent advances in the molecular pathogenesis of Ewing's sarcoma. *Oncogene* **29,** 4504–16 (2010).
130. Bachmaier, R. *et al.* O-GlcNAcylation is involved in the transcriptional activity of EWS-FLI1 in Ewing's sarcoma. *Oncogene* **28,** 1280–4 (2009).
131. Toretsky, J. A. *et al.* Oncoprotein EWS-FLI1 activity is enhanced by RNA helicase A. *Cancer Res.* **66,** 5574–81 (2006).
132. Ramakrishnan, R. *et al.* Role of protein-protein interactions in the antiapoptotic function of EWS-Fli-1. *Oncogene* **23,** 7087–94 (2004).
133. Kinsey, M., Smith, R. & Lessnick, S. L. NR0B1 is required for the oncogenic phenotype mediated by EWS/FLI in Ewing's sarcoma. *Mol Cancer Res* **4,** 851–9 (2006).
134. Zwerner, J. P. *et al.* The EWS/FLI1 oncogenic transcription factor deregulates GLI1. *Oncogene* **27,** 3282–3291 (2008).
135. Beauchamp, E. *et al.* GLI1 is a direct transcriptional target of EWS-FLI1 oncoprotein. *J. Biol. Chem.* **284,** 9074–9082 (2009).
136. Siligan, C. *et al.* EWS-FLI1 target genes recovered from Ewing's sarcoma chromatin. *Oncogene* **24,** 2512–24 (2005).
137. Luo, W. *et al.* GSTM4 is a microsatellite-containing EWS/FLI target involved in Ewing's sarcoma oncogenesis and therapeutic resistance. *Oncogene* **28,** 4126–32 (2009).
138. Tirado, O. M. *et al.* Caveolin-1 (CAV1) is a target of EWS/FLI-1 and a key determinant of the oncogenic phenotype and tumorigenicity of Ewing's sarcoma cells. *Cancer Res.* **66,** 9937–47 (2006).
139. Fuchs, B., Inwards, C. Y. & Janknecht, R. Vascular endothelial growth factor expression is up-regulated by EWS-ETS oncoproteins and Sp1 and may represent an independent predictor of survival in Ewing's sarcoma. *Clin Cancer Res* **10,** 1344–53 (2004).
140. Ohali, A. *et al.* Association between telomerase activity and outcome in patients with nonmetastatic Ewing family of tumors. *J. Clin. Oncol. Off. J. Am. Soc. Clin. Oncol.* **21,** 3836–3843 (2003).
141. Richter, G. H. *et al.* EZH2 is a mediator of EWS/FLI1 driven tumor growth and metastasis blocking endothelial and neuro-ectodermal differentiation. *Proc. Natl. Acad. Sci. U. S. A.* **106,** 5324–9 (2009).
142. Surdez, D. *et al.* Targeting the EWSR1-FLI1 oncogene-induced protein kinase PKC-β abolishes Ewing sarcoma growth. *Cancer Res.* **72,** 4494–4503 (2012).
143. Stoll, G. *et al.* Systems biology of Ewing sarcoma: a network model of EWS-FLI1 effect on proliferation and apoptosis. *Nucleic Acids Res.* (2013). doi:10.1093/nar/gkt678
144. Klevernic, I. V., Morton, S., Davis, R. J. & Cohen, P. Phosphorylation of Ewing's sarcoma protein (EWS) and EWS-Fli1 in response to DNA damage. *Biochem. J.* **418,** 625 (2009).
145. Olsen, R. J. & Hinrichs, S. H. Phosphorylation of the EWS IQ domain regulates transcriptional activity of the EWS/ATF1 and EWS/FLI1 fusion proteins. *Oncogene* **20,** 1756–64 (2001).
146. Sankar, S. *et al.* Mechanism and relevance of EWS/FLI-mediated transcriptional repression in Ewing sarcoma. *Oncogene* **17**, 5089-100 (2013).
147. Krebs, H. Otto Heinrich Warburg. 1883-1970. *Biogr Mems Fell R Soc* **18,** 628–699 (1972).
148. Warburg, O. H. Versuche an überlebendem Carcinom-Gewebe (methoden). *Biochem J* **142,** 317–333 (1923).
149. Warburg, O. H. *Uber den Stoffwechsel der Tumoren. Arbeiten aus dem Kaiser Wilhelm-Institüt für Biologie*. (Julius Springer, 1926).
150. Höxtermann, E. & Sucker, U. *Otto Warburg*. (BSB B.G. Teubner Verlagsgesellschaft, 1989).

151. Koppenol, W. H., Bounds, P. L. & Dang, C. V. Otto Warburg's contributions to current concepts of cancer metabolism. *Nat. Rev. Cancer* **11,** 325–337 (2011).
152. Warburg, O. H. On the formation of lactic acid with growth. *Biochem. J.* **160,** 307–311 (1925).
153. Warburg, O. H. The metabolism of tumors in the body. *J Gen Physiol* **8,** 519–530 (1927).
154. Cori, C. F. & Cori, G. T. The carbohydrate metabolism of tumors. I. The free sugar, lactic acid, and glycogen content of malignant tumors. *J. Biol. Chem* 11–22 (1925).
155. Cori, C. F. & Cori, G. T. The carbohydrate metabolism of tumors. II. Changes in the sugar, lactic acid, and co-combing power of blood passing through a tumor. *J. Biol. Chem* 397–405 (1925).
156. DeBerardinis, R. J. & Thompson, C. B. Cellular metabolism and disease: what do metabolic outliers teach us? *Cell* **148,** 1132–1144 (2012).
157. Kanehisa, M. Kyoto Encyclopedia of Genes and Genomes. *www.genome.jp/kegg*
158. Lum, J. J. *et al.* Growth factor regulation of autophagy and cell survival in the absence of apoptosis. *Cell* **120,** 237–248 (2005).
159. Gibbons, J. J., Abraham, R. T. & Yu, K. Mammalian target of rapamycin: discovery of rapamycin reveals a signaling pathway important for normal and cancer cell growth. *Semin. Oncol.* **36 Suppl 3,** S3–S17 (2009).
160. Hardie, D. G. AMP-activated protein kinase: an energy sensor that regulates all aspects of cell function. *Genes Dev.* **25,** 1895–1908 (2011).
161. Zhang, H. & Forman, H. J. Glutathione synthesis and its role in redox signaling. *Semin. Cell Dev. Biol.* **23,** 722–728 (2012).
162. Kaplowitz, N., Aw, T. Y. & Ookhtens, M. The regulation of hepatic GSH. *Annu Rev Pharmacol Toxicol* **25,** 714–744 (1985).
163. Akerboom, T. P., Bilzer, M. & Sies, H. The relationship of biliary glutathione disulfide efflux and intracellular glutathione disulfide content in perfused rat liver. *J. Biol. Chem.* **257,** 4248–4252 (1982).
164. Ballatori, N. *et al.* Glutathione dysregulation and the etiology and progression of human diseases. *Biol. Chem.* **390,** 191–214 (2009).
165. Forman, H. J., Zhang, H. & Rinna, A. Glutathione: overview of its protective roles, measurement, and biosynthesis. *Mol. Aspects Med.* **30,** 1–12 (2009).
166. Meredith, M. J. & Reed, D. J. Status of the mitochondrial pool of glutathione in the isolated hepatocyte. *J. Biol. Chem.* **257,** 3747–3753 (1982).
167. Hwang, C., Sinskey, A. J. & Lodish, H. F. Oxidized redox state of glutathione in the endoplasmic reticulum. *Science* **257,** 1496–1502 (1992).
168. Yuan, L. & Kaplowitz, N. Glutathione in liver diseases and hepatotoxicity. *Mol. Aspects Med.* **30,** 29–41 (2009).
169. Zhang, H. & Forman, H. J. Redox regulation of gamma-glutamyl transpeptidase. *Am. J. Respir. Cell Mol. Biol.* **41,** 509–515 (2009).
170. Griffith, O. W., Bridges, R. J. & Meister, A. Formation of gamma-glutamycyst(e)ine in vivo is catalyzed by gamma-glutamyl transpeptidase. *Proc. Natl. Acad. Sci. U. S. A.* **78,** 2777–2781 (1981).
171. Meister, A. New developments in glutathione metabolism and their potential application in therapy. *Hepatol. Baltim. Md* **4,** 739–742 (1984).
172. Lu, S. C. Glutathione synthesis. *Biochim. Biophys. Acta* **1830,** 3143–3153 (2013).
173. Biswas, S., Lunec, J. & Bartlett, K. Non-glucose metabolism in cancer cells--is it all in the fat? *Cancer Metastasis Rev.* **31,** 689–698 (2012).
174. DeBerardinis, R. J. Is cancer a disease of abnormal cellular metabolism? New angles on an old idea. *Genet. Med. Off. J. Am. Coll. Med. Genet.* **10,** 767–777 (2008).

175. Semenza, G. L. Defining the role of hypoxia-inducible factor 1 in cancer biology and therapeutics. *Oncogene* **29,** 625–634 (2010).
176. Shanware, N. P., Mullen, A. R., DeBerardinis, R. J. & Abraham, R. T. Glutamine: pleiotropic roles in tumor growth and stress resistance. *J. Mol. Med. Berl. Ger.* **89,** 229–236 (2011).
177. Jones, R. G. & Thompson, C. B. Tumor suppressors and cell metabolism: a recipe for cancer growth. *Genes Dev.* **23,** 537–548 (2009).
178. Parsons, D. W. *et al.* An integrated genomic analysis of human glioblastoma multiforme. *Science* **321,** 1807–1812 (2008).
179. Yan, H. *et al.* IDH1 and IDH2 mutations in gliomas. *N. Engl. J. Med.* **360,** 765–773 (2009).
180. Mardis, E. R. *et al.* Recurring mutations found by sequencing an acute myeloid leukemia genome. *N. Engl. J. Med.* **361,** 1058–1066 (2009).
181. Kaelin, W. G., Jr & Thompson, C. B. Q&A: Cancer: clues from cell metabolism. *Nature* **465,** 562–564 (2010).
182. Pouysségur, J., Dayan, F. & Mazure, N. M. Hypoxia signalling in cancer and approaches to enforce tumour regression. *Nature* **441,** 437–443 (2006).
183. Koukourakis, M. I., Giatromanolaki, A., Harris, A. L. & Sivridis, E. Comparison of metabolic pathways between cancer cells and stromal cells in colorectal carcinomas: a metabolic survival role for tumor-associated stroma. *Cancer Res.* **66,** 632–637 (2006).
184. Swietach, P., Vaughan-Jones, R. D. & Harris, A. L. Regulation of tumor pH and the role of carbonic anhydrase 9. *Cancer Metastasis Rev.* **26,** 299–310 (2007).
185. Fischer, K. *et al.* Inhibitory effect of tumor cell-derived lactic acid on human T cells. *Blood* **109,** 3812–3819 (2007).
186. Gatenby, R. A. & Gillies, R. J. Why do cancers have high aerobic glycolysis? *Nat. Rev. Cancer* **4,** 891–899 (2004).
187. Kroemer, G. & Pouyssegur, J. Tumor cell metabolism: cancer's Achilles' heel. *Cancer Cell* **13,** 472–482 (2008).
188. Wang, H. Q. *et al.* Positive feedback regulation between AKT activation and fatty acid synthase expression in ovarian carcinoma cells. *Oncogene* **24,** 3574–3582 (2005).
189. Wong, K.-K., Engelman, J. A. & Cantley, L. C. Targeting the PI3K signaling pathway in cancer. *Curr. Opin. Genet. Dev.* **20,** 87–90 (2010).
190. Plas, D. R. & Thompson, C. B. Akt-dependent transformation: there is more to growth than just surviving. *Oncogene* **24,** 7435–7442 (2005).
191. Elstrom, R. L. *et al.* Akt stimulates aerobic glycolysis in cancer cells. *Cancer Res.* **64,** 3892–3899 (2004).
192. Robey, R. B. & Hay, N. Is Akt the 'Warburg kinase'?-Akt-energy metabolism interactions and oncogenesis. *Semin. Cancer Biol.* **19,** 25–31 (2009).
193. Manning, B. D. & Cantley, L. C. AKT/PKB signaling: navigating downstream. *Cell* **129,** 1261–1274 (2007).
194. Cairns, R. A., Harris, I. S. & Mak, T. W. Regulation of cancer cell metabolism. *Nat. Rev. Cancer* **11,** 85–95 (2011).
195. Kuhajda, F. P. AMP-activated protein kinase and human cancer: cancer metabolism revisited. *Int. J. Obes. 2005* **32 Suppl 4,** S36–41 (2008).
196. Shackelford, D. B. & Shaw, R. J. The LKB1-AMPK pathway: metabolism and growth control in tumour suppression. *Nat. Rev. Cancer* **9,** 563–575 (2009).
197. Jones, R. G. *et al.* AMP-activated protein kinase induces a p53-dependent metabolic checkpoint. *Mol. Cell* **18,** 283–293 (2005).
198. Marshall, S., Bacote, V. & Traxinger, R. R. Discovery of a metabolic pathway mediating glucose-induced desensitization of the glucose transport system. Role of hexosamine biosynthesis in the induction of insulin resistance. *J. Biol. Chem.* **266,** 4706–4712 (1991).

199. Fang, M. *et al.* The ER UDPase ENTPD5 promotes protein N-glycosylation, the Warburg effect, and proliferation in the PTEN pathway. *Cell* **143,** 711–724 (2010).
200. Vander Heiden, M. G., Cantley, L. C. & Thompson, C. B. Understanding the Warburg effect: the metabolic requirements of cell proliferation. *Science* **324,** 1029–1033 (2009).
201. Gao, P. *et al.* HIF-dependent antitumorigenic effect of antioxidants in vivo. *Cancer Cell* **12,** 230–238 (2007).
202. Bell, E. L., Emerling, B. M. & Chandel, N. S. Mitochondrial regulation of oxygen sensing. *Mitochondrion* **5,** 322–332 (2005).
203. Takahashi, A. *et al.* Mitogenic signalling and the p16INK4a-Rb pathway cooperate to enforce irreversible cellular senescence. *Nat. Cell Biol.* **8,** 1291–1297 (2006).
204. Garrido, C. *et al.* Mechanisms of cytochrome c release from mitochondria. *Cell Death Differ.* **13,** 1423–1433 (2006).
205. Han, D., Antunes, F., Canali, R., Rettori, D. & Cadenas, E. Voltage-dependent anion channels control the release of the superoxide anion from mitochondria to cytosol. *J. Biol. Chem.* **278,** 5557–5563 (2003).
206. Fruehauf, J. P. & Meyskens, F. L., Jr. Reactive oxygen species: a breath of life or death? *Clin. Cancer Res. Off. J. Am. Assoc. Cancer Res.* **13,** 789–794 (2007).
207. Nathan, C. & Ding, A. SnapShot: reactive oxygen intermediates (ROI). *Cell* **140,** 951–951.e2 (2010).
208. Gao, P. *et al.* c-Myc suppression of miR-23a/b enhances mitochondrial glutaminase expression and glutamine metabolism. *Nature* **458,** 762–765 (2009).
209. Wise, D. R. *et al.* Myc regulates a transcriptional program that stimulates mitochondrial glutaminolysis and leads to glutamine addiction. *Proc. Natl. Acad. Sci. U. S. A.* **105,** 18782–18787 (2008).
210. DeBerardinis, R. J. *et al.* Beyond aerobic glycolysis: transformed cells can engage in glutamine metabolism that exceeds the requirement for protein and nucleotide synthesis. *Proc. Natl. Acad. Sci. U. S. A.* **104,** 19345–19350 (2007).
211. Wishart, D. S. *et al.* HMDB: the human metabolome database. *Nucleic Acids Res.* **35,** D521–526 (2007).
212. Griffin, J. L. & Shockcor, J. P. Metabolic profiles of cancer cells. *Nat. Rev. Cancer* **4,** 551–561 (2004).
213. Spratlin, J. L., Serkova, N. J. & Eckhardt, S. G. Clinical applications of metabolomics in oncology: a review. *Clin. Cancer Res. Off. J. Am. Assoc. Cancer Res.* **15,** 431–440 (2009).
214. Dehaven, C. D., Evans, A. M., Dai, H. & Lawton, K. A. Organization of GC/MS and LC/MS metabolomics data into chemical libraries. *J. Cheminformatics* **2,** 9 (2010).
215. Reitman, Z. J. *et al.* Profiling the effects of isocitrate dehydrogenase 1 and 2 mutations on the cellular metabolome. *Proc. Natl. Acad. Sci. U. S. A.* **108,** 3270–3275 (2011).
216. Nicholson, J. K. *et al.* Metabolic phenotyping in clinical and surgical environments. *Nature* **491,** 384–392 (2012).
217. Gavaghan, C. L., Holmes, E., Lenz, E., Wilson, I. D. & Nicholson, J. K. An NMR-based metabonomic approach to investigate the biochemical consequences of genetic strain differences: application to the C57BL10J and Alpk:ApfCD mouse. *FEBS Lett.* **484,** 169–174 (2000).
218. Tennant, D. A., Durán, R. V. & Gottlieb, E. Targeting metabolic transformation for cancer therapy. *Nat. Rev. Cancer* **10,** 267–277 (2010).
219. Kolb, E. A. & Gorlick, R. Development of IGF-IR inhibitors in pediatric sarcomas. *Curr. Oncol. Rep.* **11,** 307–313 (2009).
220. Vazquez-Martin, A., Colomer, R., Brunet, J. & Menendez, J. A. Pharmacological blockade of fatty acid synthase (FASN) reverses acquired autoresistance to trastuzumab (Herceptin

by transcriptionally inhibiting 'HER2 super-expression' occurring in high-dose trastuzumab-conditioned SKBR3/Tzb100 breast cancer cells. *Int. J. Oncol.* **31,** 769–776 (2007).
221. Alli, P. M., Pinn, M. L., Jaffee, E. M., McFadden, J. M. & Kuhajda, F. P. Fatty acid synthase inhibitors are chemopreventive for mammary cancer in neu-N transgenic mice. *Oncogene* **24,** 39–46 (2005).
222. Pizer, E. S. *et al.* Malonyl-coenzyme-A is a potential mediator of cytotoxicity induced by fatty-acid synthase inhibition in human breast cancer cells and xenografts. *Cancer Res.* **60,** 213–218 (2000).
223. Jang, M., Kim, S. S. & Lee, J. Cancer cell metabolism: implications for therapeutic targets. *Exp. Mol. Med.* **45,** e45 (2013).
224. Pelicano, H., Martin, D. S., Xu, R.-H. & Huang, P. Glycolysis inhibition for anticancer treatment. *Oncogene* **25,** 4633–4646 (2006).
225. Trivedi, B. & Danforth, W. H. Effect of pH on the kinetics of frog muscle phosphofructokinase. *J. Biol. Chem.* **241,** 4110–4112 (1966).
226. Reshkin, S. J. *et al.* Na+/H+ exchanger-dependent intracellular alkalinization is an early event in malignant transformation and plays an essential role in the development of subsequent transformation-associated phenotypes. *FASEB J. Off. Publ. Fed. Am. Soc. Exp. Biol.* **14,** 2185–2197 (2000).
227. Harguindey, S., Orive, G., Luis Pedraz, J., Paradiso, A. & Reshkin, S. J. The role of pH dynamics and the Na+/H+ antiporter in the etiopathogenesis and treatment of cancer. Two faces of the same coin--one single nature. *Biochim. Biophys. Acta* **1756,** 1–24 (2005).
228. Cardone, R. A., Casavola, V. & Reshkin, S. J. The role of disturbed pH dynamics and the Na+/H+ exchanger in metastasis. *Nat. Rev. Cancer* **5,** 786–795 (2005).
229. Erecińska, M., Deas, J. & Silver, I. A. The effect of pH on glycolysis and phosphofructokinase activity in cultured cells and synaptosomes. *J. Neurochem.* **65,** 2765–2772 (1995).
230. Christofk, H. R. *et al.* The M2 splice isoform of pyruvate kinase is important for cancer metabolism and tumour growth. *Nature* **452,** 230–233 (2008).
231. Mazurek, S., Boschek, C. B., Hugo, F. & Eigenbrodt, E. Pyruvate kinase type M2 and its role in tumor growth and spreading. *Semin. Cancer Biol.* **15,** 300–308 (2005).
232. Li, W., Liu, J. & Zhao, Y. PKM2 inhibitor shikonin suppresses TPA-induced mitochondrial malfunction and proliferation of skin epidermal JB6 cells. *Mol. Carcinog.* **53,** 403–412 (2014).
233. Bridges, C. B. & Brehme, K. S. The mutants of Drosophilia melanogaster. *Carnegie Inst Wash Publ* **552,** (1922).
234. Dobzhansky, T. Genetics of natural populations. XIII. Recombination and variability in populations of Drosophila pseudoobscura. *Genetic* **31,** 269–290 (1946).
235. Sturtevant, A. H. A highly specific complementary lethal system in Drosophia melanogaster. *Genetics* **41,** 118–123 (1956).
236. Bender, A. & Pringle, J. R. Use of a screen for synthetic lethal and multicopy suppressee mutants to identify two new genes involved in morphogenesis in Saccharomyces cerevisiae. *Mol. Cell. Biol.* **11,** 1295–1305 (1991).
237. Talpaz, M. *et al.* Dasatinib in imatinib-resistant Philadelphia chromosome-positive leukemias. *N. Engl. J. Med.* **354,** 2531–2541 (2006).
238. Buchdunger, E. *et al.* Inhibition of the Abl protein-tyrosine kinase in vitro and in vivo by a 2-phenylaminopyrimidine derivative. *Cancer Res.* **56,** 100–104 (1996).
239. Druker, B. J. *et al.* Effects of a selective inhibitor of the Abl tyrosine kinase on the growth of Bcr-Abl positive cells. *Nat. Med.* **2,** 561–566 (1996).
240. Druker, B. J. *et al.* Five-year follow-up of patients receiving imatinib for chronic myeloid leukemia. *N. Engl. J. Med.* **355,** 2408–2417 (2006).

241. Druker, B. J. *et al.* Efficacy and safety of a specific inhibitor of the BCR-ABL tyrosine kinase in chronic myeloid leukemia. *N. Engl. J. Med.* **344,** 1031–1037 (2001).
242. Heinrich, M. C., Blanke, C. D., Druker, B. J. & Corless, C. L. Inhibition of KIT tyrosine kinase activity: a novel molecular approach to the treatment of KIT-positive malignancies. *J. Clin. Oncol. Off. J. Am. Soc. Clin. Oncol.* **20,** 1692–1703 (2002).
243. Demetri, G. D. Targeting c-kit mutations in solid tumors: scientific rationale and novel therapeutic options. *Semin. Oncol.* **28,** 19–26 (2001).
244. Demetri, G. D. Targeting the molecular pathophysiology of gastrointestinal stromal tumors with imatinib. Mechanisms, successes, and challenges to rational drug development. *Hematol. Oncol. Clin. North Am.* **16,** 1115–1124 (2002).
245. Gerber, D. E. & Minna, J. D. ALK inhibition for non-small cell lung cancer: from discovery to therapy in record time. *Cancer Cell* **18,** 548–551 (2010).
246. Zhang, J., Yang, P. L. & Gray, N. S. Targeting cancer with small molecule kinase inhibitors. *Nat. Rev. Cancer* **9,** 28–39 (2009).
247. Weiner, L. M. An overview of monoclonal antibody therapy of cancer. *Semin. Oncol.* **26,** 41–50 (1999).
248. Garraway, L. A. & Jänne, P. A. Circumventing cancer drug resistance in the era of personalized medicine. *Cancer Discov.* **2,** 214–226 (2012).
249. Al-Lazikani, B., Banerji, U. & Workman, P. Combinatorial drug therapy for cancer in the post-genomic era. *Nat. Biotechnol.* **30,** 679–692 (2012).
250. Hartwell, L. H., Szankasi, P., Roberts, C. J., Murray, A. W. & Friend, S. H. Integrating genetic approaches into the discovery of anticancer drugs. *Science* **278,** 1064–1068 (1997).
251. Kroll, E. S., Hyland, K. M., Hieter, P. & Li, J. J. Establishing genetic interactions by a synthetic dosage lethality phenotype. *Genetics* **143,** 95–102 (1996).
252. Kaelin, W. G., Jr. Synthetic lethality: a framework for the development of wiser cancer therapeutics. *Genome Med.* **1,** 99 (2009).
253. Kaelin, W. G., Jr. The concept of synthetic lethality in the context of anticancer therapy. *Nat. Rev. Cancer* **5,** 689–698 (2005).
254. Guarente, L. Synthetic enhancement in gene interaction: a genetic tool come of age. *Trends Genet. TIG* **9,** 362–366 (1993).
255. Hartman, J. L., 4th, Garvik, B. & Hartwell, L. Principles for the buffering of genetic variation. *Science* **291,** 1001–1004 (2001).
256. Chan, D. A. & Giaccia, A. J. Harnessing synthetic lethal interactions in anticancer drug discovery. *Nat. Rev. Drug Discov.* **10,** 351–364 (2011).
257. Felsher, D. W. & Bishop, J. M. Reversible tumorigenesis by MYC in hematopoietic lineages. *Mol. Cell* **4,** 199–207 (1999).
258. Prochownik, E. V. & Vogt, P. K. Therapeutic targeting of Myc. *Genes Cancer* **1,** 650–659 (2010).
259. Pelengaris, S., Littlewood, T., Khan, M., Elia, G. & Evan, G. Reversible activation of c-Myc in skin: induction of a complex neoplastic phenotype by a single oncogenic lesion. *Mol. Cell* **3,** 565–577 (1999).
260. Harris, C. C. & Hollstein, M. Clinical implications of the p53 tumor-suppressor gene. *N. Engl. J. Med.* **329,** 1318–1327 (1993).
261. Olivier, M. *et al.* Recent advances in p53 research: an interdisciplinary perspective. *Cancer Gene Ther.* **16,** 1–12 (2009).
262. Liu, T.-C., Hwang, T.-H., Bell, J. C. & Kirn, D. H. Translation of targeted oncolytic virotherapeutics from the lab into the clinic, and back again: a high-value iterative loop. *Mol. Ther. J. Am. Soc. Gene Ther.* **16,** 1006–1008 (2008).
263. Gien, L. T. & Mackay, H. J. The emerging role of PARP inhibitors in the treatment of

epithelial ovarian cancer. *J. Oncol.* **2010,** 151750 (2010).
264. Audeh, M. W. *et al.* Oral poly(ADP-ribose) polymerase inhibitor olaparib in patients with BRCA1 or BRCA2 mutations and recurrent ovarian cancer: a proof-of-concept trial. *Lancet* **376,** 245–251 (2010).
265. Tutt, A. *et al.* Oral poly(ADP-ribose) polymerase inhibitor olaparib in patients with BRCA1 or BRCA2 mutations and advanced breast cancer: a proof-of-concept trial. *Lancet* **376,** 235–244 (2010).
266. Johannessen, C. M. *et al.* COT drives resistance to RAF inhibition through MAP kinase pathway reactivation. *Nature* **468,** 968–972 (2010).
267. Mali, P. *et al.* RNA-guided human genome engineering via Cas9. *Science* **339,** 823–826 (2013).
268. Steckel, M. *et al.* Determination of synthetic lethal interactions in KRAS oncogene-dependent cancer cells reveals novel therapeutic targeting strategies. *Cell Res.* **22,** 1227–1245 (2012).
269. Bernards, R. Finding effective cancer therapies through loss of function genetic screens. *Curr. Opin. Genet. Dev.* **24,** 23–29 (2014).
270. Elbashir, S. . *et al.* Duplexes of 21-nucleotide rnas mediate rna interference in cultured mammalian cells. *Nature* **411,** 494–498 (2001).
271. Etemadmoghadam, D. *et al.* Synthetic lethality between CCNE1 amplification and loss of BRCA1. *Proc. Natl. Acad. Sci. U. S. A.* **110,** 19489–19494 (2013).
272. Weidle, U. H., Maisel, D. & Eick, D. Synthetic lethality-based targets for discovery of new cancer therapeutics. *Cancer Genomics Proteomics* **8,** 159–171 (2011).
273. Dong, Y., Li, A., Wang, J., Weber, J. D. & Michel, L. S. Synthetic lethality through combined Notch-epidermal growth factor receptor pathway inhibition in basal-like breast cancer. *Cancer Res.* **70,** 5465–5474 (2010).
274. Michiue, H., Eguchi, A., Scadeng, M. & Dowdy, S. F. Induction of in vivo synthetic lethal RNAi responses to treat glioblastoma. *Cancer Biol. Ther.* **8,** 2306–2313 (2009).
275. Chan, N. *et al.* Contextual synthetic lethality of cancer cell kill based on the tumor microenvironment. *Cancer Res.* **70,** 8045–8054 (2010).
276. Chan, D. A. & Giaccia, A. J. Targeting cancer cells by synthetic lethality: autophagy and VHL in cancer therapeutics. *Cell Cycle Georget. Tex* **7,** 2987–2990 (2008).
277. Rottmann, S., Wang, Y., Nasoff, M., Deveraux, Q. L. & Quon, K. C. A TRAIL receptor-dependent synthetic lethal relationship between MYC activation and GSK3beta/FBW7 loss of function. *Proc. Natl. Acad. Sci. U. S. A.* **102,** 15195–15200 (2005).
278. Farmer, H. *et al.* Targeting the DNA repair defect in BRCA mutant cells as a therapeutic strategy. *Nature* **434,** 917–921 (2005).
279. Fong, P. C. *et al.* Inhibition of poly(ADP-ribose) polymerase in tumors from BRCA mutation carriers. *N. Engl. J. Med.* **361,** 123–134 (2009).
280. Bryant, H. E. *et al.* Specific killing of BRCA2-deficient tumours with inhibitors of poly(ADP-ribose) polymerase. *Nature* **434,** 913–917 (2005).
281. Jackson, S. P. & Bartek, J. The DNA-damage response in human biology and disease. *Nature* **461,** 1071–1078 (2009).
282. Chen, S. & Parmigiani, G. Meta-Analysis of BRCA1 and BRCA2 Penetrance. *J. Clin. Oncol.* **25,** 1329–1333 (2007).
283. Chambon, P., Weill, J. D. & Mandel, P. Nicotinamide mononucleotide activation of new DNA-dependent polyadenylic acid synthesizing nuclear enzyme. *Biochem. Biophys. Res. Commun.* **11,** 39–43 (1963).
284. Polo, S. E. & Jackson, S. P. Dynamics of DNA damage response proteins at DNA breaks: a focus on protein modifications. *Genes Dev.* **25,** 409–433 (2011).

285. Noël, G., Giocanti, N., Fernet, M., Mégnin-Chanet, F. & Favaudon, V. Poly(ADP-ribose) polymerase (PARP-1) is not involved in DNA double-strand break recovery. *BMC Cell Biol.* **4,** 7 (2003).
286. Haber, J. E. DNA recombination: the replication connection. *Trends Biochem. Sci.* **24,** 271–275 (1999).
287. Feng, Z. *et al.* Rad52 inactivation is synthetically lethal with BRCA2 deficiency. *Proc. Natl. Acad. Sci. U. S. A.* **108,** 686–691 (2011).
288. Kumar, M. S. *et al.* The GATA2 transcriptional network is requisite for RAS oncogene-driven non-small cell lung cancer. *Cell* **149,** 642–655 (2012).
289. Barbie, D. A. *et al.* Systematic RNA interference reveals that oncogenic KRAS-driven cancers require TBK1. *Nature* **462,** 108–112 (2009).
290. Scholl, C. *et al.* Synthetic lethal interaction between oncogenic KRAS dependency and STK33 suppression in human cancer cells. *Cell* **137,** 821–834 (2009).
291. Potratz, J. C. *et al.* Synthetic lethality screens reveal RPS6 and MST1R as modifiers of insulin-like growth factor-1 receptor inhibitor activity in childhood sarcomas. *Cancer Res.* **70,** 8770–81 (2010).
292. Pollak, M. Insulin and insulin-like growth factor signalling in neoplasia. *Nat. Rev. Cancer* **8,** 915–928 (2008).
293. Gualberto, A. & Pollak, M. Emerging role of insulin-like growth factor receptor inhibitors in oncology: early clinical trial results and future directions. *Oncogene* **28,** 3009–3021 (2009).
294. Garnett, M. J. *et al.* Systematic identification of genomic markers of drug sensitivity in cancer cells. *Nature* **483,** 570–575 (2012).
295. Uren, A. & Toretsky, J. A. Ewing's sarcoma oncoprotein EWS-FLI1: the perfect target without a therapeutic agent. *Future Oncol. Lond. Engl.* **1,** 521–528 (2005).
296. Arvand, A. & Denny, C. T. Biology of EWS/ETS fusions in Ewing's family tumors. *Oncogene* **20,** 5747–54 (2001).
297. Yun, J. *et al.* Glucose deprivation contributes to the development of KRAS pathway mutations in tumor cells. *Science* **325,** 1555–1559 (2009).
298. Furuta, E., Okuda, H., Kobayashi, A. & Watabe, K. Metabolic genes in cancer: Their roles in tumor progression and clinical implications. *Biochim. Biophys. Acta BBA - Rev. Cancer* **1805,** 141–152 (2010).
299. Dauphinot, L. *et al.* Analysis of the expression of cell cycle regulators in Ewing cell lines: EWS-FLI-1 modulates p57KIP2and c-Myc expression. *Oncogene* **20,** 3258–65 (2001).
300. Kim, J., Gao, P., Liu, Y.-C., Semenza, G. L. & Dang, C. V. Hypoxia-inducible factor 1 and dysregulated c-Myc cooperatively induce vascular endothelial growth factor and metabolic switches hexokinase 2 and pyruvate dehydrogenase kinase 1. *Mol. Cell. Biol.* **27,** 7381–7393 (2007).
301. Osthus, R. C. *et al.* Deregulation of glucose transporter 1 and glycolytic gene expression by c-Myc. *J. Biol. Chem.* **275,** 21797–21800 (2000).
302. Kim, J., Tchernyshyov, I., Semenza, G. L. & Dang, C. V. HIF-1-mediated expression of pyruvate dehydrogenase kinase: A metabolic switch required for cellular adaptation to hypoxia. *Cell Metab.* **3,** 177–185 (2006).
303. Subramanian, A. & Miller, D. M. Structural analysis of α-Enolase: mapping the functional domains involved in down-regulation of the c-myc protooncogene. *J. Biol. Chem.* **275,** 5958–5965 (2000).
304. Miller, D. M., Thomas, S. D., Islam, A., Muench, D. & Sedoris, K. c-Myc and cancer metabolism. *Clin. Cancer Res. Off. J. Am. Assoc. Cancer Res.* **18,** 5546–5553 (2012).
305. Morrish, F. *et al.* Myc-dependent mitochondrial generation of acetyl-CoA contributes to fatty acid biosynthesis and histone acetylation during cell cycle entry. *J. Biol. Chem.* **285,**

36267–36274 (2010).
306. Morrish, F. & Hockenbery, D. Myc's mastery of mitochondrial mischief. *Cell Cycle Georget. Tex* **2,** 11–13 (2003).
307. Le, A. *et al.* Glucose-independent glutamine metabolism via TCA cycling for proliferation and survival in B cells. *Cell Metab.* **15,** 110–121 (2012).
308. Scotlandi, K. *et al.* Insulin-like growth factor I receptor-mediated circuit in Ewing's sarcoma/peripheral neuroectodermal tumor: a possible therapeutic target. *Cancer Res* **56,** 4570–4 (1996).
309. Evans, A. M., DeHaven, C. D., Barrett, T., Mitchell, M. & Milgram, E. Integrated, nontargeted ultrahigh performance liquid chromatography/electrospray ionization tandem mass spectrometry platform for the identification and relative quantification of the small-molecule complement of biological systems. *Anal. Chem.* **81,** 6656–6667 (2009).
310. Ryals, J., Lawton, K., Stevens, D. & Milburn, M. Metabolon, Inc. *Pharmacogenomics* **8,** 863–866 (2007).
311. Lawton, K. A. *et al.* Analysis of the adult human plasma metabolome. *Pharmacogenomics* **9,** 383–397 (2008).
312. Sreekumar, A. *et al.* Metabolomic profiles delineate potential role for sarcosine in prostate cancer progression. *Nature* **457,** 910–914 (2009).
313. Metabolon. Result-driven metabolomics designed for action. *Work. Metabolon* at <http://www.metabolon.com/research-services/working-with-metabolon.aspx>
314. Zhang, Y. *et al.* Detrimental effects of adenosine signaling in sickle cell disease. *Nat. Med.* **17,** 79–86 (2011).
315. Lin, T.-C. *et al.* Autophagy: Resetting glutamine-dependent metabolism and oxygen consumption. *Autophagy* **8,** 1477–1493 (2012).
316. Suhre, K. *et al.* Human metabolic individuality in biomedical and pharmaceutical research. *Nature* **477,** 54–60 (2011).
317. Fong, M. Y., McDunn, J. & Kakar, S. S. Identification of metabolites in the normal ovary and their transformation in primary and metastatic ovarian cancer. *PloS One* **6,** e19963 (2011).
318. Storey, J. D. & Tibshirani, R. Statistical significance for genomewide studies. *Proc. Natl. Acad. Sci. U. S. A.* **100,** 9440–9445 (2003).
319. R Development Core Team. *R: A language and environment for statistical computing*. (R Foundation for Statistical Computing, 2008).
320. Platten, M., Wick, W. & Van den Eynde, B. J. Tryptophan catabolism in cancer: beyond IDO and tryptophan depletion. *Cancer Res.* **72,** 5435–5440 (2012).
321. Adams, S. *et al.* The kynurenine pathway in brain tumor pathogenesis. *Cancer Res.* **72,** 5649–5657 (2012).
322. Gostner, J. M., Becker, K., Fuchs, D. & Sucher, R. Redox regulation of the immune response. *Redox Rep. Commun. Free Radic. Res.* **18,** 88–94 (2013).
323. Metz, R. *et al.* IDO2 is critical for IDO1-mediated T-cell regulation and exerts a non-redundant function in inflammation. *Int. Immunol.* (2014). doi:10.1093/intimm/dxt073
324. Hissong, B. D., Byrne, G. I., Padilla, M. L. & Carlin, J. M. Upregulation of interferon-induced indoleamine 2,3-dioxygenase in human macrophage cultures by lipopolysaccharide, muramyl tripeptide, and interleukin-1. *Cell. Immunol.* **160,** 264–269 (1995).
325. Currier, A. R. *et al.* Tumor necrosis factor-alpha and lipopolysaccharide enhance interferon-induced antichlamydial indoleamine dioxygenase activity independently. *J. Interf. Cytokine Res. Off. J. Int. Soc. Interf. Cytokine Res.* **20,** 369–376 (2000).
326. Uldry, M. & Thorens, B. The SLC2 family of facilitated hexose and polyol transporters. *Pflügers Arch. Eur. J. Physiol.* **447,** 480–489 (2004).
327. Zhao, F.-Q. & Keating, A. F. Functional Properties and Genomics of Glucose Transporters.

Curr. Genomics **8,** 113–128 (2007).
328. Doege, H., Bocianski, A., Joost, H. G. & Schürmann, A. Activity and genomic organization of human glucose transporter 9 (GLUT9), a novel member of the family of sugar-transport facilitators predominantly expressed in brain and leucocytes. *Biochem. J.* **350 Pt 3,** 771–776 (2000).
329. Spiro, R. G. Protein glycosylation: nature, distribution, enzymatic formation, and disease implications of glycopeptide bonds. *Glycobiology* **12,** 43R–56R (2002).
330. Ruddock, L. W. & Molinari, M. N-glycan processing in ER quality control. *J. Cell Sci.* **119,** 4373–4380 (2006).
331. Horton, J. D., Goldstein, J. L. & Brown, M. S. SREBPs: activators of the complete program of cholesterol and fatty acid synthesis in the liver. *J. Clin. Invest.* **109,** 1125–1131 (2002).
332. Levine, A. J. & Puzio-Kuter, A. M. The control of the metabolic switch in cancers by oncogenes and tumor suppressor genes. *Science* **330,** 1340–1344 (2010).
333. Shim, H. *et al.* c-Myc transactivation of LDH-A: implications for tumor metabolism and growth. *Proc. Natl. Acad. Sci. U. S. A.* **94,** 6658–6663 (1997).
334. Dang, C. V., Le, A. & Gao, P. MYC-induced cancer cell energy metabolism and therapeutic opportunities. *Clin. Cancer Res. Off. J. Am. Assoc. Cancer Res.* **15,** 6479–6483 (2009).
335. Martinez-Outschoorn, U. E. *et al.* Oncogenes and inflammation rewire host energy metabolism in the tumor microenvironment: RAS and NFκB target stromal MCT4. *Cell Cycle Georget. Tex* **12,** 2580–2597 (2013).
336. Minchenko, A. *et al.* Hypoxia-inducible factor-1-mediated expression of the 6-phosphofructo-2-kinase/fructose-2,6-bisphosphatase-3 (PFKFB3) gene. Its possible role in the Warburg effect. *J. Biol. Chem.* **277,** 6183–6187 (2002).
337. Aebi, M. & Hennet, T. Congenital disorders of glycosylation: genetic model systems lead the way. *Trends Cell Biol.* **11,** 136–141 (2001).
338. Taylor, M. E. & Drickamer, K. *Introduction to glycobiology*. (Oxford University Press, 2011).
339. *Essentials of glycobiology*. (Cold Spring Harbor Laboratory Press, 2009).
340. Wang, M. *et al.* Regulatory role of mevalonate and N-linked glycosylation in proliferation and expression of the EWS/FLI-1 fusion protein in Ewing's sarcoma cells. *Exp. Cell Res.* **246,** 38–46 (1999).
341. Girnita, L. *et al.* Inhibition of N-linked glycosylation down-regulates insulin-like growth factor-1 receptor at the cell surface and kills Ewing's sarcoma cells: therapeutic implications. *Anticancer Drug* **15,** 67–72 (2000).
342. Carlberg, M. *et al.* Mevalonic acid is limiting for N-linked glycosylation and translocation of the insulin-like growth factor-1 receptor to the cell surface. Evidence for a new link between 3-hydroxy-3-methylglutaryl-coenzyme a reductase and cell growth. *J. Biol. Chem.* **271,** 17453–17462 (1996).
343. Dricu, A. *et al.* Mevalonate-regulated mechanisms in cell growth control: role of dolichyl phosphate in expression of the insulin-like growth factor-1 receptor (IGF-1R) in comparison to Ras prenylation and expression of c-myc. *Glycobiology* **7,** 625–633 (1997).
344. Dricu, A., Carlberg, M., Wang, M. & Larsson, O. Inhibition of N-linked glycosylation using tunicamycin causes cell death in malignant cells: role of down-regulation of the insulin-like growth factor 1 receptor in induction of apoptosis. *Cancer Res.* **57,** 543–548 (1997).
345. Wang, Q. *et al.* Activation of NAD(P)H oxidase by tryptophan-derived 3-hydroxykynurenine accelerates endothelial apoptosis and dysfunction in vivo. *Circ. Res.* **114,** 480–492 (2014).
346. Mailankot, M. *et al.* Indoleamine 2,3-dioxygenase overexpression causes kynurenine-modification of proteins, fiber cell apoptosis and cataract formation in the mouse lens. *Lab. Investig. J. Tech. Methods Pathol.* **89,** 498–512 (2009).

347. Opitz, C. A. *et al.* An endogenous tumour-promoting ligand of the human aryl hydrocarbon receptor. *Nature* **478,** 197–203 (2011).
348. Currie, E., Schulze, A., Zechner, R., Walther, T. C. & Farese, R. V., Jr. Cellular fatty acid metabolism and cancer. *Cell Metab.* **18,** 153–161 (2013).
349. Zaugg, K. *et al.* Carnitine palmitoyltransferase 1C promotes cell survival and tumor growth under conditions of metabolic stress. *Genes Dev.* **25,** 1041–1051 (2011).
350. Stoll, G. *et al.* Systems biology of Ewing sarcoma: a network model of EWS-FLI1 effect on proliferation and apoptosis. *Nucleic Acids Res.* **41,** 8853–8871 (2013).
351. Carracedo, A., Cantley, L. C. & Pandolfi, P. P. Cancer metabolism: fatty acid oxidation in the limelight. *Nat. Rev. Cancer* **13,** 227–232 (2013).
352. Olmos, D. *et al.* Safety, pharmacokinetics, and preliminary activity of the anti-IGF-1R antibody figitumumab (CP-751,871) in patients with sarcoma and Ewing's sarcoma: a phase 1 expansion cohort study. *Lancet Oncol.* **11,** 129–135 (2010).
353. Olmos, D. *et al.* Targeting the Insulin-Like Growth Factor 1 Receptor in Ewing's sarcoma: reality and expectations. *Sarcoma* **2011,** 402508 (2011).
354. Muñoz-Pinedo, C., El Mjiyad, N. & Ricci, J.-E. Cancer metabolism: current perspectives and future directions. *Cell Death Dis.* **3,** e248 (2012).
355. Cheung, H. W. *et al.* Systematic investigation of genetic vulnerabilities across cancer cell lines reveals lineage-specific dependencies in ovarian cancer. *Proc. Natl. Acad. Sci.* **108,** 12372–12377 (2011).
356. Huang, D. W., Sherman, B. T. & Lempicki, R. A. Systematic and integrative analysis of large gene lists using DAVID bioinformatics resources. *Nat. Protoc.* **4,** 44–57 (2009).
357. Huang, D. W., Sherman, B. T. & Lempicki, R. A. Bioinformatics enrichment tools: paths toward the comprehensive functional analysis of large gene lists. *Nucleic Acids Res.* **37,** 1–13 (2009).
358. Huang, D. W., Sherman, B. T. & Lempicki, R. A. Bioinformatics enrichment tools: paths toward the comprehensive functional analysis of large gene lists. *Nucleic Acids Res.* **37,** 1–13 (2009).
359. Silva, J. M. *et al.* Profiling essential genes in human mammary cells by multiplex RNAi screening. *Science* **319,** 617–620 (2008).
360. Gerdes, S. *et al.* Essential genes on metabolic maps. *Curr. Opin. Biotechnol.* **17,** 448–456 (2006).
361. Koonin, E. V. How many genes can make a cell: the minimal-gene-set concept. *Annu. Rev. Genomics Hum. Genet.* **1,** 99–116 (2000).
362. Hughes, J. *et al.* The polycystic kidney disease 1 (PKD1) gene encodes a novel protein with multiple cell recognition domains. *Nat. Genet.* **10,** 151–160 (1995).
363. Bhunia, A. K. *et al.* PKD1 induces p21(waf1) and regulation of the cell cycle via direct activation of the JAK-STAT signaling pathway in a process requiring PKD2. *Cell* **109,** 157–168 (2002).
364. Boca, M. *et al.* Polycystin-1 induces cell migration by regulating phosphatidylinositol 3-kinase-dependent cytoskeletal rearrangements and GSK3beta-dependent cell cell mechanical adhesion. *Mol. Biol. Cell* **18,** 4050–4061 (2007).
365. Boletta, A. Emerging evidence of a link between the polycystins and the mTOR pathways. *Pathogenetics* **2,** 6 (2009).
366. Qiu, N., Zhou, H. & Xiao, Z. Downregulation of PKD1 by shRNA results in defective osteogenic differentiation via cAMP/PKA pathway in human MG-63 cells. *J. Cell. Biochem.* **113,** 967–976 (2012).
367. Chapin, H. C. & Caplan, M. J. The cell biology of polycystic kidney disease. *J. Cell Biol.* **191,** 701–710 (2010).

368. Boca, M. *et al.* Polycystin-1 induces resistance to apoptosis through the Phosphatidylinositol 3-Kinase/Akt signaling pathway. *J. Am. Soc. Nephrol.* **17,** 637–647 (2006).
369. Owen, L. A., Kowalewski, A. A. & Lessnick, S. L. EWS/FLI mediates transcriptional repression via NKX2.2 during oncogenic transformation in Ewing's sarcoma. *PLoS ONE* **3,** e1965 (2008).
370. Hancock, J. D. & Lessnick, S. L. A transcriptional profiling meta-analysis reveals a core EWS-FLI gene expression signature. *Cell Cycle Georget. Tex* **7,** 250–256 (2008).
371. Scotlandi, K. *et al.* Overcoming resistance to conventional drugs in Ewing sarcoma and identification of molecular predictors of outcome. *J Clin Oncol* **27,** 2209–16 (2009).
372. Duckwall, C. S., Murphy, T. A. & Young, J. D. Mapping cancer cell metabolism with(13)C flux analysis: Recent progress and future challenges. *J. Carcinog.* **12,** 13 (2013).
373. Beischlag, T. V., Morales, J. L., Hollingshead, B. D. & Perdew, G. H. The aryl hydrocarbon receptor complex and the control of gene expression. *Crit. Rev. Eukaryot. Gene Expr.* **18,** 207–250 (2008).
374. Marinković, N., Pašalić, D., Ferenčak, G., Gršković, B. & Stavljenić Rukavina, A. Dioxins and human toxicity. *Arh. Hig. Rada Toksikol.* **61,** 445–453 (2010).
375. Furness, S. G. B. & Whelan, F. The pleiotropy of dioxin toxicity — Xenobiotic misappropriation of the aryl hydrocarbon receptor's alternative physiological roles. *Pharmacol. Ther.* **124,** 336–353 (2009).
376. Denison, M. S. & Nagy, S. R. Activation of the aryl hydrocarbon receptor by structurally diverse exogenous and endogenous chemicals. *Annu. Rev. Pharmacol. Toxicol.* **43,** 309–334 (2003).
377. Perdew, G. H. Association of the Ah receptor with the 90-kDa heat shock protein. *J. Biol. Chem.* **263,** 13802–13805 (1988).
378. Kazlauskas, A., Poellinger, L. & Pongratz, I. Evidence that the co-chaperone p23 regulates ligand responsiveness of the dioxin (Aryl hydrocarbon) receptor. *J. Biol. Chem.* **274,** 13519–13524 (1999).
379. Meyer, B. K., Pray-Grant, M. G., Vanden Heuvel, J. P. & Perdew, G. H. Hepatitis B virus X-associated protein 2 is a subunit of the unliganded aryl hydrocarbon receptor core complex and exhibits transcriptional enhancer activity. *Mol. Cell. Biol.* **18,** 978–988 (1998).
380. Chen, Y. *et al.* Nuclear receptors in the multidrug resistance through the regulation of drug-metabolizing enzymes and drug transporters. *Biochem. Pharmacol.* **83,** 1112–1126 (2012).
381. Feng, S., Cao, Z. & Wang, X. Role of aryl hydrocarbon receptor in cancer. *Biochim. Biophys. Acta BBA - Rev. Cancer* **1836,** 197–210 (2013).
382. Weigelt, B. & Reis-Filho, J. S. Histological and molecular types of breast cancer: is there a unifying taxonomy? *Nat. Rev. Clin. Oncol.* **6,** 718–730 (2009).
383. Swanton, C. Intratumor heterogeneity: evolution through space and time. *Cancer Res.* **72,** 4875–4882 (2012).
384. Marusyk, A., Almendro, V. & Polyak, K. Intra-tumour heterogeneity: a looking glass for cancer? *Nat. Rev. Cancer* **12,** 323–334 (2012).
385. Xu, C., Li, C. Y.-T. & Kong, A.-N. T. Induction of phase I, II and III drug metabolism/transport by xenobiotics. *Arch. Pharm. Res.* **28,** 249–268 (2005).
386. Muller, A. J., DuHadaway, J. B., Donover, P. S., Sutanto-Ward, E. & Prendergast, G. C. Inhibition of indoleamine 2,3-dioxygenase, an immunoregulatory target of the cancer suppression gene Bin1, potentiates cancer chemotherapy. *Nat. Med.* **11,** 312–319 (2005).
387. Uyttenhove, C. *et al.* Evidence for a tumoral immune resistance mechanism based on tryptophan degradation by indoleamine 2,3-dioxygenase. *Nat. Med.* **9,** 1269–1274 (2003).
388. Ma, Q., Baldwin, K. T., Renzelli, A. J., McDaniel, A. & Dong, L. TCDD-inducible poly(ADP-

ribose) polymerase: a novel response to 2,3,7,8-tetrachlorodibenzo-p-dioxin. *Biochem. Biophys. Res. Commun.* **289,** 499–506 (2001).
389. Platten, M., Wick, W. & Van den Eynde, B. J. Tryptophan catabolism in cancer: beyond IDO and tryptophan depletion. *Cancer Res.* **72,** 5435–5440 (2012).
390. Gramatzki, D. *et al.* Aryl hydrocarbon receptor inhibition downregulates the TGF-beta/Smad pathway in human glioblastoma cells. *Oncogene* **28,** 2593–2605 (2009).
391. Pantouris, G. & Mowat, C. G. Antitumour agents as inhibitors of tryptophan 2,3-dioxygenase. *Biochem. Biophys. Res. Commun.* **443,** 28–31 (2014).
392. Luo, B. *et al.* Highly parallel identification of essential genes in cancer cells. *Proc. Natl. Acad. Sci.* **105,** 20380–20385 (2008).
393. Moffat, J. *et al.* A lentiviral RNAi library for human and mouse genes applied to an arrayed viral high-content screen. *Cell* **124,** 1283–1298 (2006).
394. Berns, K. *et al.* A large-scale RNAi screen in human cells identifies new components of the p53 pathway. *Nature* **428,** 431–437 (2004).
395. Ngo, V. N. *et al.* A loss-of-function RNA interference screen for molecular targets in cancer. *Nature* **441,** 106–110 (2006).
396. Luo, J. *et al.* A Genome-wide RNAi Screen Identifies Multiple Synthetic Lethal Interactions with the Ras Oncogene. *Cell* **137,** 835–848 (2009).
397. Sarthy, A. V. *et al.* Survivin depletion preferentially reduces the survival of activated K-Ras-transformed cells. *Mol. Cancer Ther.* **6,** 269–276 (2007).
398. Arora, S. *et al.* RNAi phenotype profiling of kinases identifies potential therapeutic targets in Ewing's sarcoma. *Mol. Cancer* **9,** 218 (2010).
399. Cholewa, B. D., Liu, X. & Ahmad, N. The role of Polo-like Kinase 1 in carcinogenesis: cause or consequence? *Cancer Res.* **73,** 6848–6855 (2013).
400. Malumbres, M. & Barbacid, M. Cell cycle kinases in cancer. *Curr. Opin. Genet. Dev.* **17,** 60–65 (2007).
401. Yim, H. Current clinical trials with polo-like kinase 1 inhibitors in solid tumors. *Anticancer. Drugs* **24,** 999–1006 (2013).
402. Downward, J. Finding the weakness in cancer. *N. Engl. J. Med.* **361,** 922–924 (2009).
403. Yang, X. *et al.* A public genome-scale lentiviral expression library of human ORFs. *Nat. Methods* **8,** 659–661 (2011).
404. Škalamera, D. *et al.* A high-throughput platform for lentiviral overexpression screening of the human ORFeome. *PloS One* **6,** e20057 (2011).
405. Nims, N., Vassmer, D. & Maser, R. L. Transmembrane domain analysis of polycystin-1, the product of the polycystic kidney disease-1 (PKD1) gene: evidence for 11 membrane-spanning domains. *Biochemistry (Mosc.)* **42,** 13035–13048 (2003).
406. Puri, S. *et al.* Polycystin-1 activates the calcineurin/NFAT (nuclear factor of activated T-cells) signaling pathway. *J. Biol. Chem.* **279,** 55455–55464 (2004).
407. Van Adelsberg, J. S. The role of the polycystins in kidney development. *Pediatr. Nephrol. Berl. Ger.* **13,** 454–459 (1999).
408. Somlo, S. & Ehrlich, B. Human disease: calcium signaling in polycystic kidney disease. *Curr. Biol. CB* **11,** R356–360 (2001).
409. Harris, P. C. Molecular basis of polycystic kidney disease: PKD1, PKD2 and PKHD1. *Curr. Opin. Nephrol. Hypertens.* **11,** 309–314 (2002).
410. Zhou, J. Polycystins and primary cilia: primers for cell cycle progression. *Annu. Rev. Physiol.* **71,** 83–113 (2009).
411. Le, N. H. *et al.* Aberrant polycystin-1 expression results in modification of activator protein-1 activity, whereas Wnt signaling remains unaffected. *J. Biol. Chem.* **279,** 27472–27481 (2004).

412. Parnell, S. C. *et al.* The polycystic kidney disease-1 protein, polycystin-1, binds and activates heterotrimeric G-proteins in vitro. *Biochem. Biophys. Res. Commun.* **251,** 625–631 (1998).
413. Parnell, S. C. *et al.* Polycystin-1 activation of c-Jun N-terminal kinase and AP-1 is mediated by heterotrimeric G proteins. *J. Biol. Chem.* **277,** 19566–19572 (2002).
414. Arnould, T. *et al.* The polycystic kidney disease 1 gene product mediates protein kinase C alpha-dependent and c-Jun N-terminal kinase-dependent activation of the transcription factor AP-1. *J. Biol. Chem.* **273,** 6013–6018 (1998).
415. Kim, E. *et al.* The polycystic kidney disease 1 gene product modulates Wnt signaling. *J. Biol. Chem.* **274,** 4947–4953 (1999).
416. Luo, J. Glycogen synthase kinase 3beta (GSK3beta) in tumorigenesis and cancer chemotherapy. *Cancer Lett.* **273,** 194–200 (2009).
417. Nusse, R. & Varmus, H. Three decades of Wnts: a personal perspective on how a scientific field developed. *EMBO J.* **31,** 2670–2684 (2012).
418. Hedgepeth, C. M., Deardorff, M. A., Rankin, K. & Klein, P. S. Regulation of Glycogen Synthase Kinase 3β and downstream Wnt signaling by Axin. *Mol. Cell. Biol.* **19,** 7147–7157 (1999).
419. Nakamura, T. *et al.* Axin, an inhibitor of the Wnt signalling pathway, interacts with β-catenin, GSK-3β and APC and reduces the β-catenin level. *Genes Cells* **3,** 395–403 (1998).

Annexes

Annex I: List of metabolites identified in 1C timeseries
Annex II: List of metabolites identified in A673 and SKNMC
Annex III: List of essential genes in 1C and 1C dox, name and gene ID
Annex IV: List of specifically killing 1C dox, name and gene ID

Annex I

BIOCHEMICAL NAME	168h / 0h	*p*-Value	*q*-Value
glycine	0.69	0.0015	0.0008
serine	0.86	0.0118	0.0041
N-acetylserine	0.19	0.0010	0.0000
threonine	0.80	0.0095	0.0034
N-acetylthreonine	0.45	0.0061	0.0024
alanine	0.95	0.4894	0.0900
beta-alanine	0.29	0.0010	0.0003
N-acetylalanine	0.53	0.0010	0.0001
aspartate	0.90	0.2438	0.0508
N-acetylaspartate (NAA)	0.81	0.0397	0.0118
asparagine	0.35	0.0010	0.0000
glutamate	**0.87**	0.0782	0.0208
glutamine	0.53	0.0010	0.0000
gamma-aminobutyrate (GABA)	1.13	0.3081	0.0620
N-acetyl-aspartyl-glutamate (NAAG)	0.70	0.0035	0.0015
histidine	1.39	0.0010	0.0003
lysine	**1.20**	0.0615	0.0171
2-aminoadipate	0.62	0.0010	0.0004
phenylalanine	1.10	0.1242	0.0293
p-cresol sulfate	**1.39**	0.0741	0.0199
tyrosine	**1.11**	0.0943	0.0240
3-(4-hydroxyphenyl)lactate	0.57	0.0010	0.0001
kynurenine	11.82	0.0010	0.0000
tryptophan	0.96	0.5054	0.0925
isoleucine	1.04	0.6172	0.1087
leucine	1.10	0.1610	0.0358
valine	1.04	0.5489	0.0983
isobutyrylcarnitine	0.66	0.0010	0.0000
isovalerylcarnitine	0.65	0.0010	0.0002
cysteine	0.47	0.0488	0.0139
cysteine sulfinic acid	0.80	0.0249	0.0080
cystathionine	0.41	0.0010	0.0000
N-formylmethionine	0.57	0.0010	0.0002
hypotaurine	0.28	0.0010	0.0001
S-adenosylhomocysteine (SAH)	0.79	0.0444	0.0130
methionine	1.37	0.0010	0.0003
N-acetylmethionine	0.37	0.0010	0.0000
homocysteine	0.71	0.0064	0.0025
arginine	1.38	0.1312	0.0300
ornithine	**1.16**	0.0755	0.0202
urea	1.49	0.0029	0.0013
proline	**0.84**	0.0980	0.0244
trans-4-hydroxyproline	0.77	0.0010	0.0004
creatine	0.93	0.3767	0.0727
2-aminobutyrate	0.79	0.0166	0.0056
5-methylthioadenosine (MTA)	1.04	0.6029	0.1067
putrescine	1.44	0.0405	0.0120
N-acetylputrescine	1.03	0.9651	0.1606
spermidine	1.46	0.3812	0.0728
4-acetamidobutanoate	1.39	0.0015	0.0008
glutathione, reduced (GSH)	0.98	0.8384	0.1435
5-oxoproline	0.82	0.1171	0.0280
glutathione, oxidized (GSSG)	1.25	0.1319	0.0300
cysteine-glutathione disulfide	2.58	0.0049	0.0020
S-lactoylglutathione	12.43	0.0269	0.0086
glycylglycine	0.74	0.0234	0.0076
glycylisoleucine	0.74	0.1125	0.0273
glycylleucine	1.19	0.5525	0.0986
pro-hydroxy-pro	1.78	0.0010	0.0005
cysteinylglycine	0.61	0.0010	0.0001
gamma-glutamylvaline	1.15	0.2814	0.0575
gamma-glutamylleucine	1.17	0.0480	0.0138
gamma-glutamylisoleucine *	0.95	0.5484	0.0983
gamma-glutamylglutamate	1.32	0.0092	0.0034
gamma-glutamylphenylalanine	1.40	0.0377	0.0115
gamma-glutamyltyrosine	1.37	0.2169	0.0463
erythronate*	0.34	0.0010	0.0000
N-acetylneuraminate	1.28	0.1135	0.0274
fructose	0.88	0.4319	0.0808
lactose	1.15	0.7958	0.1385
mannitol	0.82	0.3973	0.0753
sorbitol	0.74	0.2786	0.0572
maltotriose	2.00	0.0352	0.0108
glycerate	1.08	0.8646	0.1474
glucose-6-phosphate (G6P)	0.67	0.2042	0.0442

ornithine	**1.16**	0.0755	0.0202
urea	1.49	0.0029	0.0013
proline	**0.84**	0.0980	0.0244
trans-4-hydroxyproline	0.77	0.0010	0.0004
creatine	0.93	0.3767	0.0727
2-aminobutyrate	0.79	0.0166	0.0056
5-methylthioadenosine (MTA)	1.04	0.6029	0.1067
putrescine	1.44	0.0405	0.0120
N-acetylputrescine	1.03	0.9651	0.1606
spermidine	1.46	0.3812	0.0728
4-acetamidobutanoate	1.39	0.0015	0.0008
glutathione, reduced (GSH)	0.98	0.8384	0.1435
5-oxoproline	0.82	0.1171	0.0280
glutathione, oxidized (GSSG)	1.25	0.1319	0.0300
cysteine-glutathione disulfide	2.58	0.0049	0.0020
S-lactoylglutathione	12.43	0.0269	0.0086
glycylglycine	0.74	0.0234	0.0076
glycylisoleucine	0.74	0.1125	0.0273
glycylleucine	1.19	0.5525	0.0986
pro-hydroxy-pro	1.78	0.0010	0.0005
cysteinylglycine	0.61	0.0010	0.0001
gamma-glutamylvaline	1.15	0.2814	0.0575
gamma-glutamylleucine	1.17	0.0480	0.0138
gamma-glutamylisoleucine *	0.95	0.5484	0.0983
gamma-glutamylglutamate	1.32	0.0092	0.0034
gamma-glutamylphenylalanine	1.40	0.0377	0.0115
gamma-glutamyltyrosine	1.37	0.2169	0.0463
erythronate*	0.34	0.0010	0.0000
N-acetylneuraminate	1.28	0.1135	0.0274
fructose	0.88	0.4319	0.0808
lactose	1.15	0.7958	0.1385
mannitol	0.82	0.3973	0.0753
sorbitol	0.74	0.2786	0.0572
maltotriose	2.00	0.0352	0.0108
glycerate	1.08	0.8646	0.1474
glucose-6-phosphate (G6P)	0.67	0.2042	0.0442

10-heptadecenoate (17:1n7)	3.72	0.0010	0.0000
oleate (18:1n9)	2.13	0.0032	0.0014
cis-vaccenate (18:1n7)	3.33	0.0010	0.0001
nonadecanoate (19:0)	2.88	0.0010	0.0000
eicosenoate (20:1n9 or 11)	3.11	0.0010	0.0000
dihomo-linoleate (20:2n6)	4.71	0.0010	0.0000
mead acid (20:3n9)	4.55	0.0010	0.0001
arachidonate (20:4n6)	6.36	0.0010	0.0000
docosadienoate (22:2n6)	2.50	0.0010	0.0000
adrenate (22:4n6)	10.99	0.0010	0.0000
4-hydroxybutyrate (GHB)	1.82	0.0028	0.0013
2-hydroxypalmitate	1.34	0.1309	0.0300
2-hydroxyglutarate	0.55	0.0010	0.0005
17-methylstearate	1.90	0.0010	0.0003
propionylcarnitine	**0.76**	0.0865	0.0224
butyrylcarnitine	0.32	0.0010	0.0000
deoxycarnitine	1.03	0.8922	0.1509
carnitine	1.30	0.0022	0.0011
acetylcarnitine	0.73	0.0010	0.0003
palmitoylcarnitine	0.62	0.2108	0.0452
oleoylcarnitine	1.47	0.2698	0.0556
taurocholate	1.49	0.3490	0.0683
choline phosphate	2.97	0.0010	0.0000
ethanolamine	1.21	0.3364	0.0671
phosphoethanolamine	5.56	0.0010	0.0000
glycerol 3-phosphate (G3P)	3.53	0.0010	0.0000
glycerophosphorylcholine (GPC)	5.18	0.0010	0.0001
cytidine 5'-diphosphocholine	1.09	0.3823	0.0728
myo-inositol	1.18	0.2874	0.0581
inositol 1-phosphate (I1P)	1.60	0.0052	0.0021
scyllo-inositol	0.88	0.3486	0.0683
1-palmitoylglycerophosphoethanolamine	0.53	0.0013	0.0007
2-palmitoylglycerophosphoethanolamine*	5.30	0.0010	0.0001
1-stearoylglycerophosphoethanolamine	1.18	0.5237	0.0954

10-heptadecenoate (17:1n7)	3.72	0.0010	0.0000
oleate (18:1n9)	2.13	0.0032	0.0014
cis-vaccenate (18:1n7)	3.33	0.0010	0.0001
nonadecanoate (19:0)	2.88	0.0010	0.0000
eicosenoate (20:1n9 or 11)	3.11	0.0010	0.0000
dihomo-linoleate (20:2n6)	4.71	0.0010	0.0000
mead acid (20:3n9)	4.55	0.0010	0.0001
arachidonate (20:4n6)	6.36	0.0010	0.0000
docosadienoate (22:2n6)	2.50	0.0010	0.0000
adrenate (22:4n6)	10.99	0.0010	0.0000
4-hydroxybutyrate (GHB)	1.82	0.0028	0.0013
2-hydroxypalmitate	1.34	0.1309	0.0300
2-hydroxyglutarate	0.55	0.0010	0.0005
17-methylstearate	1.90	0.0010	0.0003
propionylcarnitine	**0.76**	0.0865	0.0224
butyrylcarnitine	0.32	0.0010	0.0000
deoxycarnitine	1.03	0.8922	0.1509
carnitine	1.30	0.0022	0.0011
acetylcarnitine	0.73	0.0010	0.0003
palmitoylcarnitine	0.62	0.2108	0.0452
oleoylcarnitine	1.47	0.2698	0.0556
taurocholate	1.49	0.3490	0.0683
choline phosphate	2.97	0.0010	0.0000
ethanolamine	1.21	0.3364	0.0671
phosphoethanolamine	5.56	0.0010	0.0000
glycerol 3-phosphate (G3P)	3.53	0.0010	0.0000
glycerophosphorylcholine (GPC)	5.18	0.0010	0.0001
cytidine 5'-diphosphocholine	1.09	0.3823	0.0728
myo-inositol	1.18	0.2874	0.0581
inositol 1-phosphate (I1P)	1.60	0.0052	0.0021
scyllo-inositol	0.88	0.3486	0.0683
1-palmitoylglycerophosphoethanolamine	0.53	0.0013	0.0007
2-palmitoylglycerophosphoethanolamine*	5.30	0.0010	0.0001
1-stearoylglycerophosphoethanolamine	1.18	0.5237	0.0954
hypoxanthine	1.10	0.5473	0.0983
inosine	1.24	0.0452	0.0132
2'-deoxyinosine	0.43	0.0010	0.0001
inosine 5'-monophosphate (IMP)	**0.62**	0.0820	0.0214
adenine	0.86	0.1312	0.0300
adenosine	0.87	0.4051	0.0761
N1-methyladenosine	0.65	0.0350	0.0108
adenosine 3'-monophosphate (3'-AMP)	2.57	0.0018	0.0009
adenosine 5'-monophosphate (AMP)	0.86	0.4016	0.0758
adenosine 5'-diphosphate (ADP)	1.26	0.2566	0.0532
adenosine 5'-triphosphate (ATP)	1.20	0.4407	0.0817
adenylosuccinate	0.34	0.0148	0.0051
guanine	1.15	0.6881	0.1207
guanosine	1.71	0.0018	0.0009
2'-deoxyguanosine	0.45	0.0010	0.0001
guanosine 5'-diphospho-fucose	2.58	0.0010	0.0001
N2-methylguanosine	0.46	0.0010	0.0004
N2,N2-dimethylguanosine	0.49	0.0104	0.0037
allantoin	0.87	0.1360	0.0307
cytidine	0.47	0.0083	0.0031
cytidine 5'-monophosphate (5'-CMP)	0.62	0.0073	0.0028
thymine	1.19	0.1822	0.0399
thymidine 5'-monophosphate	0.41	0.0010	0.0003
uracil	3.67	0.0015	0.0008
uridine	1.55	0.0010	0.0001
pseudouridine	**0.78**	0.0544	0.0152
uridine 5'-diphosphate (UDP)	**1.54**	0.0699	0.0189
uridine 5'-triphosphate (UTP)	3.37	0.0386	0.0116
methylphosphate	1.63	0.0153	0.0052
gulono-1,4-lactone	0.30	0.0179	0.0060
5-methyltetrahydrofolate (5MeTHF)	0.97	0.5719	0.1016
nicotinamide	1.12	0.1873	0.0408

nicotinamide adenine dinucleotide (NAD+)	1.35	0.1163	0.0279
nicotinamide adenine dinucleotide reduced (NADH)	3.64	0.1274	0.0296
pantothenate	0.68	0.0010	0.0002
coenzyme A	0.41	0.0068	0.0026
3'-dephosphocoenzyme A	0.16	0.0069	0.0026
pyridoxal	**1.60**	0.0986	0.0244
flavin adenine dinucleotide (FAD)	1.18	0.0274	0.0087
riboflavin (Vitamin B2)	1.17	0.2290	0.0484
thiamin (Vitamin B1)	1.44	0.0016	0.0008
pyridoxate	0.98	0.8091	0.1402
hippurate	**1.14**	0.0680	0.0187
benzoate	2.12	0.0010	0.0002
glycerol 2-phosphate	0.51	0.0010	0.0001
phenol red	1.35	0.0013	0.0007
erythritol	0.91	0.1632	0.0361

Annex II

	A673	SKNMC	A673 siEF1/siCT		SKNMC siEF1/siCT	
Biochemical Name	**siEF1 / siCTR**	**siEF1 / siCTR**	***p*-value**	***q*-value**	***p*-value**	***q*-value**
glycine	0.87	0.59	0.1674	0.0466	0.0076	0.0341
serine	1.00	0.90	0.9764	0.1958	0.7192	0.4676
N-acetylserine	0.65	0.41	0.0163	0.0063	0.0006	0.0083
threonine	0.69	0.92	0.0047	0.0024	0.3511	0.3256
N-acetylthreonine	0.89	0.68	0.4178	0.1001	0.0947	0.1520
alanine	1.26	0.97	0.0340	0.0117	0.7632	0.4820
N-acetylalanine	0.69	0.54	0.0394	0.0131	0.0037	0.0230
aspartate	1.32	0.69	0.0105	0.0044	0.0387	0.0882
asparagine	0.57	0.85	0.0002	0.0004	0.2949	0.2984
N-acetylaspartate (NAA)	0.11	0.82	0.0000	0.0000	0.1752	0.2096
glutamate	0.95	0.83	0.5822	0.1296	0.1617	0.2002
glutamine	1.84	0.84	0.0019	0.0012	0.3652	0.3261
N-acetyl-aspartyl-glutamate (NAAG)	0.41	1.68	0.0000	0.0000	0.0462	0.0958
gamma-aminobutyrate (GABA)	0.54	0.34	0.0062	0.0030	0.0006	0.0083
histidine	0.76	1.25	0.0529	0.0167	0.0347	0.0844
lysine	1.42	1.25	0.0380	0.0128	0.0136	0.0499
2-aminoadipate	1.10	0.48	0.6550	0.1411	0.0139	0.0499
phenylalanine	0.97	1.17	0.8309	0.1725	0.0715	0.1252
tyrosine	0.92	1.13	0.4093	0.0992	0.1810	0.2096
3-(4-hydroxyphenyl)lactate	0.57	0.93	0.0005	0.0005	0.4439	0.3588
p-cresol sulfate	1.40	1.37	0.0115	0.0047	0.0154	0.0520
tryptophan	0.61	1.28	0.0019	0.0013	0.0710	0.1252
kynurenine	39.29	2.92	0.0000	0.0000	0.0005	0.0075
leucine	0.96	1.20	0.7125	0.1517	0.0906	0.1475
isovalerylcarnitine	3.12	0.70	0.0001	0.0002	0.0020	0.0187
isoleucine	0.95	1.19	0.5901	0.1307	0.0699	0.1252
valine	0.89	1.26	0.3485	0.0880	0.0150	0.0513
isobutyrylcarnitine	1.89	0.75	0.0003	0.0004	0.0435	0.0940
methionine	1.07	1.25	0.4196	0.1001	0.0427	0.0937
N-acetylmethionine	0.84	0.52	0.1072	0.0312	0.0004	0.0075
N-formylmethionine	1.22	0.83	0.0445	0.0146	0.1275	0.1780
S-adenosylhomocysteine (SAH)	1.87	0.87	0.0069	0.0033	0.2128	0.2381
homocysteine	0.66	0.86	0.0204	0.0076	0.2171	0.2406
cystathionine	0.38	0.41	0.0003	0.0004	0.0038	0.0230
2-aminobutyrate	0.70	0.83	0.0113	0.0047	0.5385	0.3877
cysteine	4.61	2.02	0.0000	0.0000	0.1218	0.1735
cysteine sulfinic acid	3.23	3.17	0.0001	0.0002	0.0001	0.0032
hypotaurine	0.28	0.88	0.0000	0.0001	0.4517	0.3600
arginine	1.23	0.92	0.1653	0.0463	0.8361	0.5085
urea	2.26	1.03	0.0059	0.0029	0.8756	0.5211
ornithine	2.04	1.60	0.0017	0.0012	0.0002	0.0054
proline	0.61	0.93	0.0053	0.0027	0.4486	0.3588
trans-4-hydroxyproline	0.47	0.80	0.0001	0.0002	0.3020	0.3017
pro-hydroxy-pro	1.61	1.64	0.0068	0.0032	0.0162	0.0539

creatine	0.68	0.56	0.0078	0.0036	0.0000	0.0006
putrescine	0.81	0.52	0.1347	0.0384	0.0009	0.0105
spermidine	1.28	0.34	0.2404	0.0637	0.0703	0.1252
5-methylthioadenosine (MTA)	1.35	0.83	0.0450	0.0147	0.0641	0.1185
N-acetylputrescine	0.50	0.59	0.0014	0.0011	0.0202	0.0619
4-acetamidobutanoate	1.54	1.03	0.0300	0.0106	0.9814	0.5486
glutathione, reduced (GSH)	2.98	1.02	0.0000	0.0000	0.7182	0.4676
glutathione, oxidized (GSSG)	2.50	1.37	0.0474	0.0153	0.1064	0.1598
cysteine-glutathione disulfide	5.30	4.02	0.0089	0.0039	0.0141	0.0499
S-lactoylglutathione	1.00	0.50			0.8278	0.5057
cysteinylglycine	3.04	1.10	0.0000	0.0000	0.5655	0.3989
5-oxoproline	2.41	0.87	0.0001	0.0002	0.4917	0.3765
gamma-glutamylglutamate	7.72	1.65	0.0000	0.0000	0.0049	0.0268
gamma-glutamylisoleucine*	1.13	1.21	0.4463	0.1052	0.8388	0.5085
gamma-glutamylleucine	1.99	0.98	0.0004	0.0004	0.9877	0.5500
gamma-glutamylphenylalanine	1.88	1.33	0.0002	0.0003	0.1425	0.1865
gamma-glutamyltyrosine	2.03	1.35	0.0001	0.0003	0.0092	0.0382
gamma-glutamylvaline	1.60	1.11	0.0118	0.0048	0.9630	0.5467
glycylglycine	1.57	0.97	0.0145	0.0057	0.7390	0.4765
glycylisoleucine	1.65	1.88	0.0135	0.0054	0.0267	0.0706
glycylleucine	1.42	1.49	0.0085	0.0038	0.1392	0.1859
glucose	24.01	3.38	0.0194	0.0073	0.0625	0.1165
glucose-6-phosphate (G6P)	16.44	1.04	0.0011	0.0008	0.6471	0.4405
glucose 1-phosphate	1.31	0.74	0.0433	0.0143	0.4201	0.3517
fructose-6-phosphate	3.89	1.42	0.0007	0.0006	0.2003	0.2284
pyruvate	1.66	0.34	0.3462	0.0880	0.0852	0.1426
lactate	1.48	0.78	0.0030	0.0017	0.4075	0.3424
glycerate	2.47	0.79	0.0211	0.0078	0.2501	0.2659
ribose 5-phosphate	1.00	0.78			0.9250	0.5378
ribulose	1.02	0.87	0.7218	0.1533	0.2342	0.2524
ribose	0.69	1.00	0.0573	0.0179	0.9927	0.5515
ribitol	0.33	0.55	0.0000	0.0000	0.0043	0.0250
xylonate	0.59	0.83	0.0084	0.0038	0.2792	0.2889
xylitol	1.20	0.56	0.1852	0.0510	0.0033	0.0228
threitol	0.91	0.81	0.5505	0.1241	0.0605	0.1145
arabitol	0.66	0.93	0.0114	0.0047	0.7865	0.4906
maltotriose	0.91	1.25	0.4124	0.0995	0.5376	0.3877
lactose	1.48	1.27	0.0085	0.0038	0.2168	0.2406
fructose	3.26	1.78	0.0012	0.0009	0.0477	0.0958
sorbitol	1.24	1.33	0.1233	0.0355	0.0315	0.0802
mannitol	0.95	1.14	0.6361	0.1379	0.3109	0.3080
UDP-glucose	1.00	1.70			0.0031	0.0219
UDP-galactose	1.03	0.67	0.6494	0.1404	0.0230	0.0654
UDP-glucuronate	1.11	1.22	0.3202	0.0830	0.0212	0.0637
guanosine 5'-diphospho-fucose	2.12	2.09	0.0020	0.0013	0.0001	0.0033
N-acetylneuraminate	5.00	1.84	0.0000	0.0001	0.0030	0.0215

erythronate*	0.50	0.81	0.0006	0.0005	0.1040	0.1582
citrate	1.16	1.28	0.4483	0.1053	0.2994	0.3017
succinate	1.06	1.13	0.8191	0.1704	0.3884	0.3300
fumarate	1.30	0.71	0.0047	0.0024	0.0307	0.0799
malate	0.91	0.63	0.3415	0.0872	0.0219	0.0637
pyrophosphate (PPi)	3.55	1.03	0.0530	0.0167	0.8891	0.5253
phosphate	2.04	1.15	0.0001	0.0002	0.1090	0.1626
caprylate (8:0)	1.00	1.29	0.9451	0.1928	0.0888	0.1455
pelargonate (9:0)	1.97	1.07	0.0026	0.0015	0.5011	0.3774
caprate (10:0)	1.26	1.06	0.0814	0.0243	0.5007	0.3774
laurate (12:0)	1.88	1.03	0.0003	0.0004	0.6722	0.4471
myristate (14:0)	1.74	1.13	0.0034	0.0019	0.1503	0.1911
myristoleate (14:1n5)	0.64	0.91	0.0062	0.0030	0.4955	0.3765
pentadecanoate (15:0)	2.68	1.22	0.0000	0.0001	0.1803	0.2096
palmitate (16:0)	1.75	1.05	0.0003	0.0004	0.6752	0.4478
palmitoleate (16:1n7)	1.29	1.71	0.0551	0.0172	0.0110	0.0441
margarate (17:0)	2.41	1.69	0.0003	0.0004	0.0057	0.0285
10-heptadecenoate (17:1n7)	2.66	2.08	0.0003	0.0004	0.0043	0.0250
oleate (18:1n9)	1.44	1.21	0.0473	0.0153	0.1426	0.1865
cis-vaccenate (18:1n7)	2.11	1.18	0.0009	0.0007	0.2604	0.2743
nonadecanoate (19:0)	2.69	1.34	0.0022	0.0014	0.1098	0.1628
eicosenoate (20:1n9 or 11)	1.87	1.41	0.0022	0.0014	0.1277	0.1780
eicosapentaenoate (EPA; 20:5n3)	3.46	4.00	0.0001	0.0002	0.0001	0.0038
docosapentaenoate (n3 DPA; 22:5n3)	4.30	3.54	0.0001	0.0001	0.0007	0.0083
docosahexaenoate (DHA; 22:6n3)	3.42	1.48	0.0000	0.0001	0.0121	0.0470
linoleate (18:2n6)	1.78	2.42	0.0271	0.0099	0.0045	0.0254
linolenate [alpha or gamma; (18:3n3 or 6	0.94	2.68	0.6960	0.1485	0.0027	0.0215
dihomo-linolenate (20:3n3 or n6)	1.35	3.97	0.0776	0.0232	0.0021	0.0187
arachidonate (20:4n6)	2.20	3.12	0.0006	0.0005	0.0003	0.0054
adrenate (22:4n6)	3.04	2.49	0.0990	0.0290	0.0035	0.0230
docosapentaenoate (n6 DPA; 22:5n6)	1.63	1.42	0.4147	0.0998	0.1031	0.1579
docosadienoate (22:2n6)	1.82	0.94	0.0030	0.0017	0.7613	0.4820
dihomo-linoleate (20:2n6)	2.01	1.89	0.0028	0.0016	0.0180	0.0589
mead acid (20:3n9)	1.94	1.64	0.0445	0.0146	0.0080	0.0352
17-methylstearate	2.54	1.04	0.0038	0.0020	0.7599	0.4820
2-hydroxyglutarate	0.59	1.30	0.0015	0.0011	0.1406	0.1859
butyrylcarnitine	1.19	0.70	0.0369	0.0126	0.0009	0.0105
propionylcarnitine	1.52	0.77	0.0024	0.0014	0.0942	0.1520
acetylcarnitine	1.24	1.10	0.0387	0.0129	0.3649	0.3261
palmitoylcarnitine	0.47	0.54	0.0006	0.0005	0.6958	0.4562
oleoylcarnitine	0.68	0.48	0.0622	0.0192	0.7641	0.4820
deoxycarnitine	1.29	1.28	0.0185	0.0070	0.0436	0.0940
carnitine	1.01	0.91	0.7725	0.1620	0.5311	0.3854
4-hydroxybutyrate (GHB)	0.80	0.68	0.0305	0.0107	0.0520	0.1026
2-hydroxypalmitate	1.39	1.04	0.0299	0.0106	0.5117	0.3805
myo-inositol	0.92	1.23	0.4617	0.1073	0.0015	0.0152

scyllo-inositol	0.68	1.27	0.0167	0.0064	0.0026	0.0215
inositol 1-phosphate (I1P)	1.97	1.07	0.0006	0.0006	0.4601	0.3630
choline phosphate	8.40	1.84	0.0000	0.0000	0.0145	0.0502
cytidine 5'-diphosphocholine	5.62	1.64	0.0000	0.0001	0.0020	0.0187
glycerophosphorylcholine (GPC)	0.51	0.55	0.0006	0.0006	0.0088	0.0380
ethanolamine	4.96	0.64	0.0000	0.0001	0.1552	0.1953
phosphoethanolamine	3.47	1.11	0.0001	0.0001	0.4731	0.3659
2-myristoylglycerophosphocholine*	1.19	0.87	0.4828	0.1107	0.8529	0.5122
2-palmitoylglycerophosphocholine*	1.34	2.43	0.9304	0.1907	0.3511	0.3256
2-palmitoleoylglycerophosphocholine*	1.09	0.76	0.7329	0.1548	0.8102	0.4986
2-oleoylglycerophosphocholine*	2.18	1.99	0.6073	0.1330	0.7859	0.4906
2-linoleoylglycerophosphocholine*	0.95	0.97	0.6000	0.1321	0.9415	0.5398
2-arachidonoylglycerophosphocholine*	1.85	1.77	0.1923	0.0526	0.6469	0.4405
2-docosahexaenoylglycerophosphocholi	3.34	0.90	0.0096	0.0041	0.8720	0.5211
1-palmitoylglycerophosphoethanolamine	3.79	0.64	0.0004	0.0004	0.0967	0.1533
2-palmitoylglycerophosphoethanolamine	11.08	2.39	0.0061	0.0030	0.5229	0.3840
1-stearoylglycerophosphoethanolamine	2.77	0.89	0.0014	0.0011	0.7549	0.4820
1-oleoylglycerophosphoethanolamine	2.66	1.03	0.0005	0.0005	0.6906	0.4541
2-oleoylglycerophosphoethanolamine*	2.32	0.95	0.0009	0.0007	0.9333	0.5378
2-linoleoylglycerophosphoethanolamine*	1.10	1.08	0.8880	0.1825	0.8752	0.5211
1-arachidonoylglycerophosphoethanolar	2.94	1.15	0.0009	0.0007	0.3470	0.3256
2-arachidonoylglycerophosphoethanolar	2.23	1.46	0.0156	0.0061	0.5315	0.3854
2-docosapentaenoylglycerophosphoetha	2.32	2.44	0.1094	0.0317	0.5517	0.3939
2-docosahexaenoylglycerophosphoethar	2.92	1.26	0.0018	0.0012	0.4280	0.3545
glycerol 3-phosphate (G3P)	0.54	0.61	0.0029	0.0017	0.0003	0.0055
2-palmitoylglycerol (2-monopalmitin)	0.56	1.18	0.0007	0.0006	0.4763	0.3671
1,2-dipalmitoylglycerol	0.91	0.91	0.4187	0.1001	0.8118	0.4986
sphinganine	2.17	1.60	0.0032	0.0018	0.5169	0.3823
palmitoyl sphingomyelin	2.55	1.85	0.0000	0.0000	0.0060	0.0287
sphingosine	3.00	2.26	0.0001	0.0002	0.4007	0.3391
cholesterol	1.81	1.41	0.0005	0.0005	0.0191	0.0602
taurocholate	1.29	1.28	0.2033	0.0553	0.1452	0.1889
inosine 5'-monophosphate (IMP)	0.12	0.89	0.0005	0.0005	0.9301	0.5378
inosine	15.18	1.36	0.0000	0.0000	0.2012	0.2284
hypoxanthine	4.22	2.02	0.0000	0.0001	0.0060	0.0287
xanthine	1.30	1.29	0.0866	0.0257	0.0764	0.1318
2'-deoxyinosine	1.00	0.67			0.4731	0.3659
allantoin	1.06	1.07	0.4742	0.1093	0.7904	0.4906
adenosine 5'-triphosphate (ATP)	5.57	0.97	0.0005	0.0005	0.7750	0.4875
adenosine 5'-diphosphate (ADP)	1.56	0.61	0.1680	0.0466	0.0884	0.1455
adenosine 5'-monophosphate (AMP)	0.30	0.63	0.0388	0.0129	0.1160	0.1683
adenosine 3'-monophosphate (3'-AMP)	6.57	1.54	0.0000	0.0001	0.2277	0.2477
adenylosuccinate	0.53	1.00	0.0359	0.0123		
adenosine	9.34	2.08	0.0019	0.0013	0.0968	0.1533
adenine	1.16	1.41	0.2343	0.0627	0.0390	0.0882
N1-methyladenosine	3.25	1.44	0.0000	0.0000	0.2840	0.2901

guanosine	16.06	1.74	0.0000	0.0000	0.0381	0.0877
guanine	9.60	1.53	0.0000	0.0000	0.0216	0.0637
N2-methylguanosine	1.84	1.12	0.0083	0.0037	0.4966	0.3765
N2,N2-dimethylguanosine	1.22	1.01	0.7572	0.1591	0.9732	0.5472
2'-deoxyguanosine	1.00	0.82			0.8479	0.5113
uridine 5'-triphosphate (UTP)	4.02	1.36	0.0087	0.0038	0.1667	0.2041
uridine 5'-diphosphate (UDP)	0.84	0.84	0.5215	0.1186	0.3826	0.3274
uridine	7.38	1.37	0.0000	0.0000	0.1587	0.1975
uracil	17.04	1.35	0.0000	0.0000	0.1307	0.1800
pseudouridine	1.47	0.84	0.0074	0.0035	0.5415	0.3878
beta-alanine	0.12	0.62	0.0000	0.0000	0.0037	0.0230
cytidine 5'-monophosphate (5'-CMP)	1.06	0.85	0.5630	0.1260	0.7242	0.4695
cytidine	1.53	1.17	0.0489	0.0157	0.5984	0.4145
thymidine 5'-monophosphate	0.51	0.35	0.0454	0.0148	0.0583	0.1113
thymine	2.27	1.30	0.0542	0.0170	0.2619	0.2746
methylphosphate	0.85	1.12	0.4048	0.0985	0.4693	0.3654
nicotinamide	1.29	0.83	0.0684	0.0207	0.4327	0.3546
nicotinamide adenine dinucleotide (NAD	2.42	1.67	0.0002	0.0003	0.0219	0.0637
nicotinamide adenine dinucleotide reduc	2.17	2.04	0.0498	0.0159	0.0452	0.0958
riboflavin (Vitamin B2)	1.10	1.11	0.4607	0.1073	0.2519	0.2665
flavin adenine dinucleotide (FAD)	2.24	1.09	0.0000	0.0001	0.1141	0.1671
pantothenate	1.07	0.64	0.3336	0.0854	0.0000	0.0006
3'-dephosphocoenzyme A	0.87	1.09	0.3808	0.0938	0.5073	0.3805
coenzyme A	1.41	0.62	0.0716	0.0215	0.1164	0.1683
gulono-1,4-lactone	0.96	0.68	0.8355	0.1730	0.0562	0.1090
5-methyltetrahydrofolate (5MeTHF)	0.28	1.00	0.0001	0.0001		
thiamin (Vitamin B1)	0.50	3.12	0.0005	0.0005	0.0054	0.0277
pyridoxal	1.49	1.18	0.0154	0.0060	0.4935	0.3765
pyridoxate	1.41	1.25	0.0602	0.0187	0.4663	0.3654
hippurate	1.24	1.26	0.0323	0.0112	0.0703	0.1252
benzoate	1.61	1.11	0.0280	0.0101	0.4620	0.3633
erythritol	0.88	1.09	0.2749	0.0722	0.6109	0.4219
glycerol 2-phosphate	0.43	0.48	0.0004	0.0004	0.0029	0.0215
phenol red	1.41	1.38	0.0076	0.0035	0.0250	0.0678

Annex III

Gene	ID						
ACTB	60	BBS9	27241	CLPS	1208	DUSP13	51207
CDC5L	988	BCAS2	10286	CLUL1	27098	DUSP26	78986
EIF3A	8661	BCCIP	56647	COG1	9382	ECM1	1893
GAPDH	2597	BCLAF1	9774	COMMD1	150684	EFEMP1	2202
KIF11	3832	BEGAIN	57596	COPE	11316	EGFLAM	133584
PLK1	5347	BEX1	55859	CORO1A	11151	EID2	163126
POLR2B	5431	BICD1	636	CPAMD8	27151	ELP4	26610
RBX1	9978	BTN2A2	10385	CPD	1362	EPDR1	54749
ACAP1	9744	BUD31	8896	CPNE1	8904	EPHA10	284656
ACSM3	6296	C12orf72	254013	CPXM2	119587	EPHA6	285220
ACTR3B	57180	C13orf27	93081	CRB1	23418	EPM2A	7957
ADAM21	8747	C14orf148	122945	CRELD1	78987	ERRFI1	54206
ADAMDEC1	27299	C14orf156	81892	CRISP3	10321	ESPL1	9700
ADAMTSL1	92949	C14orf4	64207	CRYM	1428	EVC	2121
ADCY10	55811	C19orf22	91300	CTAG2	30848	EVI2A	2123
ADM2	79924	C19orf46	163183	CTRL	1506	EXOC4	60412
AGFG2	3268	C19orf66	55337	CTSH	1512	EYA1	2138
AIF1	199	C1orf124	83932	CTSL3	392360	FAM123A	219287
AKR1CL1	340811	C20orf103	24141	CUL4B	8450	FAM171B	165215
AKR1E2	83592	C20orf141	128653	CUL5	8065	FAM3B	54097
ALDH1L2	160428	C21orf29	54084	CXADR	1525	FAM70A	55026
AMZ2	51321	C6orf138	442213	CXCL1	2919	FAP	2191
ANG	283	C6orf170	221322	CXCL14	9547	FBXO45	200933
ANGEL1	23357	C7orf31	136895	CXorf21	80231	FERMT2	10979
ANKRD11	29123	CALHM1	255022	CXXC1	30827	FGF21	26291
ANXA8	653145	CASP5	838	CYP4X1	260293	FHL1	2273
APOC4	346	CBFA2T2	9139	CYP4Z1	199974	FIG4	9896
APOL3	80833	CC2D1A	54862	DCAF12L2	340578	FIP1L1	81608
ARFRP1	10139	CCT3	7203	DDAH2	23564	FJX1	24147
ARHGAP26	23092	CDH6	1004	DDX10	1662	FKRP	79147
ARL6IP5	10550	CDH9	1007	DDX25	29118	FLJ25006	124923
ARMC1	55156	CDHR1	92211	DDX49	54555	FOXF2	2295
ARMC9	80210	CDKN2BAS	100048912	DDX5	1655	FRK	2444
ARMCX1	51309	CDON	50937	DHFRL1	200895	FTSJ1	24140
ASCL4	121549	CDR2	1039	DHX32	55760	GAK	2580
ASH2L	9070	CEBPE	1053	DIP2B	57609	GALR2	8811
ASPSCR1	79058	CEP55	55165	DIRAS3	9077	GINS1	9837
ATP6AP2	10159	CERKL	375298	DIRC2	84925	GJA8	2703
ATP7B	540	CHD1	1105	DLEC1	9940	GK	2710
ATP9A	10079	CHI3L1	1116	DNAJC10	54431	GLT1D1	144423
ATRNL1	26033	CHI3L2	1117	DND1	373863	GPER	2852
ATXN3L	92552	CHL1	10752	DONSON	29980	GPR109A	338442
ATXN7	6314	CHMP2A	27243	DPP9	91039	GPR112	139378
B3GALTL	145173	CHRFAM7A	89832	DSC2	1824	GPR155	151556
BAI2	576	CLCN3	1182	DSCR8	84677	GPR156	165829
BAT4	7918	CLIC6	54102	DSG2	1829	GPR84	53831

Gene	ID						
GRIK5	2901	KIAA1217	56243	MGST2	4258	NXF4	55999
GRK6	2870	KIAA1737	85457	MIP	4284	OGT	8473
GSDMA	284110	KIF15	56992	MLF1IP	79682	OPN4	94233
GTF2IRD2	84163	KIF6	221458	MLL3	58508	OR10G2	26534
GZMM	3004	KIR3DL1	3811	MMADHC	27249	OR13A1	79290
H2AFZ	3015	KLC3	147700	MMP24	10893	OR1G1	8390
H3F3B	3021	KLF4	9314	MOBKL2B	79817	OR1N2	138882
HAGHL	84264	KLHDC8B	200942	MORC3	23515	OR2AE1	81392
HAND2	9464	KLK12	43849	MOSPD3	64598	OR2G6	391211
HAUS1	115106	KLK14	43847	MPDZ	8777	OR2S2	56656
HDLBP	3069	LAMA3	3909	MRGPRX3	117195	OR2T6	254879
HIST1H1B	3009	LAMA5	3911	MRPS11	64963	OR3A4	390756
HLA-DRB4	3126	LAMB3	3914	MTUS2	23281	OR4C12	283093
HMHA1	23526	LASS6	253782	MUC2	4583	OR4C16	219428
HMSD	284293	LCE5A	254910	MUC5B	727897	OR4C46	119749
HOXB3	3213	LENG1	79165	MUC6	4588	OR4C6	219432
HRC	3270	LHFPL5	222662	MYO18B	84700	OR4L1	122742
HSD17B14	51171	LHX3	8022	MYO1G	64005	OR4M1	441670
HSN2	65125	LIMA1	51474	MYO3A	53904	OR4X1	390113
HTATSF1	27336	LOC389458	389458	MYO3B	140469	OR51A7	119687
HUWE1	10075	LOC730167	730167	MYOCD	93649	OR51B4	79339
HYLS1	219844	LOXL2	4017	MYST1	84148	OR51F1	256892
ICAM4	3386	LRFN2	57497	NAPSB	256236	OR51L1	119682
IER5L	389792	LRRFIP1	9208	NCALD	83988	OR52A1	23538
IGF2BP3	10643	LRRN3	54674	NCDN	23154	OR52B6	340980
IGFBPL1	347252	LSR	51599	NDC80	10403	OR52R1	119695
IGHMBP2	3508	LTK	4058	NDUFAB1	4706	OR56B1	387748
ILKAP	80895	LYVE1	10894	NEK3	4752	OR5AR1	219493
INSL3	3640	M6PR	4074	NID2	22795	OR5P3	120066
INSRR	3645	MACROD2	140733	NLRC3	197358	OR6N1	128372
INTS7	25896	MAGEC3	139081	NLRP1	22861	OR6N2	81442
IQCB1	9657	MALAT1	378938	NLRP14	338323	OR8B8	26493
IQGAP1	8826	MAP4K3	8491	NOL3	8996	OR8D1	283159
ITFG3	83986	MAPK15	225689	NPC2	10577	OR8D4	338662
ITGBL1	9358	MAPK4	5596	NPRL2	10641	OVCH2	341277
KBTBD11	9920	MARK3	4140	NPTX2	4885	OVOL2	58495
KCNA2	3737	MAST1	22983	NRIP2	83714	P2RY10	27334
KCNC3	3748	MAST2	23139	NRK	203447	P4HA2	8974
KCNE3	10008	MASTL	84930	NRSN2	80023	PABPN1	8106
KCNJ1	3758	MBD6	114785	NTS	4922	PAPPA2	60676
KCNJ15	3772	MCEE	84693	NUAK2	81788	PAQR3	152559
KCNQ4	9132	MDK	4192	NUDT5	11164	PAX7	5081
KIAA0182	23199	MED13L	23389	NUP43	348995	PAX9	5083
KIAA0196	9897	MED28	80306	NUP85	79902	PBX1	5087
KIAA0247	9766	MEPCE	56257	NUP98	4928	PCBP2	5094
KIAA1210	57481	MFSD8	256471	NUPL1	9818	PCDH9	5101

Gene	ID						
PCID2	55795	QRFPR	84109	SEPN1	57190	SYT14	255928
PCM1	5108	QTRT1	81890	SERBP1	26135	TAC3	6866
PCSK6	5046	RAB18	22931	SERPINI2	5276	TADA2A	6871
PDCL	5082	RAB9P1	9366	SF3A2	8175	tAKR	389932
PDE4DIP	9659	RABGAP1	23637	SFRP5	6425	TAOK3	51347
PDILT	204474	RABGGTB	5876	SFRS5	6430	TAS1R2	80834
PDP1	54704	RABL2A	11159	SGK269	79834	TBC1D3C	414060
PDX1	3651	RAD51AP1	10635	SH3GL1	6455	TCEB1	6921
PDYN	5173	RAET1E	135250	SHOX	6473	TCEB3	6924
PGAM2	5224	RAPGEF3	10411	SHPK	23729	TDH	157739
PGGT1B	5229	RASSF1	11186	SHPRH	257218	TDRD6	221400
PGPEP1	54858	RASSF2	9770	SIGLEC12	89858	THAP3	90326
PHLPP2	23035	RASSF7	8045	SIPA1L1	26037	THBS3	7059
PIH1D1	55011	RBAK	57786	SLC17A5	26503	THOC5	8563
PISD	23761	RBP3	5949	SLC22A3	6581	THRAP3	9967
PITRM1	10531	RFC3	5983	SLC25A15	10166	TIE1	7075
PKD2	5311	RFFL	117584	SLC25A28	81894	TINAG	27283
PLCH1	23007	RGAG4	340526	SLC31A2	1318	TMED8	283578
PLCL1	5334	RHOJ	57381	SLC35A1	10559	TMEFF1	8577
PLN	5350	RICTOR	253260	SLC35E3	55508	TMEFF2	23671
PLVAP	83483	RMI1	80010	SLC37A3	84255	TMEM37	140738
PNN	5411	RNF113A	7737	SLC40A1	30061	TMEM49	81671
PPAPDC2	403313	RNF125	54941	SLC5A2	6524	TMEM90B	79953
PPAPDC3	84814	RNF20	56254	SLC6A6	6533	TMPO	7112
PPM1H	57460	RNF217	154214	SLITRK4	139065	TMPRSS11A	339967
PPP1R14A	94274	RPE65	6121	SLURP1	57152	TMPRSS7	344805
PPP1R3B	79660	RPGRIP1L	23322	SMARCD3	6604	TMX3	54495
PPP2R3A	5523	RPL7A	6130	SMC1A	8243	TNFSF12	8742
PPRC1	23082	RPS19	6223	SMC3	9126	TNK1	8711
PRDM15	63977	RPS27	6232	SMG1	23049	TNNI2	7136
PRDM16	63976	RPS6KL1	83694	SOX11	6664	TOMM40	10452
PREPL	9581	RRBP1	6238	SPINK6	404203	TPM1	7168
PRPF4	9128	RSPO4	343637	SPRN	503542	TPRG1L	127262
PRPF6	24148	RYR1	6261	SRA1	10011	TPSD1	23430
PRR16	51334	S100A1	6271	SSB	6741	TPT1	7178
PRSS21	10942	SAFB	6294	SSBP4	170463	TRAIP	10293
PRSS8	5652	SAMM50	25813	SSH3	54961	TRHDE	29953
PSMD10	5716	SART3	9733	SSX1	6756	TRIM13	10206
PTCHD1	139411	SBF1	6305	STAG1	10274	TRIM32	22954
PTPN18	26469	SBNO1	55206	STAM	8027	TRIM33	51592
PTPN23	25930	SCRIB	23513	STARD3NL	83930	TRIM42	287015
PTPRCAP	5790	SDSL	113675	STK31	56164	TRIM6	117854
PTPRZ1	5803	SEC23A	10484	STK35	140901	TRMT61A	115708
PYGO2	90780	SEC61G	23480	STXBP2	6813	TRPC1	7220
PZP	5858	SELO	83642	SYN2	6854	TRPC4AP	26133
QDPR	5860	SEMA3D	223117	SYNM	23336	TRPC6	7225

Gene	ID						
TRPM3	80036	ZNF85	7639	GPR111	222611	RAE1	8480
TTC38	55020	ZNRD1	30834	GPR97	222487	RALGAPA2	57186
TTC5	91875	ZRANB2	9406	HIVEP3	59269	RASL11B	65997
TXNDC15	79770	ZYX	7791	HSD17B13	345275	RBM25	58517
TYRO3	7301	ARSG	22901	IL1RAPL2	26280	RBM42	79171
UBE4B	10277	C19orf23	148046	IRGQ	126298	RPS10	6204
UBQLNL	143630	EFCAB2	84288	JAKMIP2	9832	SART1	9092
UCK2	7371	P4HA1	5033	JMJD6	23210	SCNN1G	6340
UGT2B7	7364	TEX11	56159	KIAA0586	9786	SERINC3	10955
UPF1	5976	ACTL6A	86	KIAA1109	84162	SERPINB13	5275
UQCR10	29796	ACTL7A	10881	KRR1	11103	SF3B4	10262
USP26	83844	ADAMTS16	170690	KRT9	3857	SFRS1	6426
USP28	57646	AIM1	202	LOC653111	642612	SFRS3	6428
USP43	124739	AJAP1	55966	LOC727913	727913	SGOL1	151648
USP44	84101	BAGE	574	LPPR2	64748	SHROOM2	357
USP8	9101	BAT2	7916	LSM7	51690	SIAH2	6478
UTS2R	2837	BTNL3	10917	MCOLN2	255231	SKAP1	8631
VSX1	30813	C19orf26	255057	MDN1	23195	SLC17A3	10786
VWA5A	4013	CACNG5	27091	METTL2A	339175	SLC35C1	55343
WNK3	65267	CAPZB	832	MN1	4330	SLC7A7	9056
XIRP1	165904	CCT5	22948	MYST2	11143	SLIT2	9353
XPO4	64328	CCT6A	908	NCAPH2	29781	SMC2	10592
XPO5	57510	CGB8	94115	NOTCH2NL	388677	SNRPE	6635
XYLB	9942	CHD4	1108	NUCB2	4925	SPATA7	55812
YTHDF2	51441	CLIC4	25932	NUP205	23165	SPINK4	27290
ZBED4	9889	CNTN5	53942	OR4K14	122740	SPSB3	90864
ZCWPW1	55063	COPS6	10980	OR4K15	81127	SUDS3	64426
ZFAND5	7763	CPNE6	9362	OR52E4	390081	TH1L	51497
ZFP91	80829	CRNKL1	51340	OR6C74	254783	TNNT3	7140
ZMYM4	9202	CYP27C1	339761	OR8K1	390157	TPR	7175
ZNF101	94039	CYP4F8	11283	PFDN4	5203	TRIB1	10221
ZNF137	7696	DHRS11	79154	PGLYRP4	57115	TTC23	64927
ZNF154	7710	DHX15	1665	PHF12	57649	TUBA3E	112714
ZNF155	7711	DNAJC13	23317	PKD1L1	168507	TUBB	203068
ZNF211	10520	DNASE1L3	1776	PKIB	5570	TUBGCP3	10426
ZNF222	7673	E4F1	1877	PLCXD3	345557	U2AF1	7307
ZNF224	7767	ECT2	1894	PLEKHJ1	55111	UGCGL1	56886
ZNF230	7773	EIF3C	8663	PPA1	5464	USF1	7391
ZNF234	10780	ELAVL3	1995	PPP1R15A	23645	VAT1L	57687
ZNF415	55786	ERH	2079	PPP1R7	5510	VDAC1	7416
ZNF544	27300	FAM126A	84668	PRPF4B	8899	WDR12	55759
ZNF548	147694	FLG	2312	PRPSAP2	5636	WDR36	134430
ZNF586	54807	FSCB	84075	PSPC1	55269	XRRA1	143570
ZNF687	57592	GCN1L1	10985	RAB20	55647	ZFP37	7539
ZNF750	79755	GNL3	26354	RAB38	23682	ZNF283	284349
ZNF816A	125893	GPR110	266977	RAB3GAP1	22930	ZNF468	90333

Gene	ID		
ZNF616	90317	TUBGCP2	10844
ZNF630	57232	VCP	7415
ZNF8	7554	CCT8	10694
ZPBP2	124626	EIF3B	8662
ZRANB1	54764	IMP4	92856
ARL1	400	PRPF18	8559
ATOX1	475	TUBA1B	10376
C14orf179	112752		
CIRH1A	84916		
CKAP5	9793		
CSPG5	10675		
CTSZ	1522		
DHX8	1659		
DYNC1H1	1778		
EIF3E	3646		
EIF3G	8666		
EMG1	10436		
FAM188A	80013		
FCF1	51077		
INGX	27160		
MTCP1	4515		
NUP155	9631		
PHB	5245		
POMP	51371		
PRPF3	9129		
PRPF31	26121		
RANBP10	57610		
RBM10	8241		
RHCE	6006		
RPL21	6144		
RPL23A	6147		
RPL27	6155		
RPL5	6125		
RPLP2	6181		
RPS17	6218		
RPS24	6229		
RPS27A	6233		
RPS29	6235		
RPS3	6188		
RPS4X	6191		
RPS7	6201		
SETD5	55209		
SKIV2L2	23517		
STK3	6788		
TBX15	6913		
TRIP13	9319		

Annex IV

Gene	ID
BCL2L12	83596
CDK17	5128
CHMP2B	25978
DNAH11	8701
EEFSEC	60678
EWSR1	2130
GTPBP4	23560
INVS	27130
OR8G1	26494
PHIP	55023
PRUNE	58497
RGS17	26575
RPGR	6103
SETD3	84193
TXNDC17	84817
UNC5C	8633
VIPAR	63894
BFSP1	631
LMO3	55885
TBX22	50945
TTL	150465

A Ph.D. thesis in quotes: All titles from Ph.D. presentations throughout the years

"Believe you can and you are halfway there."
Theodore Roosevelt

"It is better to light a candle than to curse the darkness."
Confucius

"Metabolics, what else?"
George Clooney

"No matter how long the winter, spring is sure to follow."
Proverb

"Coincidence in logical."
Johan Cruijff

"Less is more….. or simply less."
Divine inspiration

"Great things are done by a series of small things brought together."
Vincent van Gogh

"Simplex non veri sigillum" vel "Simplex sigillum veri."
Christiaan Eijkman and Herman Boerhave

"Mystery is at the heart of creativity. That, and surprise."
Julia Cameron

"Horses: Dangerous on both ends and crafty in the middle."
Sherlock Holmes

"In order to be irreplaceable, one must always be different."
Coco Chanel

"The future is for those who believe in the beauty of their dreams."
Eleanor Roosevelt

"Everything you can imagine is real."
Pablo Picasso

"Murphy was a genius."
Divine inspiration

“Life is what happens to you while you’re busy making other plans.”
Allen Saunders

“I’m not lost for I know where I am. But however, where I am may be lost.”
A.A. Milne, Winny the pooh

“Without deviation from the norm, progress is not possible.”
Frank Zappa

“If everyday is a gift, I would like to know where I could return Monday.”
Proverb

“You dont have to see the whole staircase to take the first step.”
Martin Luther King

Résumé

Le sarcome de Ewing est la seconde tumeur pédiatrique de l'os la plus fréquente. Elle est caractérisée par une translocation chromosomique résultant à la fusion de *EWSR1* avec un membre de la famille *ETS*. Chez 85% des patients, cette fusion conduit à l'expression de la protéine chimérique EWS-FLI1 qui est l'oncogène majeur de ce sarcome. Ce dernier agit principalement par son action transcriptionelle sur des cibles qui lui sont propres. Au niveau thérapeutique, le sarcome d'Ewing est traité par chimiothérapie, chirurgie locale et par radiothérapie. La survie à long terme des patients est de l'ordre de 70%, mais beaucoup plus basse pour les patients métastatiques et quasi nulle lors d'une récidive. Parmi maintes caractéristiques, certains cancers présentent une dérégulation énergétique. L'influence d'EWS-FLI1 sur cet aspect n'a fait l'objet d'aucune étude dans le contexte du sarcome d'Ewing. Nous avons donc étudié par profilage métabolomique des cellules de sarcome d'Ewing en présence ou en absence d'EWS-FLI1. En comparant ces deux conditions, des modulations du profil énergétique relatif au cycle de Krebs, des précurseurs de le glycosylation ainsi que des métabolites de la voie de la méthionine et du tryptophane ont été observés. En parallèle, grâce à un crible de banque de shRNAs réalisé dans des conditions expérimentales similaires à l'étude métabolomique (lignée d'Ewing avec ou sans EWS-FLI1), nous avons pu identifier des gènes présentant des caractéristiques « synthétique létales », c'est-à-dire tuant uniquement les cellules du sarcome d'Ewing en présence de son oncogène.

Abstract

Ewing sarcoma, the second most commonly occurring pediatric bone tumor, is most often characterized by a chromosomal translocation between *EWSR1* and *FLI1*. The gene fusion *EWS-FLI1* accounts for 85% of all Ewing sarcoma and is considered the major oncogene and master regulator of Ewing sarcoma. EWS-FLI1 is a transcriptional modulator of targets, both directly and indirectly. Ewing sarcoma is aggressively treated with chemotherapy, localized surgery and radiation and has an overall survival of about 70%, however, survival for metastasis or relapsed cases remains low. One of the cancer hallmarks, metabolic deregulation, is most likely partly dependent on EWS-FLI1 in Ewing sarcoma cells. In order to get a better understanding of Ewing sarcoma biology and oncogenesis, it might be of high interest to investigate the metabolic influence of EWS-FLI1 in Ewing sarcoma cells. We therefore performed a global metabolic profiling of Ewing sarcoma cells with or without inhibition of EWS-FLI1. Several changes in the energy metabolism were observed throughout this study; the observed changes were consistent with an energy profile that moved from a cancer cell energy metabolism towards the energy metabolism of a more normal cell upon EWS-FLI1 inhibition, primarily based on the TCA cycle. Levels of TCA intermediates, glycosylation precursors, methionine pathway metabolites and amino acids, especially changes in the tryptophan metabolic pathway, were altered upon EWS-FLI1 inhibition. Parallel to this study, we performed a high-throughput synthetic lethality screen, in order to not only identify essential genes for cell survival and proliferation, but also to identify new synthetic lethal targets that could specifically target Ewing sarcoma cells carrying the EWS-FLI1 fusion gene.